University of Alberta

Investigation of the Kinetics of Tet(O)-mediated Tetracycline Resistance

by

Jun Li

A thesis submitted to the Faculty of Graduate Studies and Research
in partial fulfillment of the requirements for the degree of

Master of Science

in

Medical Sciences - Laboratory Medicine and Pathology

Spring 2010
Edmonton, Alberta

Examining Committee

Monika Keelan, Laboratory Medicine and Pathology

Jeff Fuller, Laboratory Medicine and Pathology

Richard Fahlman, Biochemistry

Michael Gänzle, Agricultural, Food and Nutritional Sciences

Abstract

Widespread tetracycline resistance (Tc^R) has limited the clinical use of Tc for the treatment of bacterial infections. Tet(O) protein is present in many bacteria and is the major transmissible Tc^R determinant in *Campylobacter jejuni*, a common cause of acute bacterial diarrhea worldwide. Tet(O) protects ribosomes against the inhibition of protein synthesis by Tc. Tet(O) binds to the ribosome at a similar site as EF-G, a structural homologue of Tet(O) with GTPase activity that is required for protein elongation.

EF-G interfered with the kinetics of Tet(O)-mediated Tc release suggesting that EF-G competes with Tet(O) for ribosome binding. Indirect assessment of EF-G and Tet(O) binding to 70S ribosomes by GTP hydrolysis was unable to clearly demonstrate competition for binding. This thesis contributed to the further understanding of the kinetics of Tc release by Tet(O), and may facilitate the development of novel strategies to overcome Tet(O)-mediated Tc^R in bacteria which cause human infections.

Acknowledgements

I wish to express my sincere gratitude and appreciation to the following individuals for their contributions during my graduate studies:

To Dr. Monika Keelan, my supervisor, for her guidance, support, patience and knowledge. Her enthusiasm for learning and research encouraged me to persevere and progress towards successful completion of my Master's degree program.

To Dr. Richard Fahlman and Dr. Jeff Fuller, my committee members, and Dr. Michael Gänzle, my external examiner, for their insightful comments and their critical review of this work.

To members of Dr. Richard Fahlman's lab, especially Roshani Payoe, for her enthusiasm, expertise and technical assistance in my lab work.

To Oindrila Mukherjee, Maysoon Mahmoud, and Nour Moussa, for their support, encouragement, and friendship for assisting to make this incredible journey.

To Ashlyn J. Bernier and Sherri Selby, for their insightful comments and feedback on this thesis.

To members in the Department of Laboratory Medicine and Pathology, for their support and providing me with teaching and working opportunities.

Finally, many thanks to my parents and my husband Zhi Gang Duan, for their love, support, understanding and encouragement throughout all of my endeavors which greatly helped me to achieve my goals.

Table of Contents

List of Tables

List of Figures

List of Abbreviations

aa	Amino Acids
A-site	Aminoacyl-site
aa-tRNA	Aminoacyl-tRNA
APS	Ammonium Persulfate
ATP	Adensoine 5'-Triphosphate
BSA	Bovine Serum Albumin
BW	Binding-Washing
CDC	Centers for Disease Control and Prevention
Cip	Ciprofloxacin
CPM	Counts Per Minute
cryo-EM	Cryo-Electron Microscopy
CTP	Cytidine 5'-Triphosphate
D	Aspartate
DEPC	Diethylpyrocarbonate
DMS	Dimethyl Sulfate
DPM	Decay Per Minute
DPS	Decay Per Second
DTT	Dithiothretol
E-site	Exit-site

Ery	Erythromycin
EF-G	Elongation Factor G
GBS	Guillain-Barré Syndrome
GFP	Green Fluorescent Protein
GMP	Guanosine Monophosphate
GTP	Guanosine 5'- Triphosphate
H-bond	Hydrogen bond
His-tagged	Histidine-tagged
IMAC	Immobilized Metal Affinity Chromatography
IPTG	Isopropylthio-β-D-galactoside
LB	Luria-Bertani
LOSs	lipooligosaccharides
MIC	Minimal Inhibitory Concentration
MRSA	methicillin-resistant *Staphylococcus aureus*
MW	Molecular Weight
N	Asparagine
otr	Oxytetracycline Resistance Gene
P-site	Peptidyl-site
PBS	Phosphate-Buffered Saline
PEI	Polyethyleneimine

PPi	Pyrophosphate
RPPs	Ribosomal protection proteins
RT	Room Temperature
SD	Standard Deviation
SDS-PAGE	Sodium Dodecyl Sulfate Polyacrylamide Gel Electrophoresis
Tcs	Tetracyclines
Tc^R	Tetracycline Resistance
Tc^S	Tetracycline Susceptible
tet	Tetracycline Resistance Gene
TBE	Tris/Borate/EDTA
TLC	Thin Layer Chromatography
UTP	Uridine 5'-Triphosphate
UV	Ultraviolet
VRE	Vancomycin-Resistant *Enterococci*
WT	Wild Type
XTP	Xanthosine 5'- Triphosphate

Chapter 1 Introduction

1.1 Campylobacteriosis

Infection by *Campylobacter* spp. (campylobacteriosis) is considered to be the most common cause of acute bacterial diarrhea. Approximately 400 million cases of campylobacteriosis are reported annually in the world, and over 80% of all cases are caused by *C. jejuni* [1-3]. However, the rates of *Campylobacter* infections are usually underreported because many patients with relatively mild symptoms do not seek medical care, and some hospital laboratories may not routinely culture stool samples for *Campylobacter* spp. [4]. *Campylobacter* infection in developed countries appears to have different epidemiological characteristics compared to that described for developing countries [4, 5]. The incidence of infection is high among older children and young adults (15-30 year old) in developed countries, while in developing countries *Campylobacter* infections usually affect young children (less than 5 years old) [5, 6]. The incidence of campylobacteriosis for children less than 5 years of age is much higher in developing countries with reports of 40,000-60,000 cases per 100,000 populations per year compared with 300 cases per 100,000 populations per year in developed countries [2, 6, 7].

In the United States, it has been estimated that 2.5 million people acquire food-borne campylobacteriosis each year [8]. In Canada, the reported annual

average of campylobacterioses was 11,139 cases during 2000 to 2004, which is greater than the combined total number of reported cases of gastroenteritis caused by *Salmonella* spp., *Shigella* spp., or verotoxigenic *Escherichia coli* (Table 1.1) [9]. *C. jejuni* is responsible for ~95% of all enteric *Campylobacter* infections in Canada [10]. The rates of annual *Campylobacter* infection have been declining in Canada in the last 5–10 years. The reasons for this are not clear, but may be due to improvements in food safety [10].

Campylobacteriosis is mainly acquired by the consumption and handling of contaminated chicken, pork, beef, or drinking contaminated water or raw milk [1]. The infection is characterized by watery or bloody diarrhea, abdominal pain, fever, malaise, nausea, and rarely vomiting. The duration of illness is usually no longer than 10 days, but some longer term campylobacterioses may progress to neurological complications, such as Guillain-Barré syndrome (GBS), which causes acute neuromuscular paralysis [1]. The molecular mimicry of *C. jejuni* lipooligosaccharides in human gangliosides in nervous tissue is proposed to induce cross-reactive antibodies that lead to GBS [11]. Campylobacteriosis is the infection most frequently observed before GBS. It is estimated to occur in 1 in 3000 *Campylobacter* infections [1].

Most campylobacterioses are self-limited and do not require antimicrobial therapy, unless the infections are severe and long-lasting, or are present in immunocompromised patients [12]. Erythromycin (Ery) is the drug of choice for

antimicrobial treatment of *Campylobacter* infections, while ciprofloxacin (Cip) and tetracycline (Tc) are used as alternative drugs [3, 13]. Cip is commonly offered as empirical treatment for suspected acute bacterial gastroenteritis without waiting for culture results, especially for travelers [1, 12]. However, the growing resistance to antimicrobial drugs is becoming a major public health concern [3, 13-15]. In particular, the widespread development of resistance to Tc has limited its clinical effectiveness to treat campylobacterioses and other infections.

1.2 Tetracyclines (Tcs)

1.2.1 Classification of Tcs

Tcs are a group of broad-spectrum antibiotics consisting of four fused cyclic six-membered rings (Figure 1.1), which were first discovered and isolated from *Streptomyces aureofaciens* in 1948 [16, 17]. They exert bacteriostatic activity to a wide range of gram-negative and gram-positive bacteria, chlamydiae, rickettsias, mycoplasmas, and protozoan parasites [16]. Based on their modes of action, Tcs are classified into two groups: typical (e.g. chlortetracycline, tetracycline, doxycycline, and minocycline) and atypical (e.g. chelocardin, 6-thiatetracycline and anhydrotetracycline). The typical Tcs have therapeutic value because they exhibit bacteriostatic activity by targeting bacterial ribosomes to inhibit protein synthesis. In contrast, the atypical Tcs exhibit bactericidal activity by targeting the cell membranes instead of the ribosomes to kill the cell. Despite their ability to

kill even those bacteria possessing Tc^R genes, the atypical Tcs are not of therapeutic value because of their severe toxic side effects (central nervous system lesions) which may be caused by interaction with both mammalian membranes and bacterial membranes [18].

1.2.2 Application of Tcs

Tcs are the second most commonly used antibiotics after penicillins, especially in the developing countries due to their very low cost, broad spectrum activity and minor side effects, and have been extensively used throughout the world in human medicine, veterinary medicine, agriculture, aquaculture and so on. [16, 19]. In human medicine, Tcs were used for the prophylaxis of traveler's diarrhea (e.g. *Campylobacter* spp., *Salmonella* spp., *Shigella* spp.), the plague (*Yersinia pestis*) and tularemia (*Francisella tularensis*), as well as the treatment of infections, especially respiratory tract infections (e.g. atypical pneumonia caused by *Mycoplasma pneumonia*, *Chlamydia pneumoniae*) and some sexually transmitted diseases (e.g. nongonococcal urethritis and cervicitis) [16, 20]. Due to the high prevalence of Tc^R, Tcs are no longer the drug of choice in clinics and hospitals. However, some new applications have been identified, such as a part of a triple therapy for the management of gastritis and peptic ulcer disease caused by *Helicobacter pylori*, parasite infections (e.g. malaria, filarial nematodes infection, *entamoeba histolytica* infection etc.), non-infectious conditions (e.g. rosacea,

anti-inflammation, immunosuppression, wound healing etc.), and acne [16, 20].

In veterinary medicine, in addition to the treatment of infections, Tcs have largely been used subtherapeutically as animal growth promoters (added to the feed of food-producing animals) for long periods to improve the rate of weight gain and efficiency of feed utilization. As a result, animals become healthier, grow faster and stronger, and fewer die from disease [16, 20].

Tcs have also been used to treat infections in aquaculture (salmon, catfish, lobsters), foulbrood disease of the honeybee (caused by *Bacillus larvae* or *Melissococcus pluton*), as well as plant infections (*Erwinia amylovara* infections of fruit trees, mycoplasma infections of palm trees) [16].

1.2.3 Action of Tcs

1.2.3.1 Bacterial ribosomes and protein synthesis

Tcs uniquely target 70S ribosomes of bacteria but not 80S ribosomes of eukaryotic cells. As a result, Tcs inhibit bacterial growth without causing harm to eukaryotic cells [16].

The 70S ribosome consists of two subunits: 50S and 30S. The large 50S subunit is composed of 23S rRNA, 5S rRNA, and over 30 proteins, while the small 30S subunit consists of a single 16S rRNA and 20 proteins [21, 22]. There are three tRNA-binding sites, designated the A (aminoacyl) site, the P (peptidyl) site, and the E (exit) site on the ribosome. These sites are functionally important

for protein synthesis, especially for protein elongation [21, 22]. As a critical stage in protein synthesis, the elongation cycle (Figure 1.2) involves three phases: 1) aminoacyl-tRNA (aa-tRNA) binding to the ribosomal A-site, 2) peptide-bond formation, 3) translocation; and requires two elongation factors (EF-Tu and EF-G) to assist the process [23]. EF-Tu binds to the ribosome as a ternary complex (EF-Tu•GTP•aa-tRNA) to deliver cognate aa-tRNA to the ribosomal A-site. EF-G•GTP binds to the ribosome to catalyze the translocation of peptidyl-tRNA from the ribosomal A-site to the P-site, and the deacylated tRNA from the P-site to the E-site [24]. The binding of EF-Tu complex (EF-Tu•GTP•aa-tRNA) and EF-G complex (EF-G•GTP) to the ribosomes stimulates their GTPase activity, and causes EF-Tu•GDP and EF-G•GDP release from the ribosome following GTP hydrolysis [25].

1.2.3.2 Action of Tcs

The illumination of the high resolution structures of the ribosome and the ribosome-Tc complex by X-ray crystallography has largely facilitated a basic understanding of the molecular mechanisms of protein synthesis and the action of Tcs [22, 26-31]. Tcs reversibly inhibit bacterial protein synthesis by binding to the 30S ribosomal subunit thereby preventing accommodation of aa-tRNA to the ribosomal A-site (Figure 1.2) [16, 32]. X-ray crystallography studies of the Tc-ribosome complex revealed that Tcs prevent the accommodation of incoming

aa-tRNA to the ribosomal A-site by direct steric hindrance [30, 31].

1.2.3.3 Tc binding sites

The binding sites of Tc on the 30S ribosomal subunit have been identified by X-ray crystallography studies [30, 31]. They are divided into two classes: primary site and secondary site(s). The primary Tc binding site is responsible for the inhibition of protein synthesis by interfering with the accommodation of aa-tRNA to the ribosomal A-site, which is located between the head and the body of the 30S, and close to the ribosomal A-site (Figure 1.3). In the primary site, Tc binds to an irregular minor groove of helix 34 (h34) and h31 stem-loop in the 16S rRNA, and interacts with the sugar phosphate backbone of h34 by hydrogen bonding (Figure 1.4a). The presence of Mg^{2+} is necessary for the binding of Tc to the primary site, as it facilitates formation of a salt bridge to phosphate oxygen atoms of G1197 and G1198 (Figure 1.4c) [30, 31].

In contrast, the secondary site(s) may act synergistically to contribute to the bacteriostatic effect of Tc [30, 31]. Brodersen *et al.* [30] proposed one secondary site which is located in the body of the 30S subunit (Figure 1.3a). It binds close to h44 and is sandwiched between h27 and h11 in the 16S rRNA (Figure 1.4b). At this site, Tc interacts with the 30S subunit in a similar manner to the Tet 5 site proposed by Pioletti *et al.* [31] who put forward 5 secondary sites (Tet 2-6) (Figure 1.3b).

1.3 Tetracycline resistance (Tc^R)

1.3.1 Development and incidence of Tc^R

In 1953, only 5 years after the advent of the first member of Tcs (chlortetracycline), the first Tc^R bacterium, *Shigella dysenteriae* was isolated from a case of severe bloody diarrhea [16]. Two years later, the first multidrug-resistant *Shigella* spp. (resistant to Tc, streptomycin, and chloramphenicol) was isolated. The incidence of multidrug-resistant *Shigella* spp. increased from 0.02% to 10% within 5 years (1955-1960), and by 1993, the incidence increased to over 60% [16, 33]. Tc^R quickly spread among other gram negative bacteria, as well as gram positive bacteria, and was often present with other antibiotic resistance determinants. A 1994 study indicated that approximately 90% of methicillin-resistant *Staphylococcus aureus* (MRSA), 70% of *Streptococcus agalactiae*, 70% of multidrug-resistant *Enterococcus faecalis*, and 60% of the multidrug-resistant *Streptococcus pneumonia* were also Tc^R [34].

Tcs have been largely used at sub-therapeutic levels as growth promotion agents in the animal food industry. This resulted in the development and rapid spread of Tc^R in commensal bacteria in food animals, such as *Campylobacter* spp. [1, 16]. Despite the ban on the use of Tcs for animal growth promotion in the European Union in 1970 [16], the high incidence of Tc^R persists because Tcs are still used for the therapeutic treatment of animal infections.

1.3.1.1 Incidence of Tc^R in *C. jejuni*

A high frequency of Tc^R in human *C. jejuni* isolates was also observed worldwide over the last two decades, especially in Spain (70-97%), Japan (43-69%), and Taiwan (85-95%) [35, 36]. In Canada, a high incidence of Tc^R was observed in Quebec (43-68% during 1998-2001 in Montreal) [37], and Alberta (49.8% during 1999-2002) [38]. The high rate of Tc^R in Alberta contrasted sharply with the low rates observed twenty years previously (6.8% in 1980) [39].

A high incidence of Tc^R in *C. jejuni* isolates was also observed in food-producing animals [40-44] (Table 1.2), important sources of human campylobacteriosis and significant reservoirs of antibiotic resistant *C. jejuni* [1].

1.3.1.2 Multi-drug resistance in *C. jejuni*

Multi-drug resistance was not commonly observed in *C. jejuni* isolates prior to the 1990's, but is now slowly increasing and becoming a concern. Multi-drug resistance of human isolates increased from 0-25% in Montreal during 1998-2001 for Tc + Cip (6-25%)，Tc + Ery (0-6%)，Tc + Cip + Ery (0-2%)， and Cip + Ery (1-4%) [37]. Multi-drug resistant *C. jejuni* isolates were also reported in food-producing animals. In Alberta, approximately 8% of poultry isolates exhibited resistance to Tc + nalidixic acid (NA) + Cip [40]; ~ 3% of beef cattle isolates were resistant to Tc + Ery, and 0.5% to NA + Cip [41]. In Southern Ontario, ~13% of raw turkey meat isolates were resistant to Tc + ampicillin, ~4%

to NA + Cip, and ~1% to Tc + Ery + clindamycin [43].

1.3.2 Consequence of Tc^R

Since Tcs have been used for more than 60 years, it is not surprise that the selection pressure has resulted in the high incidence of Tc^R organisms, which are often associated with multi-drug resistance [16]. Resistant infections result in delays in effective treatment, prolong the course of disease, and increase the risk of death and cost of illness. The high prevalence of Tc^R has largely limited the clinical use of Tcs to treat infections, including campylobacterioses [16, 32, 45].

1.3.3 Mechanisms of Tc^R

Many types of antibiotics were produced to fight against diverse infections caused by different pathologic microorganisms, but bacteria have an extremely strong capacity to develop various ways to protect themselves against attack from antimicrobial agents. In only 68 years since the advent of penicillin, the first antibiotic for therapeutic use in 1942, most pathogenic and opportunistic bacteria that were once susceptible to antibiotics have developed resistance to many antibiotics [46]. The mechanisms by which bacteria develop antimicrobial resistance are diverse and complex, including three main classes: 1) limiting access of the antibiotics to their targets, 2) alteration of target sites to reduce affinity to antibiotics, 3) production of enzymes to hydrolyze and inactivate

antibiotics [47, 48]. The mechanisms of Tc^R cover the three classes of antimicrobial resistance mechanisms. Tc^R is most commonly derived from the acquisition of Tc^R genes (e.g. *tet*) rather than mutation of existing chromosomal genes (e.g. 16S rRNA mutation in *Helicobacter pylori*) [45]. There are three different types of Tc^R determinants: efflux pumps, ribosomal protection proteins (RPPs), and enzymatic inactivation [16, 49].

The efflux pumps are the most common Tc^R determinant. The *tet* efflux genes code for membrane-associated proteins that pump out Tcs to reduce intracellular accumulation and thereby protect the ribosome from the action of Tcs [16]. The efflux of Tcs is very efficient, allowing resistant bacteria to survive up to 100 times the therapeutic dose of Tcs [50]. There are 26 *tet* and oxytetracycline resistance genes (*otr*) coding for efflux pumps, and these genes are broadly disseminated among diverse bacteria [16, 49, 51].

Ribosomal protection proteins (RPPs) are another common Tc^R determinant. They bind to the bacterial ribosomes and cause the release of bound Tcs, thereby protecting the ribosome from the action of Tcs. There are 11 *tet* genes encoding RPPs, and they are also widely spread among many bacteria [16, 49].

The less common Tc^R determinant is enzymatic inactivation. There are 3 *tet* genes coding for enzymatic inactivation [49]. The most studied is the *tet*(X) gene, coding for an NADPH-requiring oxidoreductase, that inactivates Tcs in the presence of oxygen and NADPH. However, it has only been found in a strict

anaerobe, *Bacteroides* spp. [52].

These three types of Tc^R determinants, are sometimes located on the chromosome, but are most frequently associated with plasmids which facilitate the spread of resistance genes among different bacteria [45, 49]. The most current information on the distribution of the genes encoding determinants of Tc^R is available from Dr. Marilyn C. Roberts's website [51], which is updated twice a year.

l.4 Ribosomal Protection Proteins (RPPs)

The presence of a RPP as a Tc^R determinant (Tet(M)) was first discovered in *Streptococcus faecalis* in 1986 [53]. To date, 11 RPPs have been discovered, including Tet(M), Tet(O), Tet(S), Tet(T), TetB(P), Tet(Q), Tet(W), Tet(32), Tet(36), Tet, and Otr(A) [16, 49]. These RPPs are a group of soluble cytoplasmic proteins that confer Tc^R by binding to the bacterial ribosome and cause the release of bound Tcs, thereby restoring protein synthesis [16, 54].

1.4.1 Distribution of *tet* genes encoding RPPs

The genes encoding RPPs are widely distributed in divergent bacteria, and are often present with other resistance determinants, like efflux pump genes, to synergistically confer Tc^R in bacteria (Table 1.3) [49, 51]. Most *tet* genes encoding RPPs are associated with mobile units in bacteria, such as plasmids (e.g. *tet(O)*),

transposons (e.g. *tet(M)*), and conjugative transposons (e.g. *tet(M)*, *tet(Q)*). These mobile elements have enabled the *tet* genes to horizontally transfer to different strains or species, or genera [16, 49]. The *tet*(M) gene has the widest host range, and has been identified in 54 genera. The *tet*(W) gene has the second largest host range, found in 21 genera. The *tet*(O) and *tet*(Q) are also widely distributed, and have been identified in 19 genera. The other *tet* genes are not commonly disseminated in bacteria [51].

1.4.2 Classification of RPPs

The number of amino acids (aa) present in RPPs range from 639 aa to 663 aa. Based on composition of the aa sequence, RPPs are divided into three groups (Table 1.4) [16, 49, 54]. In group I, Tet(O), Tet(M), Tet(S), Tet(32), and Tet(W) share aa sequence identity between 67% to 77% In group II, Otr(A) shares 36% aa sequence identity with TetB(P). In group III, Tet(T) shares 49% aa sequence identity with Tet(Q), and 52% with Tet(36), while Tet(Q) shares 60% aa sequence identity with Tet(36).

1.4.3 RPPs are GTPases

RPPs belong to the translation factor superfamily of GTPases, and share sequence similarity to the elongation factors, EF-G and EF-Tu [49, 54-56]. The greatest homology (~50%) is observed at the N-terminal domain, designated the G

domain, which displays GTPase activity as it binds and hydrolyzes GTP [16, 57-61]. GTP binding is essential for RPPs in their role to protect bacterial ribosomes from the action of Tcs [16, 56, 62-64]. The binding of RPPs to the ribosomes activates their GTPase activity and allows the dissociation of bound Tcs from ribosomes, as well as the release of bound RPPs from ribosomes following GTP hydrolysis.

1.5 Ribosomal Protection Protein: Tet(O)

1.5.1 *tet*(O) Gene is the most common Tc^R determinant present in *C. jejuni*

The *tet(O)* gene was the transmissible Tc^R determinant, which was first identified in *C. jejuni* in the 1980's [65-68]. The *tet(O)*-mediated Tc^R is usually associated with a plasmid, which facilitates rapid and spontaneous intraspecies and interspecies Tc^R transfer among *Campylobacter* spp. and other bacterial species by conjugation, even in the absence of antimicrobial selection pressure [66, 69-71]. The *tet*(O) gene was detected in all Tc^R *C. jejuni* [38]. Transmissible Tc^R was also demonstrated by transformation of the *C. jejuni tet*(O) gene into *E. coli* [67].

In addition to *Campylobacter* spp., the *tet*(O) gene has been observed in 18 other genera [51] (Table 1.3), which include some common clinically significant pathogens, such as *Streptococcus* spp., *Staphylococcus* spp., *Enterococcus* spp.,

Neisseria spp., and *Clostridium* spp.

1.5.2 Classification of Tet(O)

Tet(O) protein is classified as a group I RPP based on its aa sequence identity with other RPPs (Table 1.4) [16]. It has more than 67% aa sequence identity with other group I RPPs, in contrast to less than 45% aa sequence identity with the group II and III RPPs. Tet(O) has the highest aa sequence identity with Tet(M) (77%) and has the lowest aa sequence identity with Otr(A) (31%) (Table 1.5) [54].

1.5.3 Tet(O) is an elongation factor-like GTPase

Tet(O) is an elongation factor-like protein with GTPase activity. It is structurally more similar to EF-G than to EF-Tu (Table 1.6). The molecular weight (MW) of Tet(O) (72.5 kDa) is close to that of EF-G (77.5 kDa) [72, 73], while the MW of EF-Tu is much smaller (～43 kDa) [74]. A structural model of Tet(O) was produced based on its similarity to EF-G [75] (Figure 1.5). Both Tet(O) and EF-G are composed of 5 domains, while EF-Tu consists of 3 domains [73]. The interactions of the domains of Tet(O) and EF-G with the ribosome are very similar except for domain IV [76] (see section 1.5.7.1). Tet(O)'s G domain (1-150 residues) shares greater aa sequence identity with EF-G (51%) than with EF-Tu (31%) [59, 76] (Figure 1.6). G domain sequence analysis reveals a conserved aa in Tet(O) and EF-G that is different in EF-Tu, which may relate to

differences in GTPase activity. Tet(O) (**A10**-H-V-D-A-G-K16) shares the same essential aa residue (alanine) as EF-G (**A17**-H-I-D-A-G-K23) in the consensus motif located at the N terminus for the GTPase, in contrast to glycine in the consensus motif (**G18**- H-V-D-H-G-K24) of EF-Tu [59, 76]. EF-Tu has about two orders of magnitude higher affinity for GDP than for GTP, and therefore requires a specific nucleotide exchange factor (EF-Ts) to assist EF-Tu•GDP to recycle back to EF-Tu•GTP [74]. In contrast, EF-G and Tet(O) have a higher affinity for GTP than GDP, therefore they do not require a specific nucleotide exchange factor to assist the recycling of EF-G•GDP and Tet(O)•GDP back to EF-G•GTP and Tet(O)•GTP, respectively [78, 79].

These three GTPase proteins are present in different amounts in the cell [59], which corresponds to their functions [25, 56, 57]. Elongation factors are present in high concentrations in the cell. EF-Tu is the most abundant protein in the cell due to the need to carry large amounts of aa-tRNA for protein synthesis. The concentration of EF-Tu (100-200 μM) is equal to that of aa-tRNA and is approximately 10-fold higher than that of ribosomes and EF-G [59, 74]. In contrast, EF-G and Tet(O) are present in low amounts in the cell. One molecule of EF-G binds per ribosome [59], and the same is proposed to be true for Tet(O) [62]. No specific concentration is known for Tet(O), but it is proposed that Tet(O) is produced in very low amounts, and is likely to act in a catalytic mode rather than a stoichiometric manner [59]. In other words, one Tet(O) molecule cycles on and

off many ribosomes to release Tcs.

The structural similarities with the elongation factors suggest that Tet(O) may have evolved from EF-G, but this evolutionary relationship has not been demonstrated [80].

1.5.4 Functions of Tet(O)

1.5.4.1 Tet(O) confers Tc^R

The major function of Tet(O) is to confer Tc^R by binding to bacterial ribosomes to release bound Tc from the ribosome and restore protein synthesis. The Tc susceptibility and Tc binding assays have been used to evaluate the ability of Tet(O) to confer Tc^R *in vivo* and *in vitro*, respectively [58, 59, 62, 67, 72, 75]. *In vivo*, Tc susceptible *E. coli* (minimal inhibitory concentration (MIC) = 1 μg/mL) was converted to Tc^R (MIC = 64 μg/mL) after transformation with the *C. jejuni tet(O)* gene. This demonstrated that the *C. jejuni tet(O)* gene can be expressed in different species and confer Tc^R to the same level observed in *C. jejuni* [67]. *In vitro*, Tc binding assays indicated that the presence of purified Tet(O) protein caused the affinity of Tc for bacterial ribosomes to decrease about 6-fold (K_d=20.4, 30 μM) compared with that observed in the absence of Tet(O) (K_d = 3.4, 5 μM) [62, 72]. Tet(O)-mediated Tc release is GTP-dependent. Tet(O) cycles repeatedly by forming a complex with GTP (Tet(O)•GTP) to bind to ribosomes, release bound Tc, and dissociate from the ribosome (as Tet(O)•GDP) following GTP

hydrolysis [62]. The presence of Tet(O) and GTP caused ~50% of the bound Tc release from the ribosomes when the concentration of Tet(O) was 0.5 or 1-fold higher than the 70S ribosomes, and could not release more bound Tc even when the concentration of Tet(O) was increased to 1.5-fold higher than the 70S ribosomes [62]. This suggested that Tet(O) does not act on all Tc binding sites, only the primary Tc binding site [58].

The non-hydrolysable GTP analogue, GMPPNP, was found to have a much greater effect than GTP on the release of bound Tc from the ribosomes in the presence of excess Tet(O) [58, 62]. When the concentration of Tet(O) was 1.5-fold or 3-fold higher than the ribosomes in the presence of GMPPNP, the relative Tc binding to the ribosome decreased to about ~20% [62] or ~10% [58] of that observed in the absence of Tet(O). An excess of Tet(O) over ribosomes was required to release Tc because Tet(O) was unable to hydrolyze GMPPNP, and could not dissociate from the ribosome, and therefore was not available to recycle. Only one round of catalysis released bound Tc by Tet(O) in the presence of GMPPNP. The binding of Tet(O) was irreversible, and prevented Tc from rebinding to the ribosome [58]. Therefore, GTP hydrolysis was not necessary for Tet(O)-mediated Tc release *in vitro* [58, 62]. In contrast to Tet(O), a quite different result was observed in Tet(M), another well-studied RPP which has 77% sequence identity with Tet(O). The presence of GMPPNP could not cause Tet(M) to release bound Tc, which indicated that GTP hydrolysis was necessary for

Tet(M)-mediated Tc release *in vitro* [63, 64].

Protein synthesis was reported to be inhibited by high levels of Tet(O) (1.5-fold greater than ribosome) or Tet(M) in the absence of Tc, by 20% [62] and 40% [63], respectively. The inhibition may be due to Tet(O) (or Tet(M)) and EF-G competition for binding to the ribosome as they share an overlapping binding site on the ribosomes [58, 64, 76] (see section 1.5.7.2).

Tc binds similarly to both the 30S ribosomal subunit and the 70S ribosome, but the ability of Tet(O) to release bound Tc from the 30S subunit and 70S ribosome is different [58]. The release of bound Tc by Tet(O) occurs only in the context of intact 70S ribosomes, and not for isolated 30S subunits. This result indicated that Tet(O)-mediated Tc release is 70S ribosome-dependent.

1.5.4.2 Tet(O) is ribosome-dependent GTPase

Tet(O) is a ribosome-dependent GTPase. GTP hydrolysis is essential for Tet(O) to dissociate from the ribosomes to allow protein synthesis to continue [58, 62]. The binding of Tet(O)·GTP to the 70S ribosomes triggers dissociation of bound Tc, activates Tet(O) GTPase activity, and the subsequent GTP hydrolysis allows the release of Tet(O) from the ribosomes [56, 62]. The affinity (K_m) of Tet(O) (84±5 μM) for GTP was observed to be the same as the K_m of EF-G (80±5 μM), but the catalytic efficiency (k_{cat}/K_m) of Tet(O) was about 2.5-fold lower than that of EF-G [72]. This suggested that the affinity of Tet(O) for GTP is the same

as EF-G, but Tet(O) has a lower efficiency to convert GTP to GDP than EF-G.

1.5.4.3 Other functions

According to a study of the evolutionary origin of RPPs by a composite phylogenetic tree [80], the functions of Tet(O) may not be limited to conferring Tc^R to bacteria. The presence of Tet(O) may also provide ribosomal protection against some unknown chemical substances in the environment.

1.5.5 Conversion of substrate specificity of Tet(O) from GTP to XTP

Hwang & Miller [81] proposed that the GTP-binding consensus motif (N-K-X-**D**) is conserved in most of known GTPases, and the mutation of D to N converts a GTPase into an XTPase. This type of mutation has been proved useful to investigate the functions of many different GTPases in cells [81-84], including $Tet(O)^{D131N}$ [57].

A single amino acid substitution (D to N) at position 131 of Tet(O) was introduced by oligonucleotide site-directed mutagenesis [57]. The D131N mutation greatly reduced the Tet(O) protein's affinity for GTP; however, this mutation dramatically increased its affinity for xanthosine 5'- triphosphate (XTP). As Hwang & Miller [81] illustrated for $EF\text{-}Tu^{D138N}$, mutation of D131 to N disrupted the hydrogen bond (H-bond) acceptor function of D131 by disrupting one key H-bound between D131 and the C2 exocyclic amine of guanine, and

replaced it with an H-bound donor (Figure 1.7). The presence of an H-bond donor opposite the exocyclic amine of GTP produces a repulsive (donor-donor) interaction that would lead to the inability of Tet(O)^{D131N} to accept GTP as a substrate. In contrast, XTP contains an H-bond acceptor at the C2 position (2-carbonyl group of xanthine) which allows forming H-bond with N131. In addition, N128 in Tet(O)^{WT} and Tet(O)^{D131N} directly hydrogen bonds to the 6-carbonyl group of either GTP or XTP (Figure 1.7). Accordingly, GTP is hydrolyzed preferentially by Tet(O)^{WT}, whereas XTP is hydrolyzed preferentially by mutant Tet(O)^{D131N}.

1.5.6 Proposed Mechanism of Tet(O)-mediated Tc^{R}

The precise mechanism of Tet(O)-mediated Tc^{R} is still not clear. A model has been proposed based on cryo-electron microscopy (cryo-EM) reconstructions and dimethyl sulfate (DMS) chemical probing experiments [57, 58, 76]. In this model, Tc binds to the 30S ribosomal subunit when the ribosome is in the POST state (with peptidyl-tRNA in the P-site and deacylated tRNA in the E-site) (Figure 1.8, step ①), and blocks the A-site by inducing the conformational change of the ribosome in the decoding site. This renders the EF-Tu ternary complex (EF-Tu•GTP•aa-tRNA) unable to deliver aa-tRNA to the A-site (Figure 1.8, step ②). Tet(O)•GTP binds to the ribosome by recognizing the Tc-induced conformational change and the open A-site (Figure 1.8, step ③). The interaction of Tet(O)•GTP

with the ribosome triggers a conformational change in the decoding site and causes release of Tc. The binding of Tet(O)•GTP to the ribosome also triggers GTP hydrolysis of Tet(O) and allows Tet(O)•GDP to dissociate from the ribosome. The A-site conformational change still remains, which prefers the binding of aa-tRNA rather than the binding of Tc (Figure 1.8, step ④). The EF-Tu ternary complex delivers aa-tRNA to the A-site. The codon-anticodon matching between mRNA and aa-tRNA triggers GTP hydrolysis of EF-Tu. EF-Tu•GDP is released from the ribosome (Figure 1.8, step ⑤), and protein elongation is restored (Figure 1.8, step ⑥) [57].

1.5.7 Interaction of Tet(O) with the 70S ribosome

The interaction of Tet(O) with the 70S ribosome is essential for Tet(O) to confer Tc^R and restore protein synthesis, so understanding the interaction of Tet(O) with 70S ribosome will provide insight into the mechanism of Tet(O)-mediated Tc^R.

1.5.7.1 Comparison of domain structure of Tet(O) and EF-G interacting with 70S ribosomes

The current structure of Tet(O) and its interaction with the ribosome are mainly derived from cryo-EM reconstructions. Based on 16Å resolution cryo-EM reconstructions, it is proposed that the overall shape of Tet(O) and its interaction with the ribosome are similar to that of EF-G (Figure 1.9) [76]. Both proteins are

composed of 5 domains, and only domain IV interacts differently with the ribosome (Table 1.7). Domain IV in EF-G interacts with helix 69 of 23S rRNA, which reaches into the decoding site of the ribosome and overlaps with the A site-bound aa-tRNA. In contrast, domain IV of Tet(O) interacts with helix 18/ helix 34 of the 16S rRNA, which is close to the primary Tc binding site [30]. This difference in domain IV may determine the different function of the two proteins. Domain IV of EF-G is essential for the translocation reaction in the ribosome [85-87], while domain IV of Tet(O) is critical for Tc release because it interacts with helix 34, a component of the primary Tc binding site [30]. The key functional role of domain IV is also demonstrated by a domain-swapping experiment between Tet(O) and EF-G. After domain IV was swapped between the proteins, Tet(O) lost its ability to release bound Tc and EF-G lost its ability to catalyze the translocation reaction [75]. The other four domains of Tet(O) and EF-G interact similarly with the ribosome. In addition, all domains interact with rRNA, with the exception of domain III, which contacts ribosomal protein S12 (Table 1.7) [76].

1.5.7.2 Tet(O) and EF-G share the similar binding site on the ribosome

Studying the interaction of Tet(O) or EF-G with the ribosome by cryo-EM reconstructions also demonstrated that the binding sites of these two GTPases on the ribosome overlap, and are located at the interface of the ribosomal subunit

near the A-site, at the base of the L7/L12 stalk [56, 57, 76]. The binding site of Tet(O) does not overlap the primary Tc binding site, which suggests that Tet(O) does not directly interfere with Tc binding, but rather promotes the release of bound Tc by allosterically distorting the Tc-binding site [76].

The binding of Tet(O) or EF-G to the ribosome induces different conformational changes on the ribosome [76]. This corresponds to their different functions and binding to different functional states of the ribosome within the elongation cycle. EF-G prefers to bind the PRE state ribosome (with the peptidyl-tRNA in the A-site and deacylated-tRNA in the P-site), while Tet(O) prefers to bind the POST state ribosome (with peptidyl-tRNA in the P-site and deacylated tRNA in the E-site) [58, 76]. Cryo-EM also revealed that when EF-G binds to the ribosome, it induces the ribosome to undergo a ratchet-like subunit rearrangement in which the subunits twist relative to one another [76, 88]. The rearrangement facilitates the tRNA translocation reaction (see section 1.2.3.1) and stimulates GTP hydrolysis of EF-G. In contrast, the binding of Tet(O) to the ribosome does not cause detectable rearrangement between the two ribosomal subunits with the exception of the extension of the L7/L12 stalk, which may contribute to the conformational change in the decoding site and subsequent Tc release [76].

1.5.7.3 Interaction of Tet(O) with 70S ribosomes

The interaction of Tet(O) with 70S ribosomes was further investigated with

dimethyl sulfate (DMS) footprinting because it can detect subtle architectural changes which may not be noticed by cryo-EM [58]. As a chemical probe, DMS modifies N1 of adenine and N3 of cytosine by donating a methyl group (Figure 1.10), which can be detected by primer extension analysis [89].

When Tc is absent, the binding of Tet(O) to the 70S ribosomes changes the DMS reactivity of only two bases of the 16S rRNA (Figure 1.10): 1) at the base of helix 34 (h34), Tet(O) protects C1214 from DMS modification; and 2) within helix 44 (h44), Tet(O) enhances DMS modification of A1408 [58]. The two bases are located in the decoding site: h34 (C1214) near the primary Tc binding site, whereas h44 (A1408) is in a region away from the Tet(O) binding site visualized by cryo-EM [76]. This suggests that Tet(O) interacts with h34 to dislodge Tc from the primary binding site, and induces long-range conformational changes in h44, which alters the decoding site [58].

When Tc is present, the interaction of Tc with 16S rRNA results in the protection of A892 (part of the secondary binding site) and enhancement of C1054 (part of the primary binding site) towards DMS modification [90]. However, the binding of Tet(O) to the 70S ribosomes in the presence of Tc inhibits the enhancement of C1054 by Tc towards DMS modification, but does not affect the protection of A892 from DMS modification [58] (Figure 1.11). This demonstrates that the function of Tet(O) is to release Tc from the primary binding site but not from the secondary binding site, and the primary binding site is

essential for the action of Tc to inhibit protein synthesis [58].

1.6 Significance of studying mechanism of Tet(O)-mediated Tc^R

Understanding Tet(O)-mediated Tc^R will help to further clarify the mechanisms of RPP-mediated Tc^R in general because it has been assumed that all 11 RPPs have the same mechanism for mediating Tc^R [16, 54].

The long term goal of studying mechanisms of Tet(O)-mediated Tc^R is to develop new generation antibiotics to overcome the mechanisms of resistance and thereby offer new strategies for the treatment of serious infectious diseases. Developing derivatives from known antibiotics is easier, less costly, and safer for clinical use than developing novel antibiotics. The improved understanding of Tc^R mechanisms likely provided opportunities for the recent discovery of a new generation of Tcs, tigecycline (glycylcycline) [91]. Tigecycline was derived from the second-generation Tc, minocycline, and was licensed by the US Food and Drug Administration (FDA) in June 2005 for intravenous use in adults [92]. The action of tigecycline is similar to earlier Tcs, but the binding affinity of tigecycline to 70S ribosomes is 5-fold higher than the binding affinity of earlier Tcs to 70S ribosomes. As a consequence, tigecycline overcomes the two major efflux pump and ribosomal protection mechanisms of Tc^R [93]. In addition, tigecycline also has good efficacy against multidrug-resistant gram-negative and gram-positive bacteria, including superbugs such as MRSA, and

vancomycin-resistant *Enterococci* (VRE). Accordingly, tigecycline has been used as the last resort to treat serious infections in Intensive Care Units (ICU) [92]. However, within 2 years, tigecycline resistance was reported in *Acinetobacter baumannii*, and *Enterococcus faecalis*, isolated from ICU patients [93-97]. The rapid development of tigecycline resistance impresses the urgency of the need to find alternative effective therapies. Investigation of the mechanisms of Tet(O)-mediated Tc^R may provide information for future development of new generation antibiotics to deal with resistant infections.

1.7 Rationale of this study

Tet(O) is an EF-G like GTPase, and binds to a similar site on the 70S ribosome as EF-G. The binding of Tet(O)•GTP to the 70S ribosome is essential for the release of bound Tc and activation of GTP hydrolysis of Tet(O). Studying the interaction of Tet(O) and EF-G with 70S ribosomes is important to further understand the mechanism of Tet(O)-mediated Tc^R. To date no studies have reported whether Tet(O) and EF-G compete for binding to the 70S ribosomes, and whether the presence of EF-G interferes with Tet(O)-mediated Tc release.

In this thesis, experiments were carried out in *E. coli* instead of *C. jejuni* for several reasons. First, *E. coli* is well characterized and has been used as a genetic engineering expression host for many years. Using *E. coli* BL21(DE3) as an expression host would ensure sufficient recombinant Tet(O) protein expression in

the presence of isopropylthio-β-D-galactoside (IPTG). Second, *E. coli* grows rapidly under aerobic conditions, while *C. jejuni* requires fastidious culture conditions, as it is strictly microaerophilic (5-10% ambient oxygen), and grows slowly. It would be very difficult to produce enough Tet(O) protein to carry out the study using *C. jejuni*. Third, the engineered *E. coli* host for protein expression is a lab-adapted strain and is harmless to people. In contrast, *C. jejuni* is a biosafety level 2 pathogen and requires special safety precautions for handling in the lab.

To confirm that *E. coli* could be the host bacteria for the experiments performed in this thesis, it was necessary to demonstrate that the *C. jejuni tet(O)* gene could be transformed into *E. coli* and confer Tc^R to a level similar to that observed in *C. jejuni* as reported by others [67].

Three states of 70S ribosomes are obtained during their isolation from *E. coli*: free 70S ribosomes (devoid of mRNA and tRNA), 70S ribosome-tRNA complexes (mRNA-programmed ribosomes with tRNA bound in the ribosomal P-, A- or E-site), and free ribosomal subunits (50S, 30S) [98-100]. Free 70S ribosomes are not present *in vivo* because subunits remain separate unless they are actively involved transcribing mRNA [101]. In this thesis, "vacant" 70S ribosomes will be used to represent free 70S ribosomes, which are tightly coupled 70S ribosomes that resist dissociation into subunits during low-speed centrifugation in the presence of 5-6 mM magnesium ions [102]. The "loaded"

70S ribosomes will be used to represent the mRNA-programmed 70S ribosomes with tRNAs occupied in the ribosomal P- and A-site (PRE state). Previous studies used only vacant 70S ribosomes or 30S ribosomal subunits to evaluate the ability of Tet(O) to release bound Tc from the 70S ribosomes *in vitro* [58, 62, 72]. In order to establish the differences of Tet(O)-mediated Tc release *in vitro* in different ribosome states, this thesis will compare loaded 70S ribosomes with vacant 70S ribosomes.

Both Tet(O) and EF-G are ribosome-dependent GTPases, and bind to the same site on the 70S ribosome. When both Tet(O) and EF-G are present in the same reaction, their GTPase activities cannot be distinguished from each other. A change in substrate specificity for one protein would distinguish the GTPase activities of the two proteins. Accordingly, the Tet(O) mutant, $Tet(O)^{D131N}$, was constructed by changing a single amino acid in position 131 from aspartate (GAC) to asparagine (AAT) [57]. As a result, the substrate specificity of the $Tet(O)^{D131N}$ enzyme was changed from GTP to XTP (see section 1.5.5). The constructed $Tet(O)^{D131N}$ should possess all of the functional properties of the $Tet(O)^{WT}$ except for the enzyme activity which is an XTPase instead of a GTPase. It was necessary to demonstrate that the $Tet(O)^{D131N}$ construct could not hydrolyze GTP, and only releases bound Tc from the 70S ribosomes in the presence of XTP, but not GTP. Once these properties were confirmed, experiments were performed to determine whether Tet(O) GTP hydrolysis affects GTP hydrolysis by EF-G as an indirect

measurement of their binding to 70S ribosomes.

1.8 Hypothesis and Thesis Objectives

This thesis tested the hypothesis that EF-G decreases Tet(O)-mediated Tc release from the ribosome by competing with Tet(O) for binding to the 70S ribosome.

The following series of objectives provided a systematic approach to test the hypothesis:

1) To determine the Tc susceptibility phenotype of *E. coli* transformed with the *C. jejuni tet(O)* gene (see section 3.1.1)
2) To determine kinetics of Tet(O)-mediated Tc release *in vitro*, which consists of three specific aims:
    i) To overexpress and purify Tet(O), and EF-G (see section 3.2);
    ii) To prepare vacant and loaded 70S ribosome complexes (see section 3.3);
    iii) To determine whether A-site occupation by aa-tRNA affects Tc release by performing Tc binding assays with different 70S ribosome complexes (vacant or loaded) in the presence of Tet(O) vs EF-G (see section 3.4).
3) To confirm the phenotype of Tet(O)^{D131N}, which consists of three specific aims:

i) To determine the Tc susceptibility phenotype of *E. coli* transformed with the *tet(O)*^{D131N} gene (see section 3.1.2);

ii) To determine Tet(O)^{D131N}-mediated Tc release in the presence of GTP or XTP (see section 3.4.3);

iii) To confirm the absence of GTP hydrolysis by Tet(O)^{D131N} (see section 3.5.2)

4) To determine kinetics of GTP hydrolysis of EF-G in the absence and presence of Tet(O)^{D131N} as an indirect measure of the binding of EF-G and Tet(O) to 70S ribosomes (see section 3.5.4)

Table 1.1 Number of *Campylobacter, Salmonella, Shigella,* verotoxigenic *Escherichia coli* infection cases by year in Canada as reported to the National Notifiable Disease Summary program (NDRS) during 2000 to 2004 [9]

	2000	**2001**	**2002**	**2003**	**2004**	**Average**
Campylobacteriosis	**12,641**	**11,886**	**11,543**	**10,027**	**9,600**	**11,139**
Salmonellosis	5,780	6,177	6,092	5,185	5,213	5,689
Shigellosis	1,156	945	1,355	906	720	1,016
Verotoxigenic *E. coli* infections	3,011	1,334	1,243	1,083	1,103	1,555

Table 1.2 Incidence of Tc^R *C. jejuni* isolates in food-producing animals in Canada

Source	% of Tc^R *C. jejuni* isolates		Reference
	Alberta	Ontario	
Poultry	69%	55-69%	40, 43
Beef cattle	50-64%	43%	41, 44
Swine	35%	44%	42, 44

Table 1.3 Distribution of *tet* genes encoding RPPs and other Tc^R determinants among diverse bacteria

RPP Genes											Efflux Genes	Enzymatic Inactive Genes	Unknown Genes	Genera[c]
Group I, *tet*-					Group II		Group III, *tet*-							
(M)	*(O)*	*(W)*	*(S)*	*(32)*	*tetB(P)*[a]	*Otr(A)*	*(T)*	*(Q)*	*(36)*	*Tet*[b]				
+	-	-	-	-	-	-	-	-	-	-	-	-	-	*Arthrobacter*
+	-	-	-	-	-	-	-	-	-	-	-	-	-	*Brachybacterium*
+	-	-	-	-	-	-	-	-	-	-	-	-	-	*Eikenella*, *Kingella*
+	-	-	-	-	-	-	-	-	-	-	-	-	-	*Ralstonia*
+	-	-	-	-	-	-	-	-	-	-	-	-	-	*Pseudoalteromona*
+	-	-	-	-	-	-	-	-	-	-	-	-	-	*Abiotrophia*
+	-	-	-	-	-	-	-	-	-	-	-	-	-	*Afipia*, *Bacterionema*
+	-	-	-	-	-	-	-	-	-	-	-	-	-	*Catenibacterium*[d]
+	-	-	-	-	-	-	-	-	-	-	-	-	-	*Mycoplasma*[e]
+	-	-	-	-	-	-	-	-	-	-	-	-	-	*Erysipelothrix*
+	-	-	-	-	-	-	-	-	-	-	-	-	-	*Granulicatella*
+	-	-	-	-	-	-	-	-	-	-	-	-	-	*Ureaplasma*[e]
+	-	-	-	-	-	-	-	-	-	-	*tet(B)*	-	-	*Pantoea*
+	-	-	-	-	-	-	-	-	-	-	*tet(L)*	-	-	*Kurthia*
+	-	-	-	-	-	-	-	-	-	-	*tet(42)*	-	-	*Microbacterium*
+	-	-	-	-	-	-	-	-	-	-	*tet(A), (D)*	-	-	*Edwardsiella*
+	-	-	-	-	-	-	-	-	-	-	*tet(B), (K)*	-	-	*Haemophilus*
+	-	-	-	-	-	-	-	-	-	-	*tet(L), (42)*	-	-	*Paenibacillus*
+	-	-	-	-	-	-	-	-	-	-	*tet(Z), (33)*	-	-	*Corynebacterium*

RPP Genes											Efflux Genes	Enzymatic Inactive Genes	Unknown Genes	Genera[c]
Group I, *tet*-					Group II		Group III, *tet*-							
(M)	*(O)*	*(W)*	*(S)*	*(32)*	*tetB(P)*[a]	*Otr(A)*	*(T)*	*(Q)*	*(36)*	*Tet*[b]				
+	-	-	-	-	-	-	-	-	-	-	*tet(A), (E), (L)*	-	-	*Flavobacterium*
+	-	-	-	-	-	-	-	-	-	-	*tet(B), (D), (Y)*	-	-	*Photobacterium*
+	-	-	-	-	-	-	-	-	-	-	*tet(A), (B), (C), (D)*	-	-	*Klebsiella*
+	-	-	-	-	-	-	-	-	-	-	*tet(A), (B), (C), (D), (L)*	-	-	*Enterobacter*
+	-	-	-	-	-	-	-	-	-	-	*tet(B), (D), (H), (G), (L)*	-	-	*Pasteurella*
+	-	-	-	-	-	-	-	-	-	-	*tet(A), (B), (G), (H), (L), (39)*	-	-	*Acinetobacter*
+	-	-	-	-	-	-	-	-	-	-	*tet(A), (B), (C), (E), (41)*	*tet(34)*	-	*Serratia*
+	-	-	-	-	-	-	-	-	-	-	*tet(A), (B), (C), (D), (E), (31)*	*tet(34)*	-	*Aeromonas*
+	-	-	-	-	-	-	-	-	-	-	*tet(A), (B), (C), (E), (G), (L), (42)*	*tet(34)*	-	*Pseudomonas*
+	-	-	-	-	-	-	-	-	-	-	*tet(A), (B), (C), (D), (E), (G), (35)*	*tet(34)*	-	*Vibrio*
+	-	-	-	-	-	-	-	-	-	-	*tet(A), (B), (C), (D), (E), (G), (L), (J), (Y)*	-	-	*Escherichia*
+	+	-	-	-	-	-	-	-	-	-	-	-	-	***Aerococcus, Gemella***
+	-	-	-	-	-	-	-	+	-	-	-	-	-	*Gardnerella*
+	-	-	+	-	-	-	-	-	-	-	-	-	-	*Lactococcus*
+	-	+	-	-	-	-	-	+	-		-	-	-	*Prevotella*[d], *Selenomonas*[d]
+	+	+	-	-	-	-	-	+	-	-	*Tet(B)*	-	-	***Neisseria***
+	+	-	-	+	-	-	-	+	-	-	*Tet(K)*	-	-	*Eubacterium*[d]
+	-	+	-	-	-	-	-	-	-	-	*Tet(L)*	-	-	*Actinomyces*

RPP Genes											Efflux Genes	Enzymatic Inactive Genes	Unknown Genes	Genera[c]
Group I, *tet*-					Group II		Group III, *tet*-							
(M)	*(O)*	*(W)*	*(S)*	*(32)*	*tetB(P)*[a]	*Otr(A)*	*(T)*	*(Q)*	*(36)*	*Tet*[b]				
+	+	+	-	-	-	-	-	-	-	-	*Tet (L)*	-	-	***Bifidobacterium***[d,h]
+	-	+	+	-	-	-	-	+	-	-	*Tet (A), (L)*	-	-	*Veillonella*[d]
+	+	+	-	-	-	-	-	+	-	-	*Tet (G), (L)*	-	-	***Fusobacterium***[d]
+	-	-	+	-	-	-	-	-	-	-	*Tet(K), (L)*	-	-	*Listeria*
+	-	+	-	-	-	-	-	-	-	-	*Tet(K), (L), (42)*	-	-	*Bacillus*
+	+	-	-	-	-	-	-	+	-	-	*Tet(K), (L)*	-	-	***Peptostreptococcus***[d]
+	+	-	+	+	-	-	-	-	-	-	*Tet(K), (L)*	-	*tet(U)*	***Enterococcus***
+	+	+	-	+	-	-	+	+	-	-	*Tet(K), (L)*	-	*tet(U)*	***Streptococcus***
+	+	+	-	+	+	-	-	+	+	-	*Tet(K), (L), A(P), (40)*	-	-	***Clostridium***[d,h]
+	+	+	+	-	-	-	-	-	-	-	*Tet(K), (L), (38), (42)*	-	*tet(U)*	***Staphylococcus***
+	+	+	+	-	-	-	-	+	+	-	*Tet(K), (L), (Z)*	-	-	***Lactobacillus***[h]
+	-	-	-	-	-	+	-	-	-	-	*Tet(K), (L), (V), Otr(B)*	-	-	*Mycobacterium*[f]
+	-	+	-	-	-	+	-	-	-	+	*Tet(K), (L), (B), (C), tcr*[b]	-	-	*Streptomyces*[g]
+	-	+	-	-	-	-	-	+	+	-	-	*tet(X)*	-	*Bacteroides*[d]
-	+	-	-	-	-	-	-	-	-	-	-	-	-	***Campylobacter***
-	+	-	-	-	-	-	-	-	-	-	-	-	-	***Psychrobacter***
-	-	-	-	-	-	-	-	+	-	-	-	-	-	*Capnocytophaga*[d]
-	-	-	-	-	-	-	-	+	-	-	-	-	-	*Ruminococcus*[d]
-	-	+	-	-	-	-	-	-	-	-	-	-	-	*Acidaminococcus*[d]
-	-	+	-	-	-	-	-	-	-	-	-	-	-	*Roseburia*

RPP Genes											Efflux Genes	Enzymatic Inactive Genes	Unknown Genes	Genera[c]
Group I, *tet*-					Group II		Group III, *tet*-							
(M)	*(O)*	*(W)*	*(S)*	*(32)*	*tetB(P)*[a]	*Otr(A)*	*(T)*	*(Q)*	*(36)*	*Tet*[b]				
-	-	+	-	-	-	-	-	-	-	-	-	-	-	*Arcanobacterium*
-	-	+	-	-	-	-	-	+	-	-	-	-	-	*Mitsuokella*[d]
-	-	+	-	-	-	-	-	+	-	-	-	-	-	*Porphyromonas*[d]
-	-	+	-	-	-	-	-	+	-	-	-	-	-	*Subdolgranulum*[d]
-	+	-	-	-	-	-	-	+	-	-	-	-	-	***Anaerovibrio***[d]
-	+	-	-	-	-	-	-	+	-	-	-	-	-	***Mobiluncus***[d]
-	+	+	-	-	-	-	-	-	-	-	-	-	-	***Butyrivibrio***[d]
-	+	+	-	-	-	-	-	-	-	-	-	-	-	***Megasphaera***[d,h]
-	+	-	-	-	-	-	-	-	-	-	*tet*(B), *tet*(H), *tet*(L)	-	-	***Actinobacillus***

[a] *tetB*(P) is not found alone, which is one part of *tet*(P). Another part tet*A*(P) of tet(P) encodes for efflux pump protein.

[b] *tet* and *tcr* have not been given number designations

[c] Shaded genera represent gram-negative bacteria; un-shaded genera represent gram-positive bacteria, *Mycobacterium*, *Mycoplasma*, *Nocardia*, *Streptomyces* and *Ureaplasma*

[d] Anaerobic genus

[e] Cell-wall-free bacteria with a Gram-positive metabolism

[f] Acid-fast bacteria

[g] Multicellular bacteria

[h] Mosaic ribosomal protection genes (O/W/32)

The bold genera possess *tet(O)* gene.

Data on *tet* genes encoding RPPs and other Tc^R determinants, as well as their distribution obtained from the website of Dr. Roberts MC. at http://faculty.washington.edu/marilynr/, which is updated twice per year [51].

Table 1.4 Classification of RPPs [16, 49, 54]

Group	RPPs	aa Sequence Identity
I	Tet(M), **Tet(O)**, Tet(W), Tet(S), Tet(32)	67%-77%
II	Otr(A), TetB(P)	36%
III	Tet(T), Tet(Q), Tet(36)	49%-60%
Unknown	Tet	-

Table 1.5 Amino acid sequence identity of RPPs compared with Tet(O)

RPPs	aa	Sequence identity	Host	Genbank No.
Tet(O)	639	100%	*Camylobacter jejuni*	M18896
Tet(M)	639	77%	*Enterococcus faecalis*	X04388
Tet(S)	641	72%	*Listeria monocytogenes*	L09756
Tet(32)	639	70%	*Streptococcus salivarius*	DQ647324
Tet(W)	639	67%	*Butyrivibrio fibrisolvens*	AJ222769
Tet(T)	651	44%	*Streptococcus pyogenes*	L42544
Tet(36)	640	41%	*Bacteroides coprosuis*	AJ514254
TetB(P)	652	40%	*Clostridium perfringens*	L20800
Tet(Q)	641	38%	*Bacteroides thetaiotaomicron*	X58717
Otr(A)	663	31%	*Streptomyces rimosus*	X53401

Amino acid sequence alignment was performed by DNAMAN software (Lynnon Corporation, Quebec, Canada).

Table 1.6 Similarities between Tet(O) and elongation factors

G protein	MW (kDa)	aa sequence identity to Tet(O) G domain	Essential aa for GTPase	Structure domains	Protein:70S ribosome
Tet(O)	72.5	-	**A10**-H-V-D-A-G-K16	5	≤ 1:1
EF-G	77.5	51%	**A17**-H-I-D-A-G-K23	5	~ 1:1
EF-Tu	43	31%	**G18**-H-V-D-H-G-K24	3	≥ 10:1

Table 1.7 Comparison of Tet(O) and EF-G interactions with the ribosome by cryo-EM reconstruction [76]

Domains	Tet(O)	EF-G
G	H95	H95
II	h5	h5
III	S12	S12
IV	**h18/h34**	**H69**
V	H43/H44	H43/H44

A lowercase h refers to a helix within the 16S rRNA, whereas an uppercase H refers to a helix within the 23S rRNA.

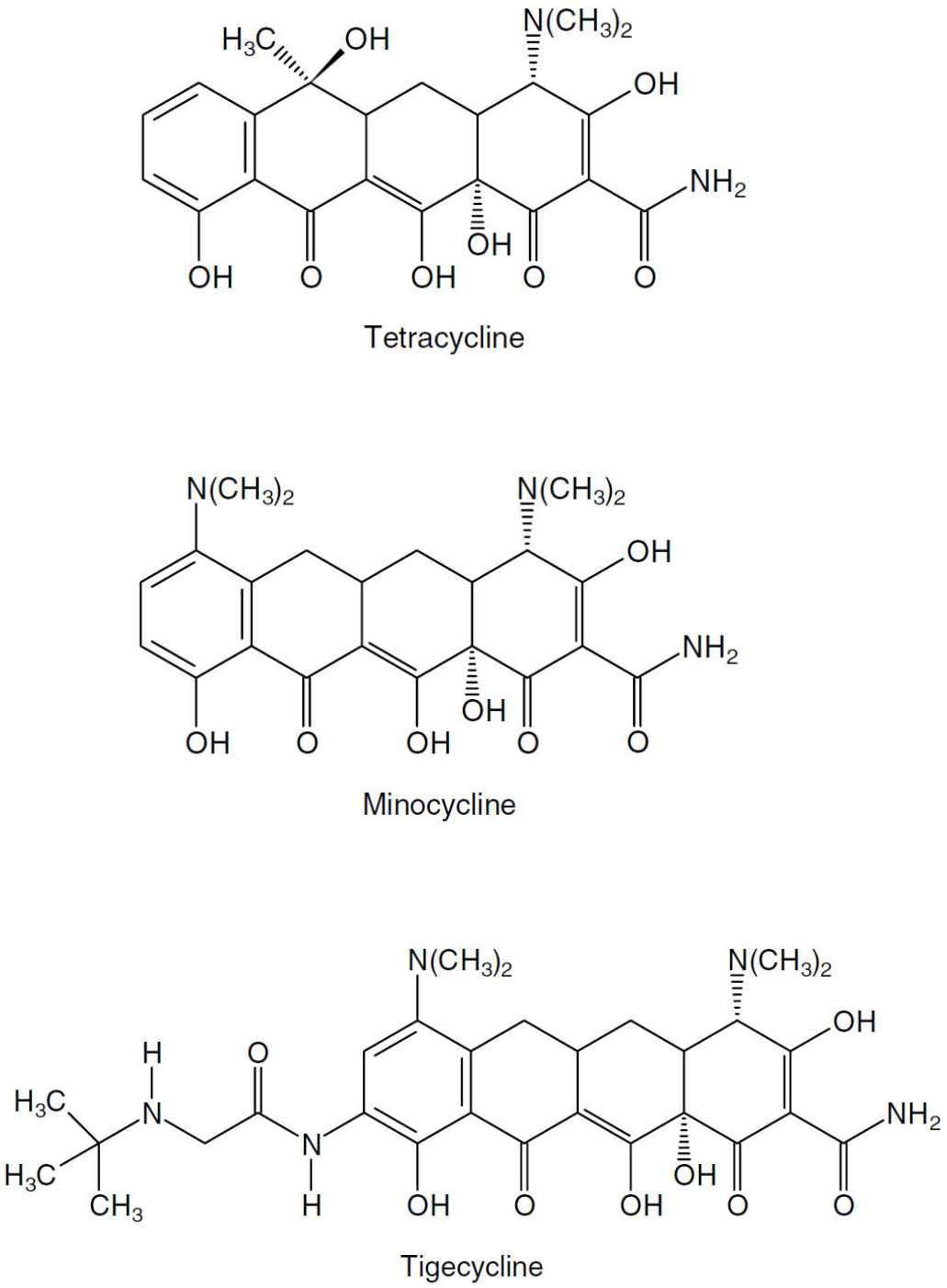

Figure 1.1 Chemical structures of tetracyclines [16]

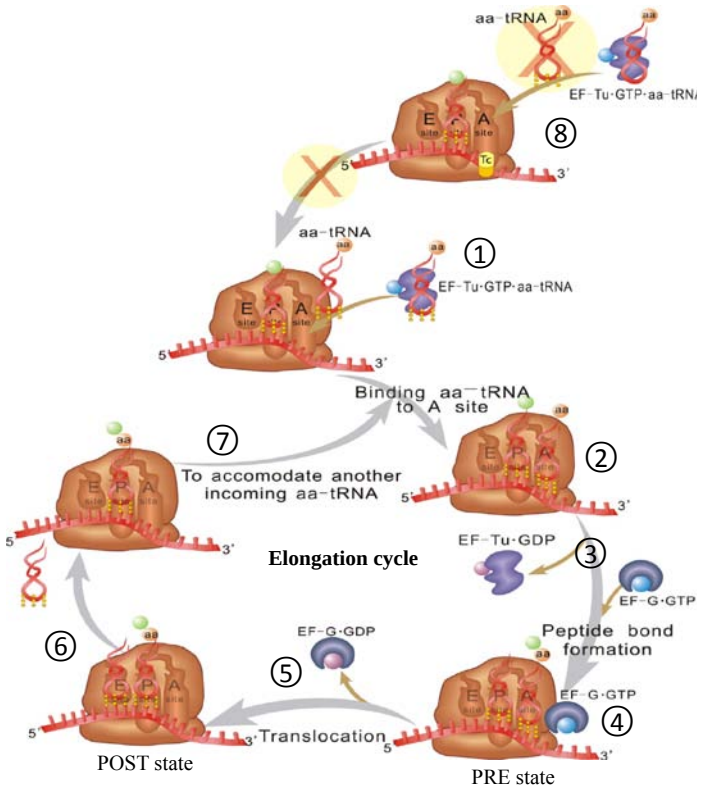

Figure 1.2 Action of tetracycline on elongation cycle of protein synthesis

① EF-Tu ternary complex (EF-Tu•GTP•aa-tRNA) carries and delivers aa-tRNA to the ribosomal A-site.

② Cognate codon-anticodon matching occurs between mRNA and aa-tRNA on the ribosomal A-site.

③ Cognate decoding on the ribosomal A-site triggers GTP hydrolysis of EF-Tu, and EF-Tu•GDP leaves the ribosome.

④ Peptide bond is formed between the amino acids on the ribosomal A-site and P-site, then EF-G•GTP binds to the PRE state-ribosome (a peptidyl-tRNA in the ribosomal A-site and deacylated tRNA in the ribosomal P-site).

⑤ EF-G•GTP catalyzes the translocation reaction following GTP hydrolysis, and EF-G•GDP leaves the ribosome. The ribosome changes from the PRE state to POST state (the peptidyl-tRNA and the deacylated tRNA translocate from the ribosomal A- and P-site to the ribosomal P- and E-site).

⑥ The deacylated tRNA leaves the ribosome from the ribosomal E-site.

⑦ The ribosomal A-site is empty to accommodate another incoming cognate aa-tRNA.

⑧ When tetracycline (Tc) is present, it binds to the 30S ribosomal subunit and prevents EF-Tu ternary complex from delivering aa-tRNA to the ribosomal A-site; thus interrupts protein elongation cycle and stops protein synthesis.

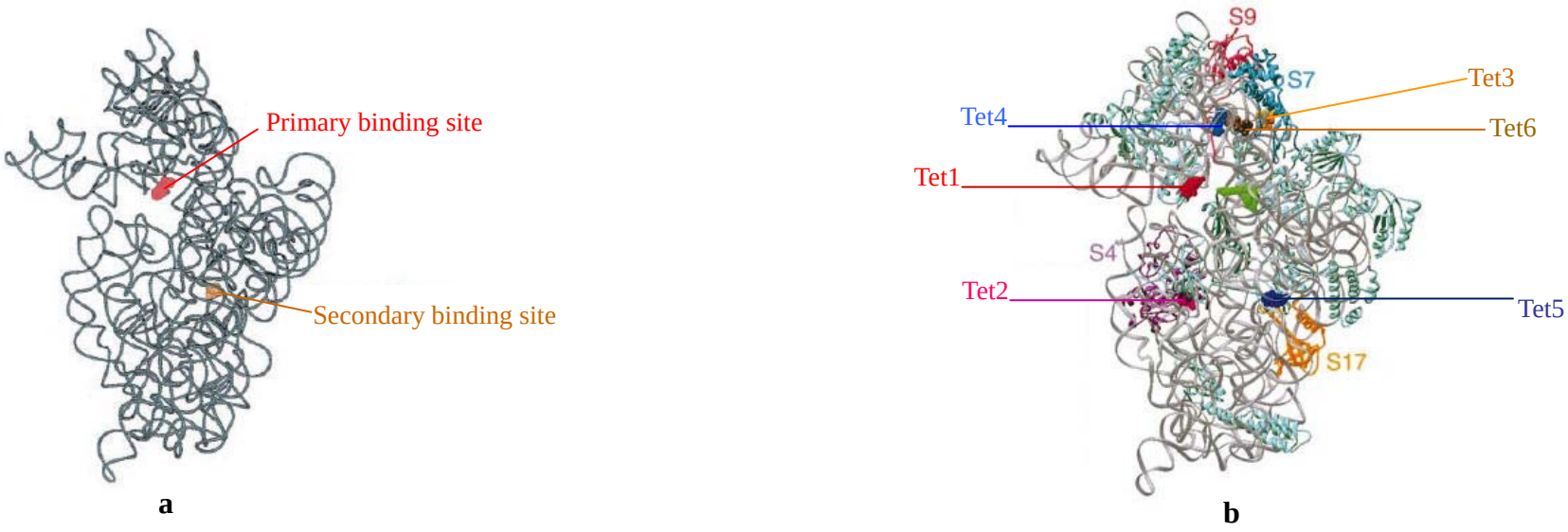

Figure 1.3 Ribosomal binding sites of tetracycline [56]

a. Two ribosomal binding sites of tetracycline (primary binding site and secondary binding site) on the 30S ribosomal subunit were proposed by Brodersen *et al.* [30] using X-ray crystallography at 3.3-3.4Å.

b. Six ribosomal binding sites of tetracycline on the 30S ribosomal subunit were proposed by Pioletti *et al.* [31] using X-ray crystallography at 3.2Å. Tet1: primary binding site, Tet2-6: secondary binding sites

Note: This figure was reproduced with permission from the publisher.

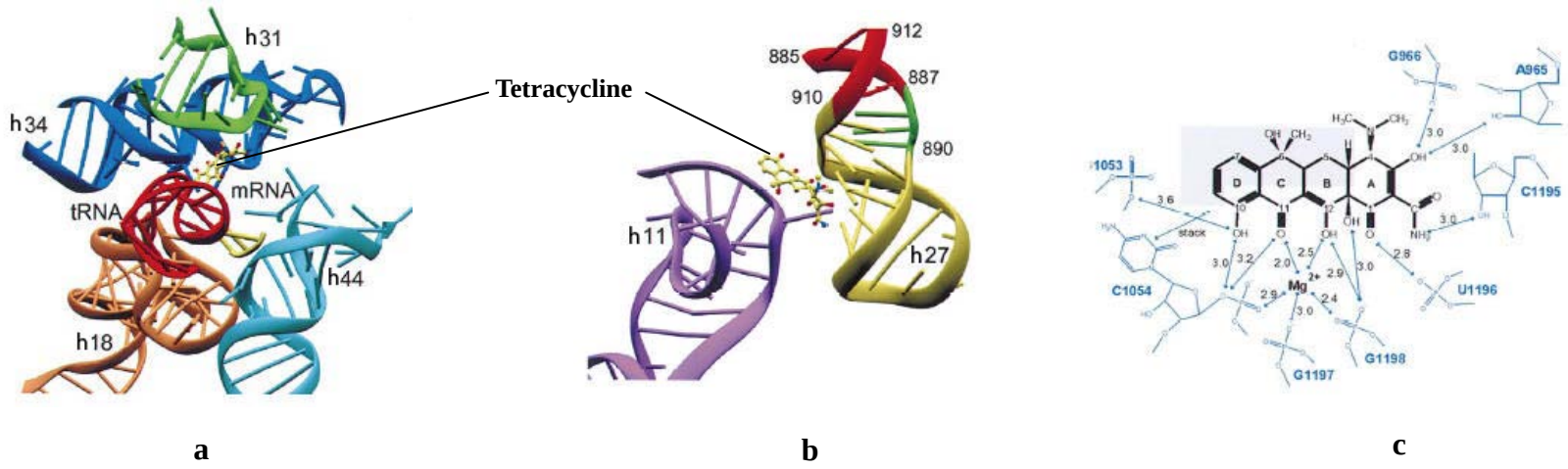

Figure 1.4 Structures of tetracycline binding sites in the 16S rRNA [30]

a. The primary tetracycline binding site

b. The secondary tetracycline binding site

c. The interaction of tetracycline with 16S rRNA and Mg^{2+}

Note: This figure was reproduced with permission from the publisher.

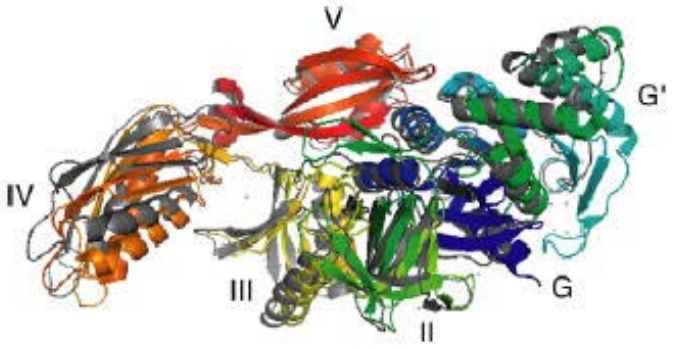

Figure 1.5 Homology-modeled structure of Tet(O) with EF-G [75]
The domains of *C. jejuni* Tet(O) (color-coded) were superimposed onto the known structure of *Thermus thermophilus* EF-G (gray).

Note: This figure was reproduced with permission from the publisher.

Figure 1.6 Amino acid sequence alignment of G domains of Tet(O) vs. elongation factors

The sequence of Tet(O) is from *C. jejuni*, Genbank No. M18896. EF-G (*fus*A) and EF-Tu (*tuf*A) are from *E. coli*, Genbank No. NC000913, NC007946. Alignment was performed by DNAMAN software (Lynnon Corporation, Quebec, Canada).

Underlined in red is the motif N-K-X-D which is conserved in most known GTPases [81].

* The mutation of D to N converts a GTPase into an XTPase, as evidenced by EF-Tu^{D138N} [81] and Tet(O)^{D131N} [57].

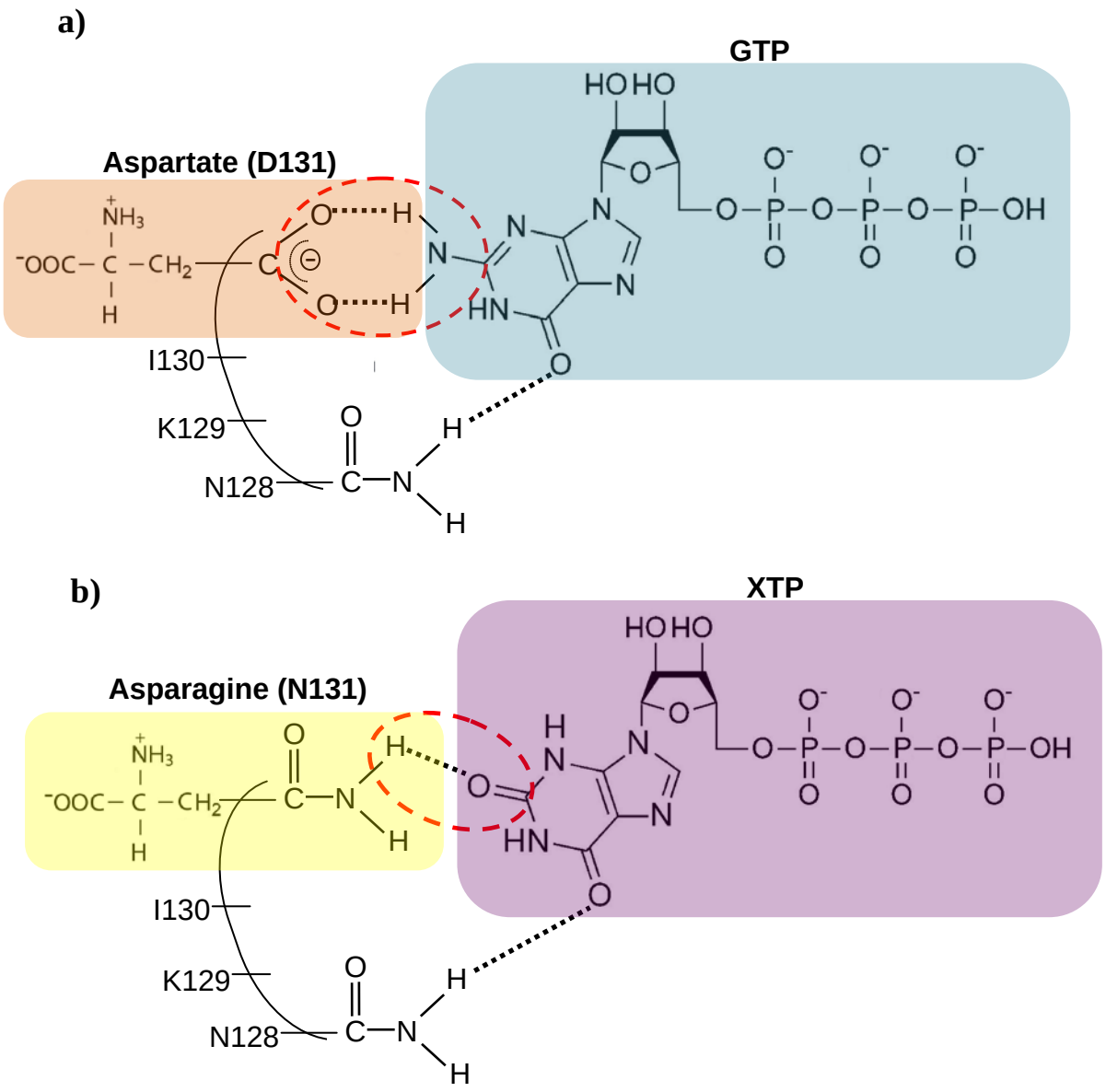

Figure 1.7 Interactions between purine ring of GTP/XTP and amino acid at position 131 of Tet(O)

Hydrogen bonding interactions (red hyphenated circles) between (a) guanine of GTP (shaded in blue) and Tet(O)^{WT} D131 (shaded in pink), and (b) xanthine of XTP (shaded in purple) and Tet(O)^{D131N} N131(shaded in yellow).
Concept based on similar interactions described for EF-Tu^{D138N} [81]

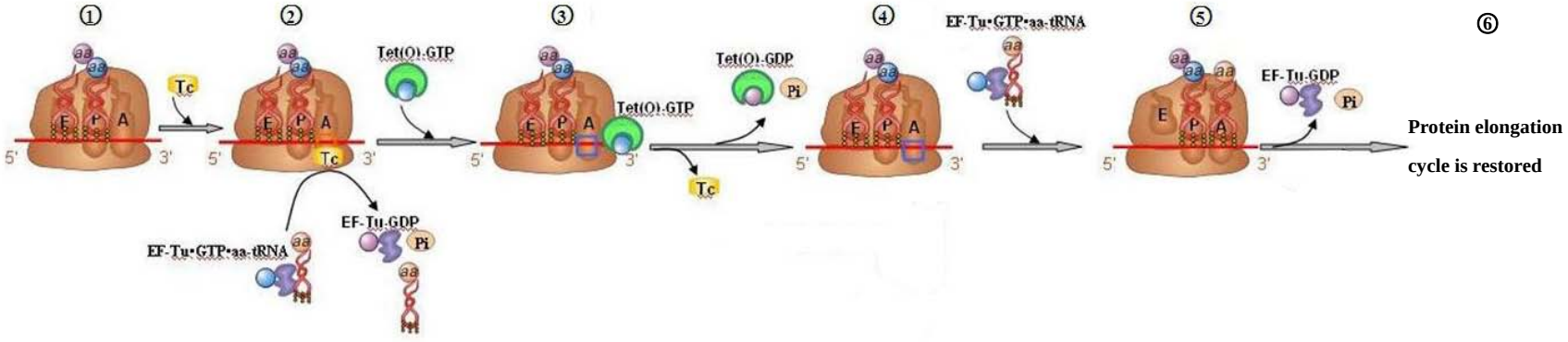

Figure 1.8 A model of Tet(O)-mediated Tc^R (modified from [57])

① The 70S ribosome is in the POST state with peptidyl-tRNA in the P-site and deacylated tRNA in the E-site.

② Tc binds to the 30S ribosomal A-site and causes a conformational change in the decoding site (indicated by a pink box line). The conformational change prevents EF-Tu ternary complex (EF-Tu·GTP·aa-tRNA) from delivering aa-tRNA to the A-site.

③ Tet(O)·GTP binds to the Tc-blocked ribosome by recognizing the conformational change, and triggers the release of the bound Tc by changing the conformation of the decoding site (indicated by a blue box line). Then Tet(O)·GDP is dissociated from the ribosome by GTP hydrolysis.

④ The A-site maintains the conformational change (indicated by a blue box line), which disfavors Tc re-binding, but favors aa-tRNA binding.

⑤ EF-Tu ternary complex delivers aa-tRNA to the A-site. The codon-anticodon matching in the decoding site triggers GTP hydrolysis of EF-Tu, and EF-Tu·GDP is released from the ribosome.

⑥ The protein elongation cycle is restored.

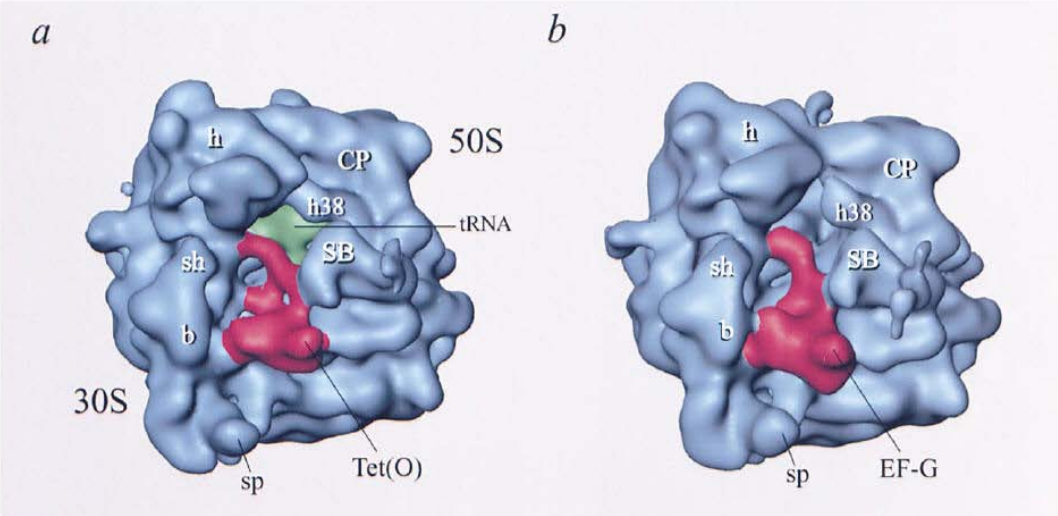

Figure 1.9 Location of Tet(O) or EF-G on the 70S ribosome by cryo-EM reconstructions [76]

a) Tet(O)•GTPγS (noncleavable GTP analog) bound to *E. coli*-70S ribosome with fMet-tRNA in the P site.

b) EF-G•GMPPCP (noncleavable GTP analog) bound to *E. coli*-70S ribosome.

Tet(O) and EF-G are shown in red, and the tRNA is shown in green. The view is from the L7/L12 site. Small subunit: h – head, b – body, sh – shoulder, sp – spur. Large subunit: CP – central protuberance, SB – stalk base, h38 – helix 38 of 23S rRNA.

Note: This figure was reproduced with permission from the publisher.

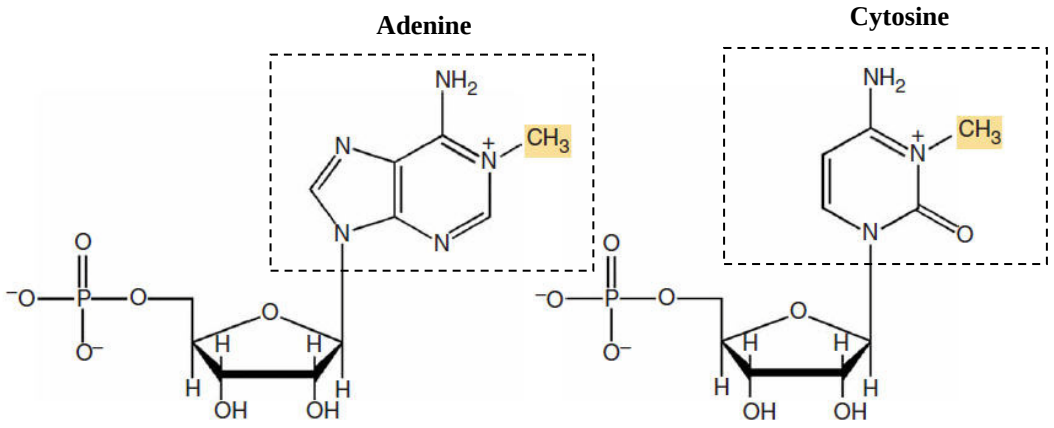

Figure 1.10 DMS Modification by methylation at N1 of Adenine and N3 of Cytosine (modified from [89])

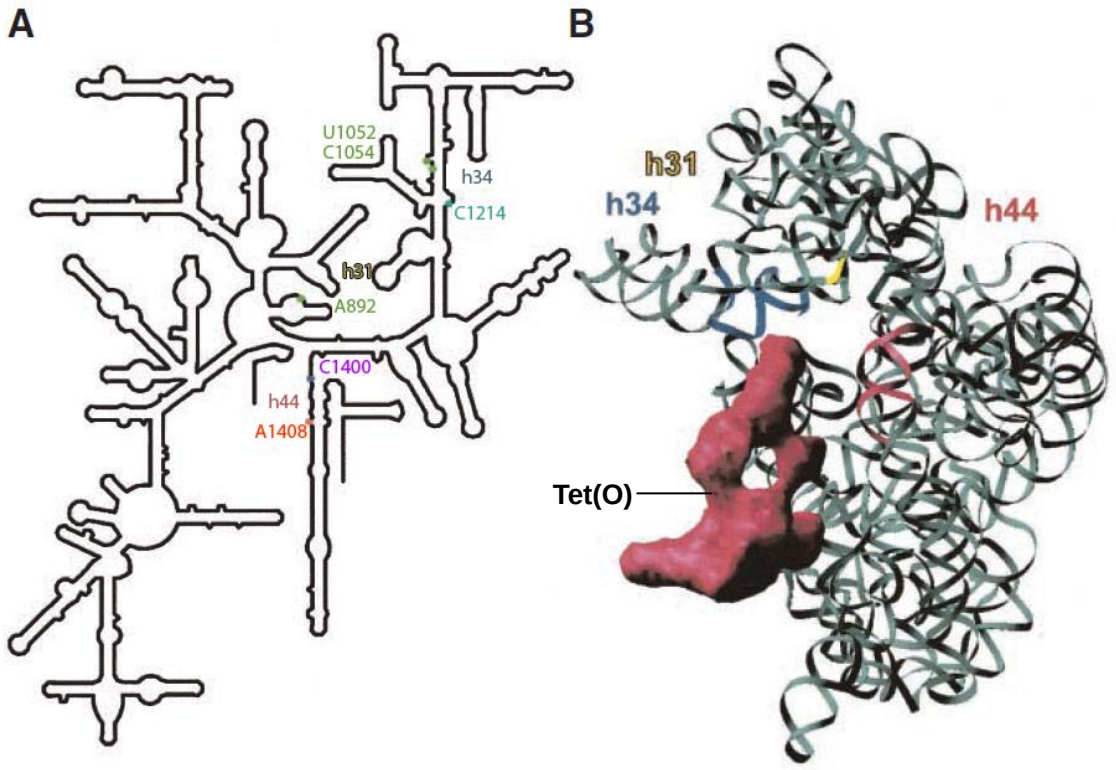

Figure 1.11 rRNA bases that are altered in DMS modification by the binding of Tet(O) around the decoding centre [58]

A. The *E. coli* 16S rRNA secondary structure is shown with the tetracycline-dependent changes in DMS modification (U1052, C1054, A892) marked in green, the Tet(O)-specific C1214 protection in cyan, the EF-G-dependent enhancement (C1400) in violet, and the A1408 enhancement, which is common to both Tet(O) and EF-G, in orange.

B. The overall orientation of Tet(O) (red density) bound to the 30S subunit

Note: This figure was reproduced with permission from the publisher.

Chapter 2 Materials and Methods

2.1 Bacterial strains

Escherichia coli BL21 Star^{TM} (DE3) (Invitrogen, Burlington, ON, Canada) was used as a host for the expression of recombinant proteins Tet(O) wild type (Tet(O)^{WT}), Tet(O) mutant (Tet(O)^{D131N}) and elongation factor G (EF-G) respectively. The strains contain the λ DE3 lysogen which carries the gene for T7 RNA polymerase under the control of the *lac*UV5 promoter [103].

E. coli TOP10 (Invitrogen, Burlington, ON, Canada) was used as a host for characterization and maintenance of transformants of pET200-*tet(O)*^{WT}, pET200-*tet(O)*^{D131N}, and pET200-*fusA*. The strain can maintain the stability of the constructs due to the absence of T7 RNA polymerase [103].

E. coli MRE 600 (kindly provided by Dr. R. P. Fahlman, Department of Biochemistry, University of Alberta) was used for the preparation of tight-coupled 70S ribosomes because this strain displays negligible ribonuclease activity due to lack of ribonuclease I [104, 105].

All *E. coli* strains were incubated in 2% Luria–Bertani (LB) (BD Biosciences, Oakville, ON, Canada) broth at 37°C for 12-14 h, and then stored at -80°C in 50% glycerol LB broth.

2.2 Reagents and equipment

Reagents, chemicals and equipment were purchased from Fisher Scientific, Ottawa, ON, Canada unless otherwise stated.

2.3 Construction of recombinant plasmids pET200-*tet(O)*^{WT}, pET200-*tet(O)*^{D131N} and pET200-*fusA*

The recombinant plasmids pET200-*tet(O)*^{WT}, pET200-*tet(O)*^{D131N} and pET200-*fusA* (expression of EF-G) were constructed and transformed to *E. coli* TOP 10 and *E. coli* BL21(DE3) by Dr. N. S. Thakor [72] as outlined in Figure 2.1. The recombinant genes of *tet(O)*^{WT} and *tet(O)*^{D131N} were cloned from a *C. jejuni tet(O)* gene (from plasmid pMS119EH), and *fusA* was cloned from an *E. coli fusA* gene (from plasmid pET24b) by PCR. The primers used to amplify the above genes are listed in Table 2.1.

The cloned genes of *tet(O)*^{WT}, *tet(O)*^{D131N} and *fusA* were individually inserted into the pET200/D-TOPO plasmid (Figure 2.2) (Invitrogen, Burlington, ON, Canada) using TOPO cloning reactions according to the user manual [103]. The reactions (6 μL) containing 2 μL PCR amplified *tet(O)*^{WT}, *tet(O)*^{D131N} or *fusA* gene, 1 μL salt solution (1.2 M NaCl, 0.06 M $MgCl_2$), 1 μL pET200/D-TOPO vector, and 2 μL sterile MilliQ water, were incubated at room temperature (RT) for 5 min, and placed on ice.

The constructed plasmids pET200-*tet(O)*^{WT}, pET200-*tet(O)*^{D131N}, and

pET200-*fusA* were transformed to *E. coli* TOP10 competent cells by chemical transformation according to the user manual [103]. TOPO cloning reactions (3 μL) were added to separate vials containing One Shot *E. coli* TOP10 competent cells. These cells were mixed gently, and incubated on ice for 20 min. The cells were then heat-shocked for 30 sec at 42°C without shaking, and immediately placed on ice. Then 250 μL of S.O.C. medium (2% tryptone, 0.5% yeast extract, 10 mM NaCl, 2.5 mM KCl, 10 mM $MgCl_2$, 10 mM $MgSO_4$, 20 mM glucose) was added in the cells at RT, shaken horizontally (200 rpm) at 37°C for 1 h, and 100-200 μL was spread onto a prewarmed antibiotic selective plate (2% LB agar supplemented with 50 μg/mL kanymycin). The plate was incubated overnight at 37°C. After confirming the gene sequence of the transformants at The Applied Genomic Centre Core Sequence Facility in the Department of Medical Genetics at the University of Alberta [72], the constructed plasmids were transformed to *E. coli* BL21(DE3) as described above for *E. coli* TOP10.

2.4 Determination of tetracycline susceptibility of *E. coli* transformants

To evaluate the ability of the *C. jejuni tet(O)*^{WT} gene to confer Tc^R to *E. coli*, Tc susceptibility of *E. coli* BL21(DE3)-pET200-*tet(O)*^{WT} was determined by the agar dilution method as described by Thakor *et al.* [75] with a few modifications (Figure 2.3). *E. coli* BL21(DE3)-pET200-*tet(O)*^{WT} was grown in 5 mL of 2% LB broth supplemented with 50 μg/mL kanamycin (Sigma-Aldrich, Oakville, ON,

Canada) to mid-log phase (OD_{600}=0.6-0.7) at 37°C with shaking at 200 rpm. (Forma Orbital Shaker, Thermo Electron Corporation, Gormley, ON, Canada). Then a 5 μL aliquot of culture was spotted onto LB agar plates containing two-fold increasing concentrations (1-256 μg/mL) of Tc (Sigma-Aldrich, Oakville, ON, Canada) and IPTG (Invitrogen, Burlington, ON, Canada). IPTG (25 μL of 1 M IPTG) was spread onto the Tc LB agar plates. IPTG is a highly stable synthetic analog of lactose. It prevents the *lac* repressor (encoded by *lacI*) from binding to the *lac* operator (*lacO*), and therefore allows *E. coli* BL21(DE3) to express T7 RNA polymerase which then binds to the T7*lac* promoter to actively transcribe the *tet(O)*^{WT} gene. The LB agar plates were then incubated at 37°C for 48 h to observe the growth of *E. coli*. Tc-free LB agar plates and IPTG-free Tc agar plates were used as growth control plates. The Tc minimal inhibitory concentration (MIC) was determined as the lowest concentration of Tc to prevent growth of macroscopically visible colonies on Tc agar plates with IPTG present.

The Tc susceptibility of *E. coli* TOP 10-pET200-*tet(O)*^{WT} was determined as the same as described above. The strain *E. coli* TOP 10 does not produce T7 RNA polymerase, so cannot express Tet(O)^{WT} even when treated with IPTG. Compared with the Tc MIC of *E. coli* BL21(DE3)-pET200-*tet(O)*^{WT}, a lower MIC was expected for *E. coli* TOP 10-pET200-*tet(O)*^{WT}.

Since the substrate specificity of Tet(O)^{D131N} is XTP and *E. coli* cannot produce internal XTP, the Tc susceptibility of *E. coli*

BL21(DE3)-pET200-*tet(O)*^{D131N} was determined as described above with the following modification: XTP (100 μL of 1 mM) was spread onto the IPTG-Tc agar plates to observe whether *E. coli* BL21(DE3)-pET200-*tet(O)*^{D131N} utilizes external XTP to exhibit Tc^R.

E. coli BL21(DE3)-pET200-*fusA* served as a Tc susceptible control to ensure that the pET200 vector and the *fusA* gene could not confer Tc^R to Tc susceptible (Tc^S) *E. coli*-BL21(DE3).

2.5 Overexpression and Purification of Tet(O)^{WT}, Tet(O)^{D131N}, and EF-G

Overexpression and purification of Tet(O)^{WT}, Tet(O)^{D131N}, and EF-G were performed according to the methods proposed by Thakor *et al.* [72] with some modifications (Figure 2.4).

2.5.1 Overexpression of Tet(O)^{WT}, Tet(O)^{D131N}, and EF-G

A single colony of *E. coli* BL21 (DE3)-pET200-*tet(O)*^{WT}/*tet(O)*^{D131N}/*fusA* was inoculated in 2% LB broth (100 mL) supplemented with 50 μg/mL kanamycin. After 12-14 h incubation at 37°C with shaking (200 rpm), the culture was transferred to a 10-fold increased volume of 2% LB broth supplemented with 50 μg/mL kanamycin, 1% glycerol, 17 mM KH_2PO_4, 72 mM K_2HPO_4 and shaking (200 rpm) continued at 37°C. When cells reached mid-log phase of growth (OD_{600}=0.6-0.7), IPTG was added to a final concentration of 0.5 mM to induce target protein overexpression and the temperature was reduced to 30°C for

Tet(O)^{WT} or EF-G (to 18°C for Tet(O)^{D131N}) to increase protein solubility. About four hours later, the cells were harvested by centrifugation at 5,000×*g* (SORVALL RC2-B, GSA rotor) for 10 min. The harvested cells were washed with 20 mM phosphate-buffered saline (PBS), pH7.4 and stored at -80°C.

2.5.2 Purification of Tet(O)^{WT}, Tet(O)^{D131N}, and EF-G

Frozen cells (~20 g) were thawed on ice, then suspended and lysed in 200 mL binding buffer (20 mM Hepes pH 7.0, 200 mM KCl, 10% Glycerol) supplemented with 2 mg/mL lysozyme (Sigma-Aldrich, Oakville, ON, Canada), 1500 U of DNAse I (Invitrogen, Burlington, ON, Canada), 2 tablets of Complete^{TM} EDTA-free protease inhibitor cocktail (Roche, Mississauga, ON, Canada), and 3 mM $MgCl_2$ at RT for 30 min. The suspension was sonicated on ice with ten 10 sec pulses separated by 10 sec pauses (model 500, Sonic Dismembrator, Fisher Scientific). The lysates were added 1.5 mL Triton X-100 and stirred at RT for 30 min. After centrifugation at 5,000×*g* (SORVALL RC2-B, GSA rotor) for 20 min, the supernatant was filtered through a 0.45 μm filter (Millipore, Toronto, ON, Canada). The filtered supernatant was then applied to a 5.0 mL HisTrap high performance (HP) Ni^{2+} column (GE Healthcare, Uppasalla, Sweden) equilibrated with binding buffer. After washed with 5 column volume of binding buffer to wash away the unbound proteins, the column was eluted with increasing concentrations of imidazole (25-500 mM) to elute out the bound His-tagged

protein. The eluate fractions were collected separately and the proteins separated on 10% sodium dodecyl sulfate polyacrylamide gel electrophoresis (SDS-PAGE) to detect the target protein bands of $Tet(O)^{WT}$ (72.5 kDa), $Tet(O)^{D131N}$ (72.5 kDa), or EF-G (77.5 kDa) at the expected molecular weight (see section 2.5.3). The target protein fractions (~25 mL) were then concentrated to less than 2.5 mL (Amicon Ultra-15 Centrifugal Filter Devices, 30K MWCO, Millipore, Toronto, ON, Canada) and dialyzed with a Tube-O-Dialyzer (15K MWCO, G-Biosciences, Brockville, ON, Canada) against the Binding Buffer supplemented with 1 mM dithiothretol (DTT) (Sigma-Aldrich, Oakville, ON, Canada). The dialyzed proteins were stored at -80°C in protein storage buffer (20 mM Hepes pH 7.0, 200 mM KCl, 50% Glycerol, 1 mM DTT).

2.5.3 SDS-PAGE

Purified proteins were separated by 10% SDS-PAGE to evaluate protein molecular weight and purity on a Mini-PROTEAN Tetra Electrophoresis System (Bio-Rad, Mississauga, ON, Canada). SDS is an anionic detergent that disrupts proteins structure to produce a linear polypeptide chain coated with negatively charged SDS molecules, and separate denaturated proteins by molecular mass. The preparation of the 10% separating gel and stacking gel was described in Table 2.3. Each protein sample (20 μL) was treated with an equal volume of 2×SDS Loading Buffer (0.125 M Tris-HCl pH 6.8, 5% SDS, 0.02% bromophenol blue,

25% glycerol, 0.2 M DTT), and boiled for 3~5 min. The samples and the PageRuler™ Plus Prestained Protein Ladder (Fermentas, Burlinton, ON, Canada) were then loaded into the wells of the stacking gel, and run at constant voltage (150 V) for ~ 1 h in SDS-PAGE Running Buffer (25 mM Tris, 192 mM glycine, 0.1% SDS). The gel was washed three times with MilliQ water for 10 min each time on an orbital shaker, and then stained with Bio-Safe Coomassie G250 stain (Bio-Rad, Mississauga, ON, Canada) for 20 min to visualize the protein bands. The stained gel was rinsed with MilliQ water, and then destained in MilliQ water for 20 min to eliminate background staining.

2.5.4 Bradford protein assay

The protein concentrations were determined by the Bradford assay [106] using bovine serum albumin (BSA) as a standard. The assay is based on an absorbance shift from 365 nm to 595 nm when the red form of Coomassie Brilliant Blue G-250 is converted to blue form upon binding of the dye to basic (especially arginine) and aromatic amino acid residues (e.g. phenylalanine, tryptophan, tyrosine) [106]. According to the manufacturer's instruction (Quick Start™ Bradford Protein Assay, Bio-Rad, Mississauga, ON, Canada), a series of BSA standards (2, 4, 6, 8, 10 μg/mL) and two-fold dilutions (1/2-1/128) of the purified protein samples (previously diluted ten-fold in MilliQ water) were prepared in MilliQ water. The BSA standards and diluted protein samples were

then mixed with equal volumes (150 μL) of 1× dye reagent (Bio-Rad, Mississauga, ON, Canada) and incubated at RT for 5 min. The absorbance was measured at 595 nm on a Microplate spectrophotometer (XMark, Bio-Rad, Mississauga, ON, Canada) against a MilliQ water blank. Diluted sample protein concentrations (μg/mL) were derived from the standard curve that was obtained by linear regression analysis (Microsoft Excel statistic function) of A_{595} vs concentrations of BSA standards. The protein concentration (μM) was directly calculated from protein concentration (μg/mL) by the following equation.

$$Protein\ concentration\ (\mu M) = \frac{protein\ concentration\ (\mu g/mL)}{MW\ (\mu g/\mu mol)} \times 1000^{*}$$

Where : MW of Tet(O) = 72,562.62

MW of EF-G = 77,580.46

*1000 converts # μmol/mL to # μmol/L

2.6 Preparation of tight-coupled 70S Ribosomes

Previous studies were carried out *in vitro* to use vacant 70S ribosomes or 30S ribosomal subunits to evaluate the ability of Tet(O) to release bound Tc from the ribosomes [57,58,62,72]. In order to establish the differences of Tet(O)-mediated Tc release *in vitro* in different ribosome states, the study was determined in the presence of loaded 70S ribosomes and compared with vacant 70S ribosomes.

To prevent the degradation of 70S ribosomes from RNase contamination, all glassware was baked at 150°C overnight, and plasticware was soaked in 0.1%

(v/v) diethylpyrocarbonate (DEPC) at 37°C for 2 h to destroy all RNase activity. This was followed by extensive rinsing with sterile MilliQ water and autoclaving to inactivate the toxicity of DEPC. All buffers were prepared in autoclaved 0.1% DEPC water, and then autoclaved or passed through a 0.22 μm filter. Reagents used should be of the highest quality and RNase free.

The tight-coupled 70S ribosomes were isolated from *E. coli* MRE 600 as previously described with some modifications [102]. *E. coli* MRE 600 cells were grown in 1 L 2% LB broth at 37°C to mid-log phase (A_{600}= ~0.5), and then cooled on ice for 30 min to produce run-off 70S ribosomes (completion of translation and dissociated from mRNA and tRNA). The cells were harvested at 4°C by centrifugation at 5000×*g* (SORVALL RC2-B, GSA rotor) for 15 min. The pellets were stored at -80°C. The frozen pellets were thawed on ice and suspended in 50 mL Lysis Buffer (50 mM Tris-HCI pH 7.5, 10 mM $MgCl_2$, 1 M NH_4Cl, 6 mM β-mercaptoethanol, 0.5 mM EDTA), and passed through a high pressure homogenizer (EmulsiFlex-MSC475, Avestin Inc, Ottawa, ON, Canada) 3-5 times at 25,000 psi to lyse cells. The cell lysate was centrifuged at 61,334×*g* (28,000 rpm, 45Ti rotor, Beckman Coulter, Mississauga, ON, Canada) for 15 min to remove nuclei, cell debris and some organelles. The supernatant was centrifuged at the same speed for 30 min at 4°C, and then at 111,921×*g* (39,000 rpm, 70Ti rotor, Beckman Coulter) for 14 h at 4°C to pellet crude 70S ribosomes. The pellets were resuspended in 4×1.5 mL Buffer 1 (50 mM Tris-HCI pH 7.5, 6 mM $MgCl_2$,

1 M NH_4Cl, 6 mM β-mercaptoethanol), and stirred at 4°C for 4-6 h. After centrifugation at 5000×*g* (SORVALL RC2-B, GSA rotor) for 5 min at 4°C, the supernatant was laid onto 6×38 mL 10-40% sucrose gradient solution made in Buffer 1, and centrifuged at 55,070×g (20,400 rpm, SW27 rotor, Beckman Coulter) for 13 h at 4°C. The 70S ribosome fraction was identified and collected under a UV detector (UA-6 ISCO UV/Vis Detector, Biostad, Saint-Julie, Québec, Canada) at 260 nm. The Mg^{2+} concentration of 70S ribosome fraction was adjusted from 6 mM to 10 mM, and then centrifuged at 72,551×g (31,400 rpm, 70Ti rotor, Beckman Coulter) for 20 h at 4°C. The pure 70S ribosome pellets were dissolved in 500 μL Buffer 2 (50 mM Tris-HCl pH 7.5, 10 mM $MgCl_2$, 100 mM NH_4Cl, 1 mM DTT), aliquoted, quick-frozen in liquid nitrogen, and stored at -80°C. The absorbance of the 70S ribosome preparation was determined at 260 nm (Beckman DU530 spectrophotometer, Beckman Coulter, Mississauga, ON, Canada). The concentration (μM) of 70S ribosomes was directly calculated from A_{260} by the following equation:

$$Conc.\ of\ 70S\ (\mu M) = \frac{A_{260} \times 23 \times Dilution\ times}{1000^*}$$

Where: $1A_{260}$ = 23 pmol/mL [102]

*1/1000 converts # pmol/mL to # μmol/L

2.7 Preparation of loaded 70S Ribosomes

The loaded 70S ribosomes were prepared according to the method reported

by Fahlman *et al.* [107] with some modifications. The $mRNA^{Phe}$, $tRNA^{Met}$ (P-site tRNA), and $tRNA^{Phe}$ (A-site tRNA) must be generated separately for subsequent assembly with vacant 70S ribosomes. To prevent the degradation of mRNA, tRNA and 70S ribosomes from RNase contamination, all glassware, plasticware, water and solutions should be treated as described in section 2.6.

2.7.1 Preparation of $mRNA^{Phe}$, $tRNA^{Met}$, and $tRNA^{Phe}$

2.7.1.1 Generation of mRNA and tRNA DNA templates

The DNA templates of $mRNA^{Phe}$, $tRNA^{Met}$, and $tRNA^{Phe}$ were generated by PCR reactions in a total volume of 50 μL containing 1 μM oligonucleotide pairs, $mRNA^{Phe}$(+)/$mRNA^{Phe}$(-), $tRNA^{Met}$(+)/$tRNA^{Met}$(-) or $tRNA^{Phe}$(+)/$tRNA^{Phe}$(-) (synthesized by Integrated DNA Technologies, Toronto, ON, Canada) (Table 2.2); 1×PCR reaction buffer (10 mM Tris-HCl pH 8.3, 50 mM KCl); 0.25 mM dNTPs (Invitrogen, Burlington, ON, Canada); 3 mM $MgCl_2$; and 1U of Taq DNA Polymerase (Invitrogen, Burlington, ON, Canada). Five cycles of amplification consisted of a 30 sec denaturation at 94°C, 30 sec annealing at 45°C, and 48 sec extension at 72°C. The PCR products were separated by 3% agarose gel electrophoresis run at constant voltage (100 V) for 30 min and the size (~90 bp) confirmed against a 100 bp DNA ladder (Invitrogen, Burlington, ON, Canada). After confirmed the size, the remaining PCR products were then extracted by phenol/chloroform (1:1, v/v) extraction, mixed with 1/10 volume of 3 M NaOAc

(pH 7.0) and 2.5 volumes of ice-cold 95% ethanol. The solution was placed at -80°C for at least 15 min to allow DNA precipitation. The DNA was pelleted by centrifugation at 12,000×g for 30 min at 4°C. The DNA pellets were then washed with 70% ethanol, and centrifuged at 12,000×g for 10 min at 4°C. The 70% ethanol was carefully removed. The pellets were resuspended in 50 μL MilliQ water after the last visible traces of ethanol had evaporated. It was important to not allow the pellets to become dessicated; otherwise they will be difficult to dissolve.

2.7.1.2 Transcription of mRNA and tRNA

The resuspended DNA templates (50 μL) were heated at 80°C for 2 min, and cooled at RT for at least 15 min. The cooled DNA templates were transcribed in a total volume of 500 μL containing 1×Transcription buffer (40 mM Tris-HCl pH 8.0, 1 mM Spermidine, 0.01% Triton X-100, 0.1% PEG), 1 mM NTPs (adensoine 5'-triphosphate (ATP), cytidine 5'-triphosphate (CTP), guanosine 5'-triphosphate (GTP) and uridine 5'-triphosphate (UTP)) (Invitrogen, Burlington, ON, Canada), 10 mM $MgCl_2$, 5 mM β-mercaptoethanol, 5 mM Guanosine Monophosphate (GMP), 20 μg/mL of T7 polymerase (kindly provided by Dr. R. P. Fahlman, Department of Biochemistry, University of Alberta), and 1×RNase inhibitor (Invitrogen, Burlington, ON, Canada). The transcription reactions were carried out at 41°C for 6 hours.

2.7.1.3 Isolation of mRNA and tRNA from denaturing acrylamide gel

The transcribed products (500 μL) were precipitated by the addition of 50 μL of 3 M NaOAc (pH 5.0) and 550 μL of isopropanol and incubation at -80°C for 15 minutes to allow RNA precipitation. After centrifugation at 12,000×g for 30 min at 4°C, the RNA pellets were washed with 70% ethanol, and centrifuged at 12,000×g for 10 min at 4°C. The 70% ethanol was carefully removed. The RNA pellets were then resuspended in 250 μL loading buffer (95% deionized formamide, 0.025% (w/v) bromophenol blue, 5 mM EDTA pH 8.0, 0.005% SDS) and heated at 81°C for 2 min. The samples were then loaded onto a 10% denaturing acrylamide gel, and run at constant Watts (15 Watts) for ~2.5 hours in 1×TBE (Tris/Borate/EDTA) buffer. The tRNA and mRNA were visualized as dark bands against a green background on a fluorescence-coated silica gel thin layer chromatography (TLC) plate (13181 Silica gel, Fisher Scientific) by a technique known as UV shadowing [108]. The bands were cut out, crushed with a spatula, and incubated overnight at 4°C in 5 mL of 300 mM NaOAc (pH 5) on an Orbitron Rotator (Fisher Scientific). After centrifugation at 5,000×g for 10 min at 4°C, the supernatant was filtered through a 8 μm μStar filter (Costar, Cambridge, MA, USA), 45 mL butanol was added, and the tube was centrifuged at 5,000×g for 20 min to concentrate the RNA preparation to less than 0.5 mL. The concentrated RNA sample was then precipitated with 2.5 volumes of 95% ethanol and washed with 70% ethanol as described in section 2.7.1.1. The pellets were dissolved in 50

μL of 5 mM NaOAc (pH 5.0). The concentrations (ng/μL) of the RNA preparations were determined by measuring the absorbance at 260 nm (NanoDrop 1000 spectrophotometer, Thermo Scientific, Wilmington, USA). The concentration (μM) of $mRNA^{Phe}$, $tRNA^{Phe}$, and $tRNA^{Met}$ were calculated from ng/μL according to the following equation:

$$Conc.\ (\mu M) = \frac{Conc.\ (ng/\mu L) \times 1000^{*}}{MW\ (\mu g/\mu mol)}$$

Where: MW (g/mol) = number of nucleotides (nt)×average MW of RNA nt (340 Da)

MW of $mRNA^{Phe}$ = 26×340 = 8,840

MW of $tRNA^{Phe}$ = 75×340 = 25,500

MW of $tRNA^{Met}$ = 76×340 = 25,840

* 1000 converts # ng/μL to μg/L

2.7.2 Assembly of ribosome complexes with mRNA and tRNA

The tight-coupled 70S ribosomes were heat activated at 42°C for 2 min, and cooled at RT for at least 15 min. The activation at 42°C introduces enough energy for tight-coupled 70S ribosomes to rearrange their distorted structures at the molecular level caused by ultracentrifugation. The $mRNA^{Phe}$, P-site tRNA ($tRNA^{Met}$), and A-site tRNA ($tRNA^{Phe}$) were added sequentially at 1.5 times the concentration of ribosomes and incubated at RT for 2 min, 10 min, and 1 h respectively due to the significantly different rates of association for the different RNAs for the ribosome [107].

2.8 Verification of tRNA loading in the ribosomal A- and P-site

2.8.1 Preparation of radio-labeled tRNA

The [3'-^{32}P] labeling of $tRNA^{Met}$ and $tRNA^{Phe}$ was prepared by an [α-^{32}P]ATP-PPi exchange reaction (Figure 2.5) catalyzed by *E. coli* tRNA-terminal nucleotidyltransferase (CCA-adding enzyme). The reactions were performed as described by Ledoux *et al.* [109] with some modifications. The reactions (100 μL) containing 50 mM glycine-HCl buffer pH 9.0, 10 mM $MgCl_2$, 1 μM tRNA, 0.3 μM 0.2 Ci [α-^{32}P] ATP (3000 Ci/mmol, Perkin-Elmer, Boston, MA, USA), 50 μM sodium pyrophosphate (PPi), and 92 μg/mL CCA-adding enzyme were incubated at 37°C for 5 min. Then 2 μL of 50 μM CTP (final concentration 1 μM) and 5 μL of 10 U/mL (final concentration 0.5 U/mL) pyrophosphatase (Invitrogen, Burlington, ON, Canada) was added, and incubated at 37°C for an additional 2 min. The reactions were then extracted by phenol/chloroform (1:1, v/v) extraction, desalted by loading samples to 0.5 mL Zeba desalt spin columns (Pierce, Rockford, USA), and centrifuged at 1,500×*g* for 2 min to collect desalted sample, and then precipitated by 95% ethanol and washed by 70% ethanol as previously described in section 2.7.1.1. The pellets were dissolved in 5 mM NaOAc (pH 5.0).

2.8.2 Assessment of tRNA binding to the ribosomal A- and P-site

Determination of the association efficiency of [3'-^{32}P]-tRNA to the ribosomal

A-site & P-site was performed by a double-filter binding method [107, 110] with a 96-well Dot-Blot System (Whatman, Florham Park, NJ, USA) (Figure 2.6). An upper NitroBind nitrocellulose membrane (Osmonics, Cole-Parmer, Montreal, QC, Canada) and a lower nylon membrane (Amersham Hybond-N^+, GE Healthcare, Baie d'Urfe, Quebec, Canada) were sandwiched between two blocks of the 96-well apparatus after pre-soaking in Binding-Washing (BW) buffer (20 mM Hepes pH7.4, 6 mM MgAc, 150 mM NH_4Cl, 4 mM β-mercaptoethanol, 0.05 mM spermine, and 2 mM spermidine) for at least 10 min. The upper nitrocellulose membrane traps tRNA bound to the ribosome, while the lower nylon membrane traps free tRNA.

The binding of tRNA to the ribosomal P-site was performed in 25 μL reactions containing 1 μM 70S ribosomes, 1.5 μM $mRNA^{Phe}$, and 5 nM [3'-^{32}P] $tRNA^{Met}$ in the BW buffer. The vacant 70S ribosomes were heat activated at 42°C for 2 minutes, and cooled at RT for at least 15 min. The $mRNA^{Phe}$ was added and incubated at RT for 2 min, and then [3'-^{32}P] $tRNA^{Met}$ was added and incubated at RT for 10 min. The reactions were diluted (5× and 10× dilution) and filtered by the double-filter dot-blot apparatus, and immediately washed with BW buffer. The dilution was done to prevent filter saturation and induce dissociation of weakly bound tRNA. The undiluted reactions were also filtered and washed with BW buffer to determine the fraction initially bound.

The binding of tRNA to the ribosomal A-site was performed in 25 μL

reactions containing 1 μM 70S ribosomes, 1.5 μM $mRNA^{Phe}$, 1.5 μM $tRNA^{Met}$, and 5 nM [3'-^{32}P] $tRNA^{Phe}$. As mentioned above, the $mRNA^{Phe}$ and $tRNA^{Met}$ were sequentially added and incubated with vacant 70S to fill in the ribosomal P-site. The [3'-^{32}P] $tRNA^{Phe}$ was then added in the reactions and incubated at RT for 1 h to load in the ribosomal A-site. The undiluted and diluted (5× and 10× dilution) reactions were filtered, following immediately washed with BW buffer.

The nitrocellulose membrane and nylon membrane were removed, dried, wrapped with SARAN plastic film, and exposed on a phosphorimager plate (Fujifilm, Mississauga, ON, Canada) overnight. The images were then obtained by scanning with a PhosphorImager (Storm 840, GE Healthcare, Baie d'Urfe, Quebec, Canada) and analyzed by ImageQuant (GE Healthcare, Baie d'Urfe, Quebec, Canada). The association efficiency (%) of tRNA bound to the ribosomal A- and P-site was calculated from the signal by the following equation:

$$Association\ Efficiency\ (\%) = Signal_{Nitrocellulose}/(Signal_{Nitrocellulose} + Signal_{Nylon})$$

Where: $Signal_{Nitrocellulose}$ = 70S ribosome-[3'-^{32}P] tRNA complex

$Signal_{Nylon}$ = free [3'-^{32}P] tRNA

2.9 Determination of Tet(O)-mediated Tc release *in vitro* by Tc binding Assay

To assess the ability of Tet(O) to release bound Tc from the 70S ribosomes in different conditions, the Tc binding assay was used to determine the affinity of [^{3}H]-Tc bound to vacant and loaded 70S ribosomes. A nitrocellulose filtration

method [72] was used to measure Tc binding to 70S ribosomes with some modifications (Figure 2.7). When Tet(O) was absent, a high affinity of [^{3}H]-Tc bound to 70S ribosomes was expected because [^{3}H]-Tc-70S ribosome complex was trapped on the 0.45 μm nitrocellulose filter. In contrast, when Tet(O) was present, a lower affinity of [^{3}H]-Tc bound to 70S ribosomes was expected because Tet(O) released bound [^{3}H]-Tc from 70S ribosomes and the free [^{3}H]-Tc was passed through the filter.

2.9.1 Determination of binding affinity of [^{3}H]-Tc to loaded 70S ribosomes in the absence and presence of Tet(O)^{WT}

The affinity of [^{3}H]-Tc bound to loaded 70S ribosomes was determined in the absence and presence of Tet(O)^{WT}. Two-fold increasing concentrations (1-40 μM) of 0.1Ci/mmol [^{3}H]Tc (Perkin-Elmer, Boston, MA, USA) were incubated with 0.5 μM loaded 70S ribosomes and 50 μM GTP in BW buffer (as described in section 2.7.2) at 37°C for 20 min in the absence or presence of 2 μM Tet(O)^{WT}. The reactions incubated with vacant 70S ribosomes were used as controls. The 20 μL reactions were then diluted with 1 mL of BW buffer and immediately vacuum filtered through 0.45 μM nitrocellulose filters (Millipore, Toronto, ON, Canada) that have been preincubated with BW buffer for 30 min. The filters were washed twice (10 mL each) with ice-cold BW buffer, and placed in scintillation vials. Then 10 mL scintillation fluid (CytoSinct ES^{TM}, MP Biomedicals, Ottawa, ON,

Canada) was added to each vial, vortexed 10 sec, and the radioactivity retained on the filter was determined on a liquid scintillation counter (LS6500, Beckman Coulter, Mississauga, ON, Canada). The amount of [^{3}H]-Tc bound to the ribosomes was calculated directly from the counts decay minute^{-1} (dpm) using the following equation.

$$pmol\ of\ 70S\text{-}[^3H]\text{-}Tc = \frac{(dps^{Total} - dps^{Bkgd})/37{,}000}{specific\ activity\ of\ [^3H]\text{-}Tc}$$

Where: dps = counts decay second^{-1}= dpm/60

1 μCi = 37,000 dps

Specific activity of [^{3}H]Tc = 0.1 Ci/mmol= 0.0001μCi/pmol

Background levels of radioactivity (dps^{Bkgd}) reflected the non-specific binding of [^{3}H]-Tc (1-40 μM) to the filter, and were subtracted from the total counts to obtain the radioactivity of specific binding of [^{3}H]-Tc to the ribosomes. The [^{3}H]-Tc dps was then converted to μCi, and then to pmol. The amount (pmol) of [^{3}H]-Tc specifically bound to the ribosomes (70S-[^{3}H]-Tc) was plotted against the concentration of [^{3}H]-Tc (1-40 μM) to obtain a rectangular hyperbola of one-site binding (GraphPad Prism 5.0, La Jolla, CA, USA). The dissociation constant, K_d (μM) (measure of binding affinity of Tc to the 70S ribosomes) was derived from the following equation:

$$Y = \frac{B_{max} \times [[^3H]\text{-}Tc]}{K_d + [[^3H]\text{-}Tc]}$$

which was rearranged to solve for K_d:

$$K_d = \frac{[[^3H]\text{-}Tc]\ (B_{max} - Y)}{Y}$$

Where: Y = pmol of 70S-[^{3}H]-Tc complex

B_{max} = maximal # pmol of [^{3}H]-Tc bound per μmol 70S ribosomes

K_d = concentration of [^{3}H]-Tc when half the binding sites on the 70S ribosomes are occupied at equilibrium

2.9.2 Determination of binding affinity of [^{3}H]Tc to vacant 70S ribosomes in the presence of Tet(O)^{WT} and EF-G

To investigate whether EF-G interferes with Tet(O)-mediated Tc release as a consequence of binding to the same ribosomal site, the affinity of [^{3}H]-Tc bound to vacant 70S ribosomes was determined in the presence of equal concentrations (2 μM) of Tet(O)^{WT} and EF-G as previously described in section 2.9.1. In order to do this experiment, it was necessary to control for the amount of [^{3}H]-Tc bound to vacant 70S ribosomes, vacant 70S ribosomes with EF-G present, and vacant 70S ribosomes with Tet(O)^{WT} present. The affinity of[^{3}H]-Tc bound to vacant 70S ribosomes in the presence of Tet(O)^{WT} and EF-G was then compared with the controls.

2.9.3 Determination of binding affinity of [^{3}H]-Tc to vacant 70S ribosomes in the presence of Tet(O)^{D131N} and GTP or XTP

To evaluate the ability of Tet(O)^{D131N} to release bound Tc from 70S ribosomes, the affinity of [^{3}H]-Tc bound to vacant 70S ribosomes in the presence

of Tet(O)^{D131N} and GTP or XTP was determined as described in section 2.9.1. In order to do this experiment, it was necessary to control for the amount of [^{3}H]-Tc bound to vacant 70S ribosomes, and vacant 70S ribosomes with Tet(O)^{WT} and GTP present. The affinity of [^{3}H]-Tc bound to vacant 70S ribosomes in the presence of Tet(O)^{D131N} and GTP or XTP was then compared with the controls.

2.10 Investigation of GTP hydrolysis kinetics of Tet(O) and EF-G

The ribosome-dependent GTP hydrolysis is necessary for Tet(O)^{WT} to dissociate the ribosome and consequently to repeatedly recycle on and off 70S ribosomes to release Tc [57, 58, 62]. To investigate the kinetics of GTP hydrolysis of Tet(O)^{WT} in different conditions, the GTP hydrolysis assay was performed as described by Thakor *et al.*[72] with some modifications (Figure 2.8).

2.10.1 Determination of GTP hydrolysis by Tet(O)^{WT} with time

To determine the kinetic GTP hydrolysis of Tet(O)^{WT}, it was necessary to establish the optimal incubation time for performing GTP hydrolysis assays. The reactions were performed in a total volume of 20 μL containing 0.2 μM vacant 70S ribosomes, 0.05 μM Tet(O)^{WT}, and 200 μM 0.5 μCi [γ-^{32}P]GTP (6000 Ci/mmol, Perkin-Elmer, Boston, MA, USA) in reaction buffer (30 mM Tris-HCl pH8.0, 80 mM NH_4Cl, and 20 mM $MgCl_2$), and incubated at 37°C for 1, 2, 5, 10, 15, 20, 30, 40, 60, 90, and 120 min. After incubation, 1 μL of each sample was

removed and quenched by mixing with 1 μL of 30% (v/v) formic acid. Then 1 μL of the quenched sample was loaded onto a water-treated polyethyleneimine (PEI) cellulose thin layer chromatography (TLC) plate (Sigma-Aldrich, Oakville, ON, Canada) and developed in 4 M sodium formate (pH 3.5), followed by an acetone rinse to allow plate to dry quickly. The treated TLC plates were wrapped with SARAN plastic film, exposed overnight on a phosphorimager plate (Fujifilm, Mississauga, ON, Canada), and scanned on a FLA5100 imaging system (Fujifilm, Mississauga, ON, Canada). The images were analyzed by ImageQuant (GE Healthcare, Baie d'Urfe, Quebec, Canada) to obtain the signal volume. The percent (%) of hydrolyzed [γ-^{32}P]GTP was calculated from the signal volume by the following equation.

$$Hydrolyzed\ [\gamma\text{-}^{32}P]GTP\ (\%) = \frac{V_{[\gamma\text{-}^{32}P]Pi}}{V_{[\gamma\text{-}^{32}P]GTP} + V_{[\gamma\text{-}^{32}P]Pi}} \times 100$$

Where: $V_{[\gamma\text{-}^{32}P]Pi}$ = signal volume of hydrolyzed [γ-^{32}P]GTP

$V_{[\gamma\text{-}^{32}P]GTP}$ = signal volume of unhydrolyzed [γ-^{32}P]GTP

The percent (%) of hydrolyzed [γ-^{32}P]GTP was then plotted versus the incubation time (min) by a non-linear regression analysis using GraphPad Prism 5.0 (La Jolla, CA, USA) .

2.10.2 Confirmation of absence of GTP hydrolysis by Tet(O)^{D131N}

The GTP hydrolysis assay of Tet(O)^{D131N} was performed to determine whether this Tet(O) mutant could hydrolyze GTP or not. As described in section

2.10.1, 0.05 μM Tet(O)^{D131N} was incubated with 0.2 μM vacant 70S ribosomes and 200 μM 0.5 μCi [γ-^{32}P]GTP for 5, 15 and 30 min in reaction buffer. The controls include: the reactions 1) in the presence of 70S ribosomes and Tet(O)^{WT}, to confirm Tet(O)^{WT} has GTPase activity to hydrolyze GTP; 2) in the presence of Tet(O)^{WT} and absence of 70S ribosomes, to confirm the GTPase activity of Tet(O)^{WT} is ribosome-dependent; 3) in the absence of 70S ribosomes and Tet(O)^{WT}/Tet(O)^{D131N}, to confirm [γ-^{32}P]GTP does not auto-hydrolyze.

2.10.3 Determination of kinetics of GTP hydrolysis by EF-G in the presence of Tet(O)^{WT} by using Tet(O)^{D131N}

Tet(O)^{WT} is an "EF-G like" GTPase, and has the similar ribosomal binding site as EF-G [57, 58, 76]. GTP hydrolysis cannot occur without Tet(O)^{WT} or EF-G binding to the 70S ribosome. Determination of the kinetics of GTP hydrolysis by EF-G in the presence of Tet(O)^{WT} by using Tet(O)^{D131N} may provide an indirect measure of the EF-G binding to the 70S ribosomes in the presence of Tet(O)^{WT} and insight into whether Tet(O)^{WT} competes with EF-G for binding to the 70S ribosomes.

The GTP hydrolysis by EF-G in the presence of Tet(O)^{D131N} was performed as described in section 2.10.1 with the following modifications. The 20 μL reactions containing 0.2 μM vacant 70S ribosomes, 0.05 μM EF-G and Tet(O)^{D131N}, 10-500 μM (10, 20, 50, 100, 200, 300, 400, 500 μM) of 0.5 μCi

[γ-^{32}P]GTP and non-radiolabelled XTP in reaction buffer were incubated at 37°C for 1-30 min. Three reactions were set up for each GTP concentration at different incubation times (10, 20 μM: 1, 2, 5 min; 50 μM: 2, 5, 10 min; 100, 200 μM: 5, 10, 20 min; 300, 400, 500 μM: 5, 15, 30 min). The following reactions were set as controls: 1) in the presence of Tet(O)^{WT}, to obtain the kinetics of GTP hydrolysis by Tet(O)^{WT}; 2) in the presence of EF-G, to obtain the kinetics of GTP hydrolysis by EF-G; 3) in the presence of Tet(O)^{WT} and EF-G, to obtain the kinetics of combined GTP hydrolysis by Tet(O)^{WT} and EF-G; 4) in the presence of Tet(O)^{D131N}, to obtain the kinetics of GTP hydrolysis due to by Tet(O)^{D131N}.

The velocity of the reactions, measured as the concentration (μM) of [γ-^{32}P]GTP hydrolyzed by per μM GTPases (Tet(O)^{WT} and/or EF-G) per second, was indirectly calculated according to the following equation:

$$Y = \frac{V_{[\gamma\text{-}^{32}P]Pi}}{V_{[\gamma\text{-}^{32}P]GTP} + V_{[\gamma\text{-}^{32}P]Pi}} \times \frac{Conc.\ of\ [\gamma\text{-}^{32}P]GTP}{Conc.\ of\ GTPases\ (Tet(O)^{WT}\ and/or\ EF\text{-}G)}$$

Where: Y = μM hydrolyzed [γ-^{32}P]GTP per μM GTPases

$V_{[\gamma\text{-}^{32}P]Pi}$ = signal volume of hydrolyzed [γ-^{32}P]GTP

$V_{[\gamma\text{-}^{32}P]GTP}$ = signal volume of unhydrolyzed [γ-^{32}P]GTP

[[γ-^{32}P]GTP] = 10, 20, 50, 100, 200, 300, 400, or 500 μM

[GTPases] = 0.05 μM

The Y (μM hydrolyzed [γ-^{32}P]GTP per μM GTPases) at each concentration of [γ-^{32}P]GTP was then plotted against its corresponding incubation times (10, 20 μM:

1, 2, 5 min; 50 μM: 2, 5, 10 min; 100, 200 μM: 5, 10, 20 min; 300, 400, 500 μM: 5, 15, 30 min) for subsequent linear regression analysis. The slope (a) represented the μM GTP hydrolyzed per minute when Y = aX+b, R^2>0.95, and was then divided by 60 to obtain the velocity of the GTPase reactions as $\mu M \cdot s^{-1}$.

The velocity was then plotted versus the increasing concentrations (10-500 μM) of [γ-^{32}P]GTP. The enzyme kinetic parameters (K_m, k_{cat}, V_{max}) were derived by a non-linear regression analysis using GraphPad Prism 5.0 (La Jolla, CA, USA) according to the following equation:

$$V\,(\mu M \cdot s^{-1}) = \frac{V_{max} \times [S]}{K_m + [S]}$$

Where: V ($\mu M \cdot s^{-1}$) = velocity of GTPase reaction

V_{max} ($\mu M \cdot s^{-1}$) = the maximal GTPase velocity

[S] (μM) = concentration of substrate, [γ-^{32}P]GTP

Apparent K_m (μM) = Michaelis-Menten constant, the concentration of [γ-^{32}P]GTP needed to achieve half-maximal GTPase velocity

$$k_{cat}\,(s^{-1}) = \frac{V_{max}}{[GTPase]}$$

Where: k_{cat} (s^{-1}) = turnover number per second, the number of [γ-^{32}P]GTP converted to GDP and [γ-^{32}P]Pi by GTPase (Tet(O)^{WT}/EF-G) per second when the Tet(O)^{WT}/EF-G is fully saturated with [γ-^{32}P]GTP.

[GTPase] = 0.05 μM, the concentration of Tet(O)^{WT} or EF-G

$$\textit{Specificity constant } (\mu M^{-1} \cdot s^{-1}) = \frac{k_{cat}}{K_m}$$

The specificity constant ($\mu M^{-1} \cdot s^{-1}$) was used to compare the catalytic efficiency of $Tet(O)^{WT}$ and EF-G.

2.11 Statistical analyses

Linear regression analysis was performed by Microsoft Excel (Microsoft, Redmond, WA, USA). All other statistical parameters were calculated and analyzed by using GraphPad Prism 5.0 (La Jolla, CA, USA). The results were expressed as mean ± standard deviation (SD) of 3-5 experiments. Each experiment of Tc binding assay was done in triplicate. The differences among the 4 groups were compared by One-way Analysis of Variance (1 way ANOVA), and were determined to be statistically significant when $p < 0.05$.

Table 2.1 Primers used to amplify *tet(O)*^{WT}, *tet(O)*^{D131N}, and *fusA* gene

Gene	Primers	Sequence (5'→3')
tet(O)^{WT}	P1-F	CACCAAAATAATTAACTTAGGCAT
	P1-R	**TTA**AGCTAACTTGTGGAACATATGC
tet(O)^{D131N}	P1-F	CACCAAAATAATTAACTTAGGCAT
	P2-R	TCCCCTCTTGATTAATTTTATTGA
	P2-F	TCAATAAAATT**AAT**CAAGAGGGGA
	P1-R	**TTA**AGCTAACTTGTGGAACATATGC
fusA	P3-F	CACCGCTCGTACAACACCCATC
	P3-R	**TTA**TTTACCACGGGCTTCAATTACG

Underlined sequence is the recognition site for TOPO isomerase.
Bold sequence is the recognition site for the stop codon.
Underlined bold sequence is the 131 position amino acid changed from GAC (aspartate, D, for *tet(O)*^{WT}) to AAT (asparagine, N).

Table 2.2 Primers used to amplify the DNA templates of $tRNA^{Phe}$, $tRNA^{Met}$ and $mRNA^{Phe}$

Primers	Sequence (5'→3')
$mRNA^{Phe}$(+)	**TAA TAC GAC TCA CTA TAG** GCA AGG AGG TAA AAA TG
$mRNA^{Phe}$(-)	ACG TGC GAA CAT **TTT** TAC CTC CTT GCC TAT AGT GAG TCG TAT TA
$tRNA^{Met}$(+)	**TAA TAC GAC TCA CTA TAG** GCT ACG TAG CTC AGT TGG TTA GAG CAC ATC ACT **CAT** AAT GAT GGG
$tRNA^{Met}$(-)	TGG TGG CTA CGA CGG GAT TCG AAC CTG TGA CCC CAT CAT TAT GAG T
$tRNA^{Phe}$(+)	**TAA TAC GAC TCA CTA TAG** CCC GGA TAG CTC AGT CGG TAG AGC AGG GGA TTG **AAA** ATC C
$tRNA^{Phe}$(-)	TGG TGC CCG GAC TCG GAA TCG AAC CAA GGA CAC GGG GAT TTT CAA TCC

In bold is the T7 promoter site.
Underlined sequence of $mRNA^{phe}$(+) is the recognition site for Shine-Dalgarno sequence.
Underlined bold sequence highlights the Phe codon in $mRNA^{Phe}$(-), the Met anticodon in $tRNA^{Met}$(+), and the Phe anticodon in $tRNA^{Phe}$(+).
Shaded sequences represent complementary binding between primers for the complete DNA template.

Table 2.3 Preparation of 10% SDS-PAGE gel

Components	10% Separating gel	Stacking gel
MilliQ H_2O	3.6 mL	2.0 mL
40% Acrylamide/Bis Solution 29:1	1.9 mL	0.3 mL
1.5M Tris-HCl, pH8.8	1.9 mL	-
1.0M Tris-HCl, pH6.8	-	0.313 mL
10% SDS	75 μL	25 μL
10% Ammonium Persulfate (APS)	75 μL	25 μL
TEMED	4 μL	4 μL

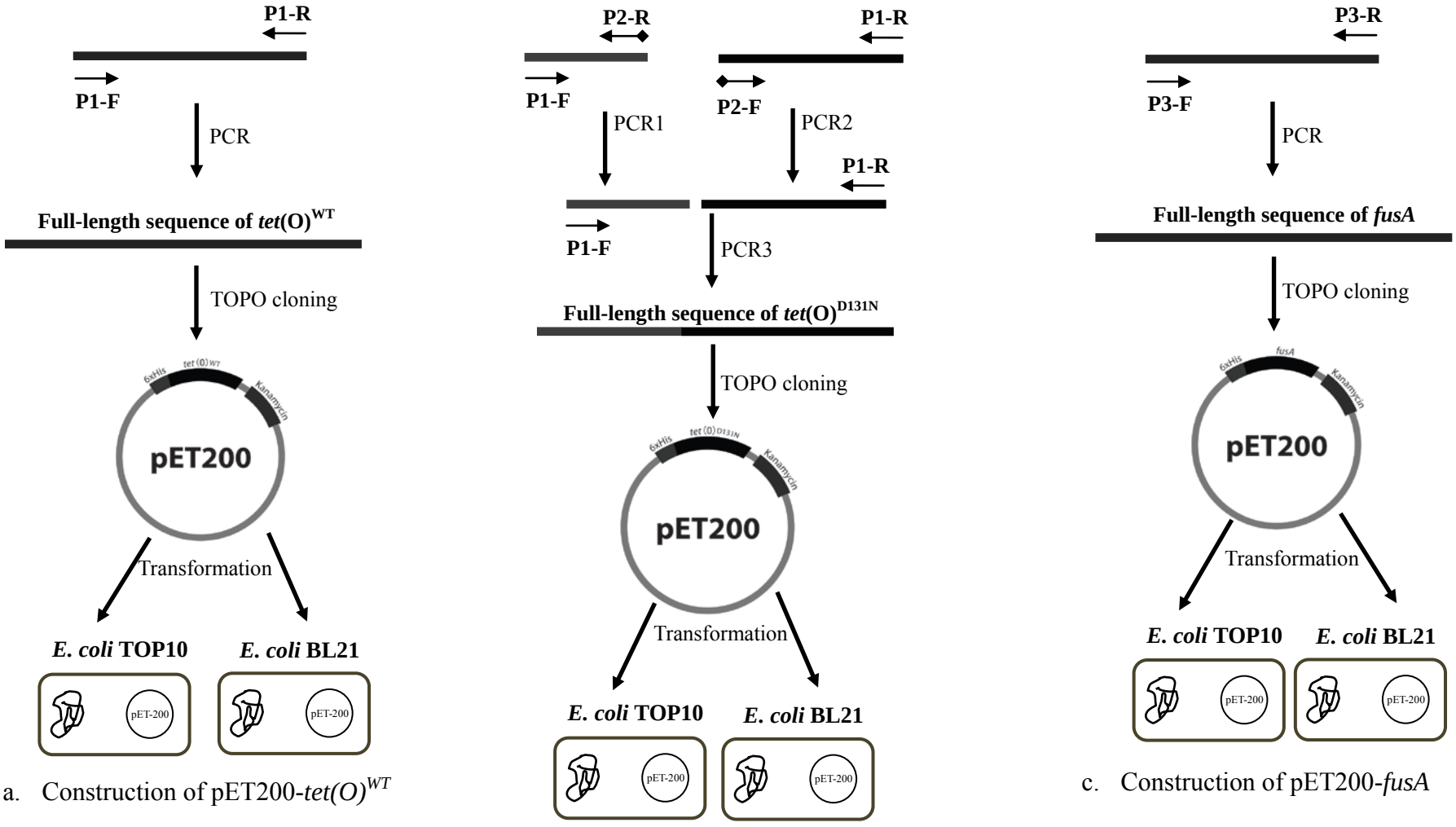

a. Construction of pET200-*tet(O)*^{WT}

b. Construction of pET200-*tet(O)*^{D131N}

c. Construction of pET200-*fusA*

Figure 2.1 Construction of pET200-*tet(O)*^{WT}, *tet(O)*^{D131N}, or *fusA*

Primers are described in Table 2.1.

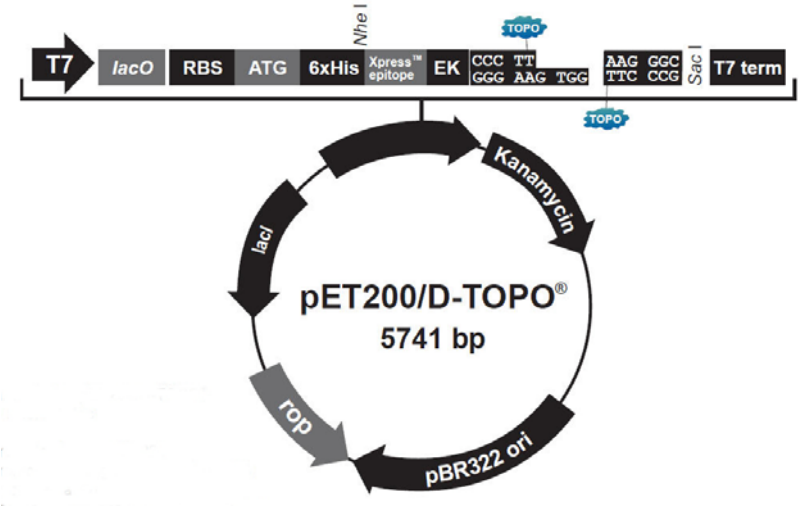

Figure 2.2 Map and features of pET 200/D-TOPO vector [103]

T7 promoter: Permits high-level, IPTG-inducible expression of recombinant protein in *E. coli* BL21(DE3) which supplies T7 RNA polymerase in a regulated manner

T7 forward priming site: Allows sequencing in the sense orientation

lac operator (lacO): Binding site for lac repressor that serves to reduce basal expression of recombinant protein

Ribosome binding site: Optimally spaced from the TOPO Cloning site for efficient translation of PCR product

ATG: Start codon

N-terminal 6×His tag: Permits purification of recombinant protein on IMAC (immobilized metal affinity chromatography). In addition, allows detection of recombinant protein with the Anti-HisG Antibodies

Xpress™ epitope (Asp-Leu-Tyr-Asp-Asp-Asp-Asp-Lys): Allows detection of the fusion protein by the Anti-Xpress™ Antibodies.

Enterokinase (EK) recognition site (Asp-Asp-Asp-Asp-Lys): Allows removal of the N-terminal tag from recombinant protein using an enterokinase such as EKMax™.

TOPO Cloning site (directional): Permits rapid cloning of PCR product for expression in *E. coli* BL21(DE3).

T7 Reverse priming site: Allows sequencing of the insert.

T7 transcription termination region: Sequence from bacteriophage T7 which permits efficient transcription termination.

Kanamycin resistance gene: Allows selection of the plasmid in *E. coli* BL21(DE3).

pBR322 origin of replication (*ori*): Permits replication and maintenance in *E. coli* BL21(DE3)

ROP ORF: Interacts with the pBR322 origin to facilitate lowcopy replication in *E. coli* BL21(DE3).

lacI ORF: Encodes lac repressor which binds to the T7*lac* promoter to block basal transcription of the gene of interest and binds to the *lacUV5* promoter to repress transcription of T7 RNA polymerase.

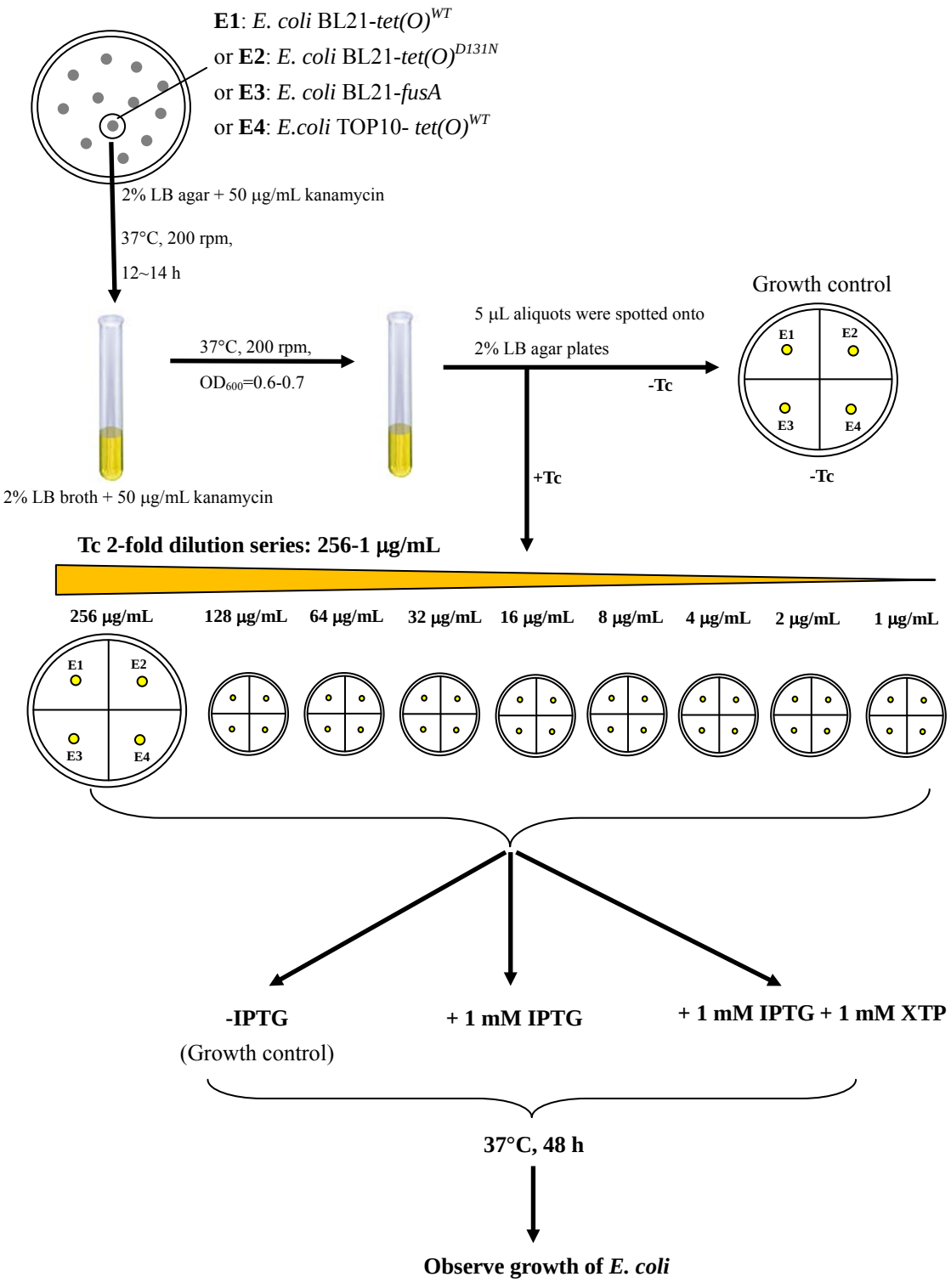

Figure 2.3 Determination of Tet(O)-mediated Tc^R *in vivo* by Tc susceptibility

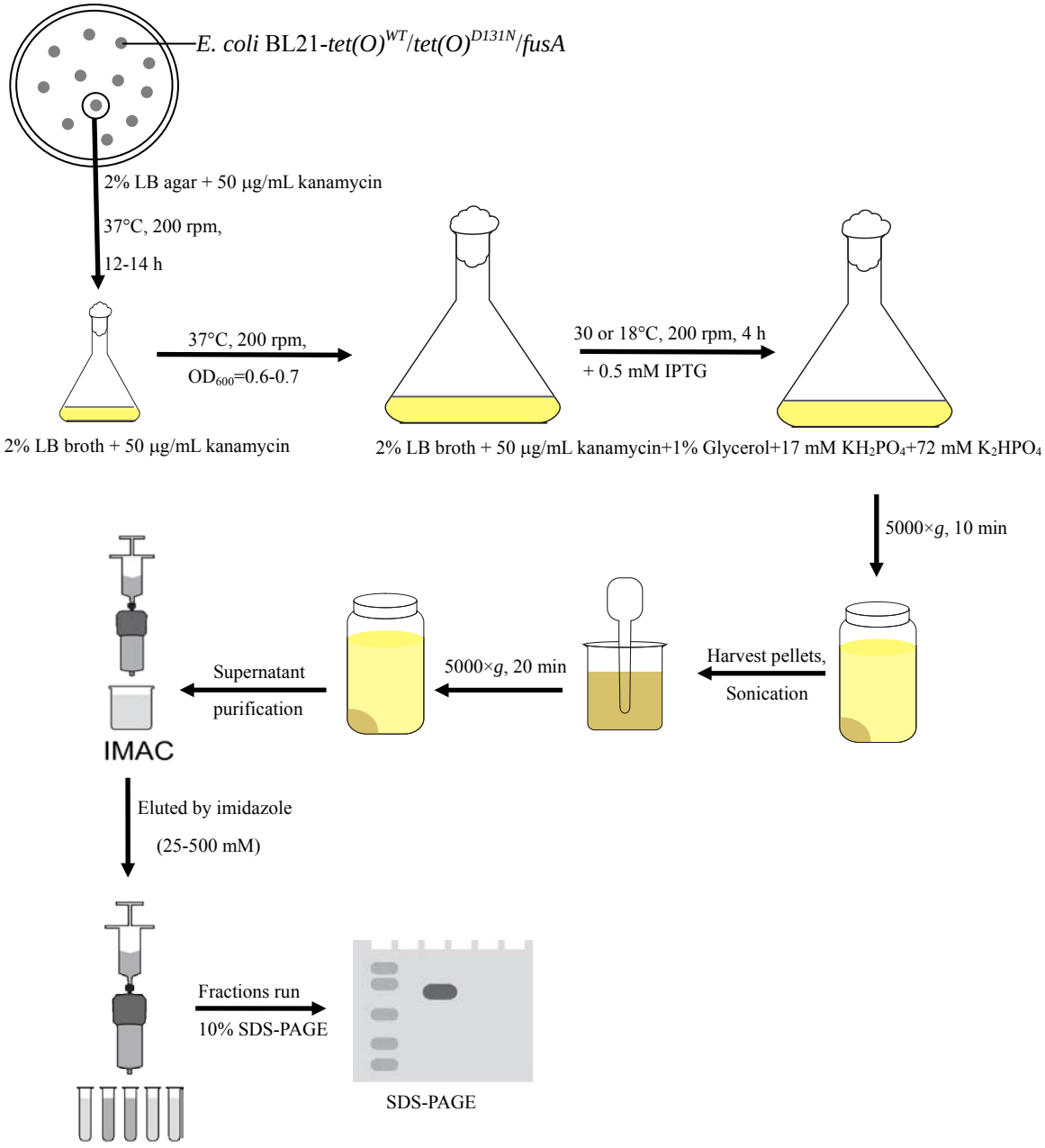

Figure 2.4 Overexpression and purification of Tet(O)^{WT}, Tet(O)^{D131N} & EF-G

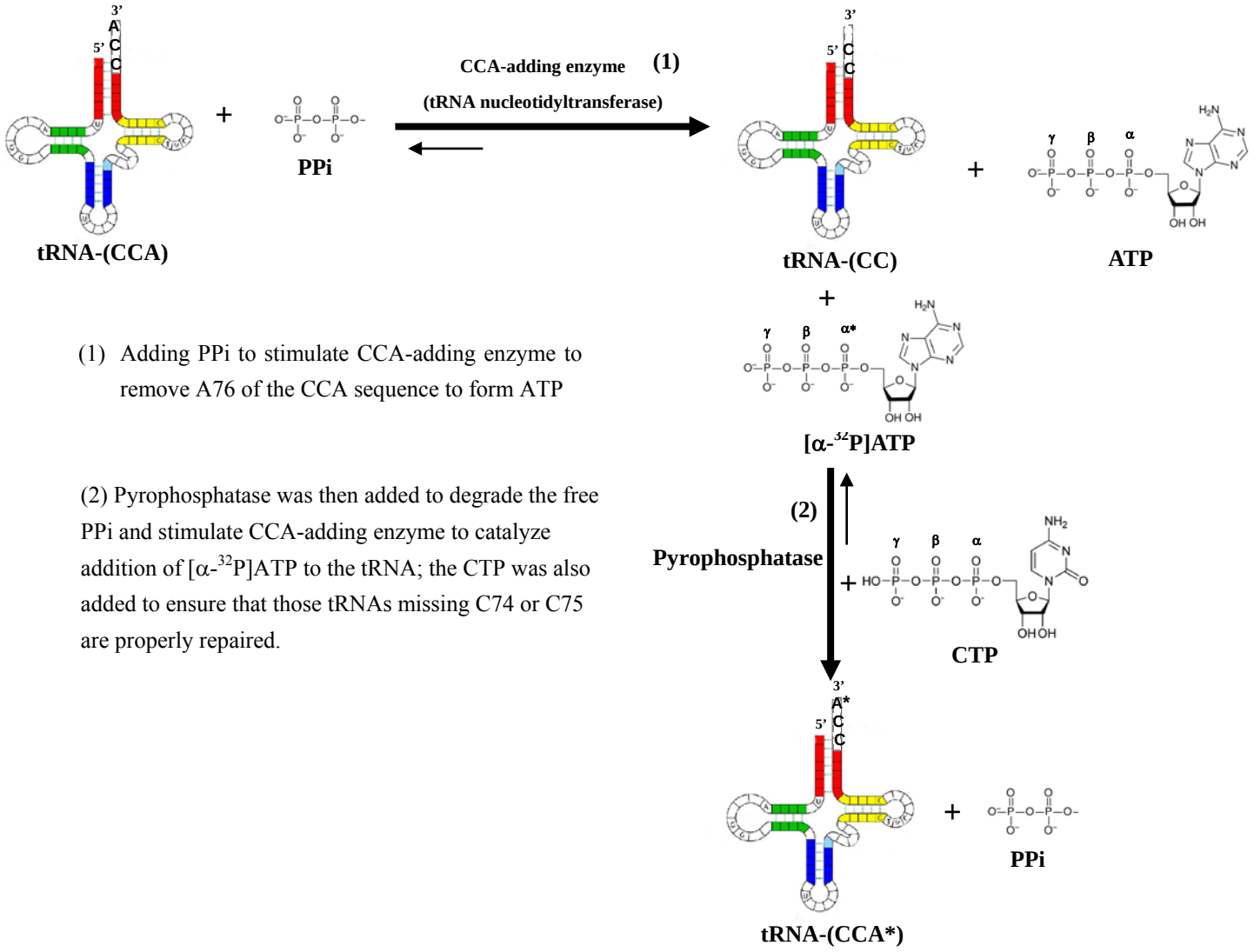

(1) Adding PPi to stimulate CCA-adding enzyme to remove A76 of the CCA sequence to form ATP

(2) Pyrophosphatase was then added to degrade the free PPi and stimulate CCA-adding enzyme to catalyze addition of [α-^{32}P]ATP to the tRNA; the CTP was also added to ensure that those tRNAs missing C74 or C75 are properly repaired.

Figure 2.5 [3'-^{32}P]-tRNA labeled by [α-^{32}P]ATP-PPi exchange

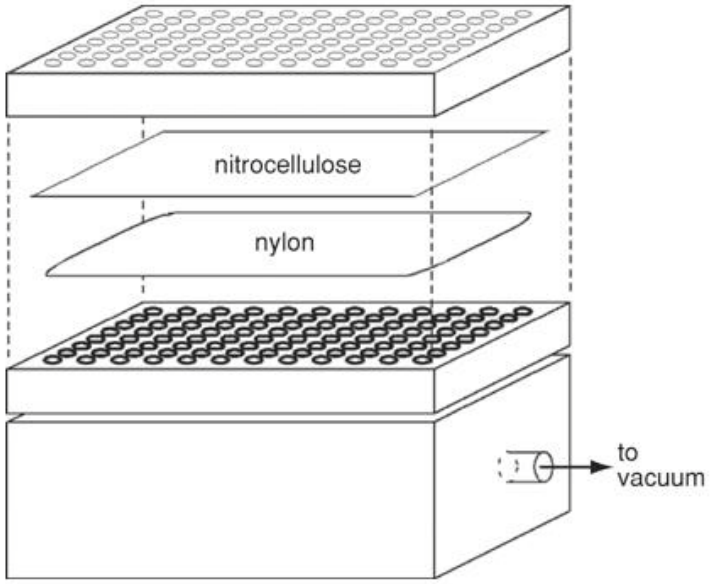

Figure 2.6 Double-filter dot-blot apparatus

An upper nitrocellulose membrane and a lower nylon membrane were sandwiched between two sets of rubber O-rings of the 96-well apparatus. The nitrocellulose membrane traps 70S ribosome- tRNA complexes; the nylon membrane traps free tRNAs.

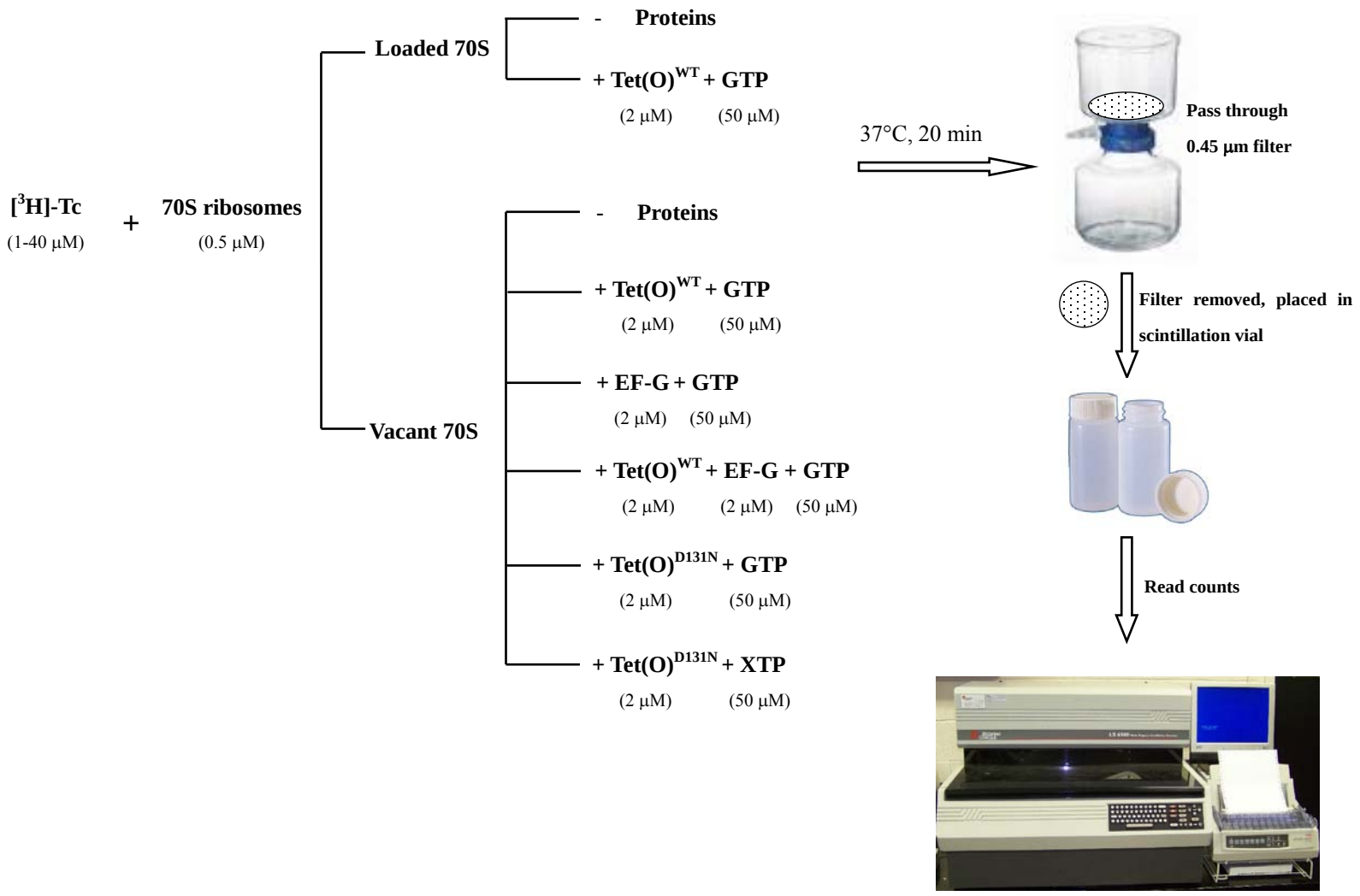

Figure 2.7 Determination of Tet(O)-mediated Tc release *in vitro* by Tc binding Assay

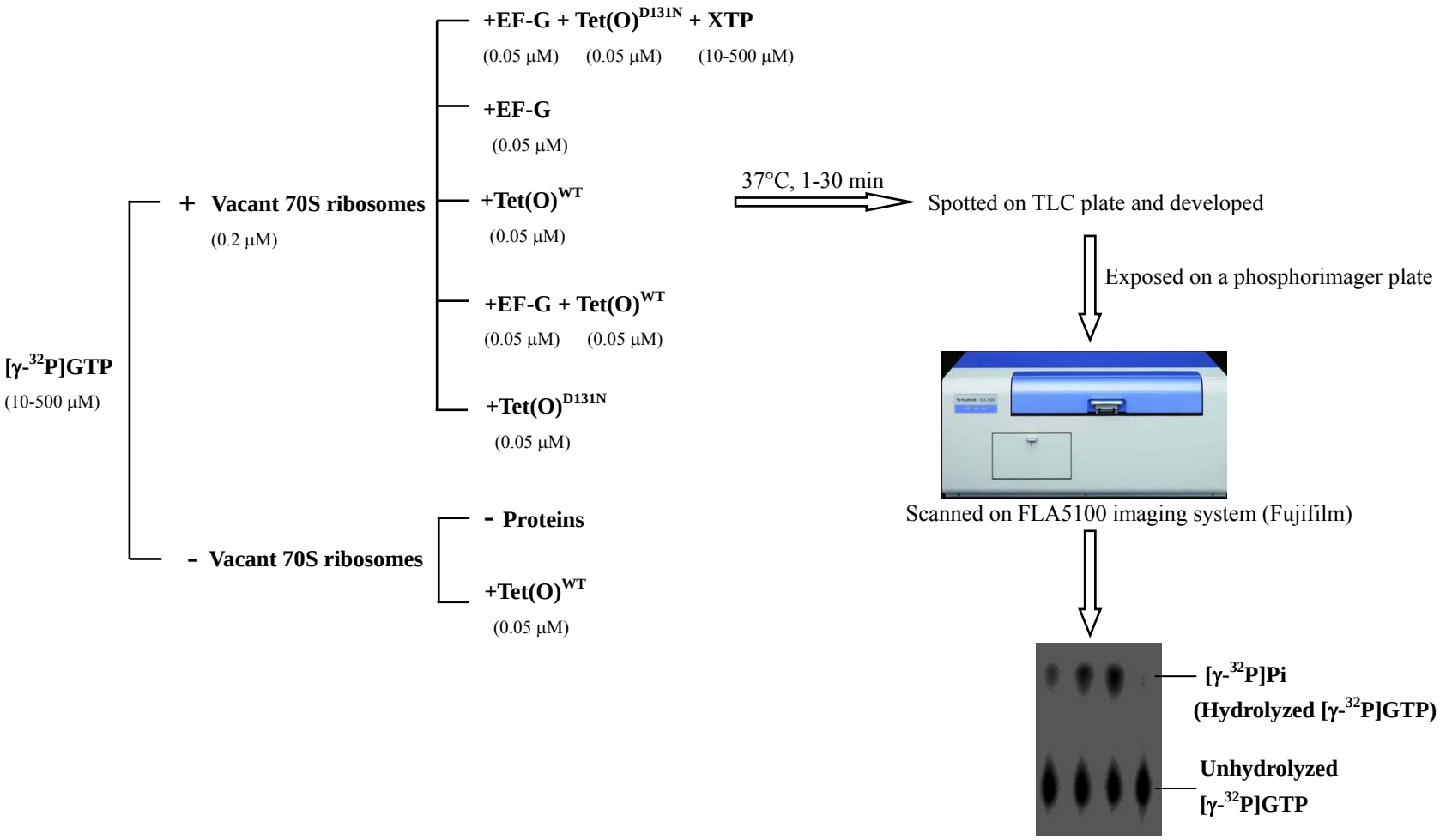

Figure 2.8 Determination of GTP hydrolysis kinetics by EF-G in the presence of Tet(O)^{WT} by using Tet(O)^{D131N}

Chapter 3 Results

3.1 *In vivo* Tc susceptibility phenotype conferred by *C. jejuni tet(O)* gene to *E. coli*

3.1.1 *C. jejuni tet(O)*^{WT} gene conferred Tc^{R} to *E. coli*

The ability of *C. jejuni tet(O)*^{WT} gene to confer Tc^{R} to *E. coli* is shown in Table 3.1. Tc^{S} *E. coli* BL21(DE3) transformed with the *fusA* gene (encodes EF-G) remained susceptible to Tc in the absence or presence of IPTG (MIC=4 μg/mL). In contrast, Tc^{S} *E. coli* BL21(DE3) became resistant to Tc when transformed with the *C. jejuni tet(O)*^{WT} gene, as observed with the 4-fold increased MIC in the absence of IPTG (16 μg/mL), and 16-fold increased MIC in the presence of IPTG (64 μg/mL).

E. coli TOP10 also became resistant to Tc when transformed with the *C. jejuni tet(O)*^{WT} gene, as demonstrated by the observed 4-fold increased MIC in the absence or presence of IPTG (16 μg/mL). This MIC was the same as observed for *E. coli* BL21(DE3) transformed with the *tet(O)*^{WT} gene in the absence of IPTG, but 4-fold less than the MIC observed in the presence of IPTG (64 μg/mL).

3.1.2 The *tet(O)*^{D131N} gene could not confer Tc^{R} to *E. coli*

E. coli BL21(DE3) remained susceptible to Tc when transformed with the

tet(O)^{D131N} gene in the absence or presence of IPTG and XTP (MIC = 8 μg/mL, Table 3.1). The MICs of *E. coli* BL21(DE3) transformed with *tet(O)*^{WT} or *fusA* gene, or *E. coli* TOP10 transformed with *tet(O)*^{WT} gene did not change in the presence of XTP.

3.2 Tet(O)^{WT}, Tet(O)^{D131N}, and EF-G were successfully overexpressed and purified

The three recombinant proteins Tet(O)^{WT}, Tet(O)^{D131N}, and EF-G were successfully overexpressed in soluble form in *E. coli* BL21(DE3) following IPTG induction at sub-optimal growth temperature. The proteins were then individually purified by immobilized metal affinity chromatography (IMAC) using a HisTrap HP Ni^{2+} column and eluted with increasing concentration of imidazole. The purified proteins were greater than 90% pure as assessed by 10% SDS-PAGE (Figure 3.1) with molecular weights around 70 kD, corresponding to the previously reported sizes of these proteins: 72.5 kDa for Tet(O)^{WT} and Tet(O)^{D131N} [72], and 77.5 kDa for EF-G [73]. The protein concentrations of purified Tet(O)^{WT}, Tet(O)^{D131N}, and EF-G were 3.0 mg/mL (41.3 μM), 1.5 mg/mL (20.7 μM), and 5.4 mg/mL (69.6 μM) respectively, as determined by the Bradford protein assay. The standard curve was shown in Figure 3.2. The overall yield of Tet(O)^{WT} was 11-13 mg from ~20 g (0.5-0.6 mg/g) of wet cell mass obtained from 2 L of the culture, while the yield of Tet(O)^{D131N} (0.2-0.3 mg/g) was about half of

Tet(O)^{WT}. In contrast, a much higher yield was obtained for EF-G (16-18 mg from ~2 g of wet cell mass obtained from 0.2 L of the culture, 8-9 mg/g).

3.3 tRNA was bound to the P- and A-site of mRNA programmed ribosome to generate loaded 70S ribosome complexes

PCR products (~100 bp) of DNA templates of tRNA^{Phe}, tRNA^{Met} and mRNA^{Phe} were successfully generated as shown in Figure 3.3. A representative gel demonstrating the successful transcription of the DNA templates was shown for transcription products of mRNA^{Phe} and tRNA^{Phe} (Figure 3.4). Sufficient yields of the transcription products were obtained for mRNA^{Phe} (95.9 μM), P-site tRNA (tRNA^{Met}, 56.1 μM), and A-site tRNA (tRNA^{Phe}, 46.1 μM). The tight-coupled 70S ribosomes were successfully prepared and purified on sucrose gradient as shown in Figure 3.5. This final vacant 70S ribosome concentration was 34.5 μM.

The vacant 70S ribosomes were programmed with mRNA^{Phe}, and then assembled with [3'-^{32}P]tRNA^{Met} and [3'-^{32}P]tRNA^{Phe}. The association of tRNAs to the P-site and A-site of mRNA-programmed ribosomes were shown in Figure 3.6**.** The high percent association of tRNAs to the P-site (80.6-85.1%) and A-site (76.4-90.6%) of mRNA-programmed ribosomes confirmed the successful preparation of mRNA programmed 70S ribosome-tRNAs complexes (loaded 70S ribosomes).

3.4 Tet(O) mediated Tc release from 70S ribosomes

3.4.1 Tet(O)-mediated Tc release was similar from loaded or vacant 70S ribosomes

The binding affinity of Tc to the loaded or vacant 70S ribosomes was determined in the absence and presence of $Tet(O)^{WT}$ and GTP. The binding affinity was described by the dissociation constant, K_d, which is inversely proportional to the relative binding affinity of Tc to the ribosomes. A high K_d indicates low binding affinity of Tc to the ribosomes, while a low K_d represents high binding affinity of Tc to the ribosomes.

The nonspecific binding of [^{3}H]-Tc to 0.45 μm nitrocellulose filters in the absence of ribosomes and purified proteins, increased linearly with the increasing concentration of [^{3}H]-Tc (Figure 3.7). The specific binding of [^{3}H]-Tc to 70S ribosomes was determined following subtraction of the nonspecific background activity from the total [^{3}H]-Tc activity.

The K_d of [^{3}H]-Tc binding to the vacant 70S ribosomes in the absence of $Tet(O)^{WT}$ was 2.9±0.7 μM, which represented the maximal binding affinity of Tc to 70S ribosomes. In contrast, the K_d of [^{3}H]-Tc binding to the vacant 70S ribosomes in the presence of $Tet(O)^{WT}$ and GTP was increased ~3.6-fold to 10.6±4.1 μM (Figure 3.8a, Table 3.2). This demonstrated that the presence of $Tet(O)^{WT}$ • GTP decreased the binding affinity of Tc to the ribosomes, and therefore was responsible for the release of Tc from 70S ribosomes.

The K_d of [^{3}H]-Tc binding to the loaded 70S ribosomes in the absence (3.7±1.4 μM) and presence (7.7±2.2 μM) (Figure 3.8b, Table 3.2) of Tet(O)^{WT} and GTP was not significantly different (p>0.05) from vacant 70S ribosomes.

3.4.2 EF-G interfered with Tet(O)-mediated Tc release

The low K_d (2.8±0.8 μM) of [^{3}H]-Tc binding to the 70S ribosomes in the presence of EF-G (Figure 3.9b, Table 3.3) was not significantly different (p>0.05) from the K_d (2.9±0.7 μM) of [^{3}H]-Tc binding to the 70S ribosomes alone (Figure 3.9a, Table 3.3). This demonstrates that EF-G cannot release bound Tc from 70S ribosomes. In contrast, when both EF-G and Tet(O)^{WT} were present in equal concentrations, the K_d (5.6±2.8 μM) of [^{3}H]-Tc binding to the ribosomes (Figure 3.9b, Table 3.3) was increased about 2-fold as compared to the K_d with only EF-G present (p<0.05). However, the K_d in the presence of EF-G and Tet(O)^{WT} was still ~1.9-fold lower than the K_d (10.6±4.1 μM) with only Tet(O)^{WT} present (p<0.05, Figure 3.9a, Table 3.3).

3.4.3 Tet(O)^{D131N}-mediated Tc release was XTP dependent

The low K_d (3.0±1.0 μM) of [^{3}H]-Tc binding to the 70S ribosomes in the presence of Tet(O)^{D131N} and GTP (Figure 3.10b, Table 3.4) was not significantly different (p>0.05) from the K_d (2.9±0.7 μM) of [^{3}H]-Tc binding to the ribosomes alone (Figure 3.10a, Table 3.4). This demonstrated that Tet(O)^{D131N} could not use

GTP as the substrate to release bound Tc from 70S ribosomes. In contrast, when Tet(O)^{D131N} was present with XTP, the K_d was increased to 9.1±4.3 μM (Figure 3.10b, Table 3.4), and it was not significantly different (p>0.05) from the K_d (10.6±4.1 μM) of [^{3}H]-Tc binding to the ribosomes with Tet(O)^{WT} and GTP present (Figure 3.10a, Table 3.4). The increased K_d demonstrated that the ability of Tet(O)^{D131N} to promote bound Tc release from 70S ribosomes is similar to Tet(O)^{WT}, but depended on the presence of XTP not GTP.

3.5 GTP hydrolysis of Tet(O)^{WT} and EF-G

3.5.1 Time course of GTP hydrolysis of Tet(O)^{WT}

The time course test showed that GTP hydrolysis of Tet(O)^{WT} increased linearly in the first 30 min (Figure 3.11). It suggested that the optimal incubation time should be ≤ 30 min for the kinetics studies of GTP hydrolysis by Tet(O)^{WT}.

3.5.2 Tet(O)^{D131N} could not hydrolyze GTP

Tet(O)^{D131N} could not hydrolyze [γ-^{32}P]GTP in the presence of 70S ribosomes as shown in Figure 3.12, which demonstrated that Tet(O)^{D131N} is not GTPase. In contrast, the control in the presence of Tet(O)^{WT} and 70S ribosomes can hydrolyze [γ-^{32}P]GTP, and it demonstrated Tet(O)^{WT} is a ribosome-dependent GTPase. Similar to Tet(O)^{D131N} in the presence of 70S ribosomes, the control in presence of Tet(O)^{WT} and absence of 70S ribosomes could not hydrolyze

[γ-^{32}P]GTP, and it demonstrated GTP hydrolysis of Tet(O)^{WT} was ribosome dependent. The control in the absence of purified proteins (Tet(O)^{WT}/ Tet(O)^{D131N}) and 70S ribosomes could not hydrolyze [γ-^{32}P]GTP, and it demonstrated [γ-^{32}P]GTP was not auto-hydrolyzed.

3.5.3 Catalytic efficiency of Tet(O)^{WT} for GTP was higher than EF-G

The affinity (apparent K_m) of Tet(O)^{WT} for GTP (69.0±19.8 μM) was similar to (p>0.05) that of EF-G (81.5±16.0 μM), but the catalytic efficiency (k_{cat}/K_m) of Tet(O)^{WT} for GTP (0.51±0.14 $\mu M^{-1}\cdot s^{-1}$) was ~1.5-fold higher than that of EF-G (0.33±0.10 $\mu M^{-1}\cdot s^{-1}$) (p<0.05). When Tet(O)^{WT} was present with EF-G in equal concentrations, the apparent K_m or k_{cat} of the mixture appeared to be equal to the sum of the individual apparent K_m or k_{cat}; the k_{cat}/K_m of the mixture was ~1.3-fold lower than Tet(O)^{WT} alone (p<0.05), but was not significantly different from EF-G alone (p>0.05) (Figure 3.13a, Table 3.5).

3.5.4 Tet(O)^{D131N} did not affect GTP hydrolysis by EF-G

The affinity (apparent K_m) and catalytic efficiency (k_{cat}/K_m) of EF-G for GTP in the absence of Tet(O)^{D131N} (81.5±16.0 μM, 0.33±0.10 $\mu M^{-1}\cdot s^{-1}$) was similar to that in the presence of Tet(O)^{D131N} and XTP (67.3±17.4 μM, 0.41±0.11 $\mu M^{-1}\cdot s^{-1}$) (p>0.05) (Figure 3.13b, Table 3.5). When Tet(O)^{D131N} and EF-G were present in equal concentrations, Tet(O)^{D131N} did not affect GTP hydrolysis by EF-G.

Table 3.1 *C. jejuni tet(O)*^{WT} gene conferred Tc^{R} to Tc susceptible *E. coli*

	Tc MIC[a] (μg/mL)			
	E. coli BL21-*fusA*	*E. coli* BL21-*tet(O)*^{WT}	*E. coli* TOP10-*tet(O)*^{WT}	*E. coli* BL21-*tet(O)*^{D131N}
-IPTG	4	16	16	8
+IPTG	4	64	16	8
+IPTG+XTP	4	64	16	8

[a] MIC≥16 μg/mL is defined as Tc^{R}

Table 3.2 The binding of [^{3}H]-Tc to vacant and loaded 70S ribosomes in the absence or presence of Tet(O)^{WT}

Conditions	K_d (μM)	*p* value
Vacant 70S	2.9±0.7	-
Loaded 70S	3.7±1.4	-
Vacant 70S+Tet(O)^{WT}+GTP	10.6±4.1	0.004*
Loaded 70S+Tet(O)^{WT}+GTP	7.7±2.2	0.005†

Values represent mean±SD

*: vs vacant 70S

†: vs loaded 70S

Table 3.3 The binding of [^{3}H]-Tc to vacant 70S ribosomes in the absence or presence of Tet(O)^{WT} and/or EF-G

Conditions	Kd (μM)	*p* value
70S	2.9±0.7	-
70S+EF-G+GTP	2.8±0.8	-
70S+Tet(O)^{WT}+GTP	10.6±4.1	0.004*
70S+Tet(O)^{WT}+EF-G+GTP	5.6±2.8	0.001*, 0.03†

Values represent mean±SD

*: vs 70S

†: vs 70S+Tet(O)^{WT}+GTP

Table 3.4 The binding of [^{3}H]-Tc to vacant 70S ribosomes in the absence or presence of Tet(O)^{D131N} and GTP/XTP

Conditions	Kd (μM)	*p* value
70S	2.9±0.7	-
70S+Tet(O)^{D131N}+GTP	3.0±1.0	-
70S+Tet(O)^{WT}+GTP	10.6±4.1	0.004*
70S+Tet(O)^{D131N}+XTP	9.1±4.3	0.002*

Values represent mean±SD

*: vs 70S

Table 3.5 Kinetic parameters of GTP hydrolysis of Tet(O)^{WT} or EF-G in the absence or presence of Tet(O)^{D131N}

Conditions	K_m (μM)	k_{cat} (s^{-1})	k_{cat}/K_m ($\mu M^{-1} \cdot s^{-1}$)	V_{max} ($\mu M \cdot s^{-1}$)
+Tet(O)^{WT}	69.0±19.8 *	35.0±2.8 *	0.51±0.14	1.75 *
+EF-G	81.5±16.0 *	26.6±1.6 *†	0.33±0.10 †	1.33 * †
+Tet(O)^{D131N}+EF-G	67.3±17.4 *	27.5±2.0 * †	0.41±0.11 †	1.37 * †
+Tet(O)^{WT}+EF-G	162.9±51.1	61.8±10.4	0.38±0.15 †	3.09

n=4, values represent mean±SD

* $p<0.05$, vs +Tet(O)^{WT}+EF-G

† $p<0.05$, vs +Tet(O)^{WT}

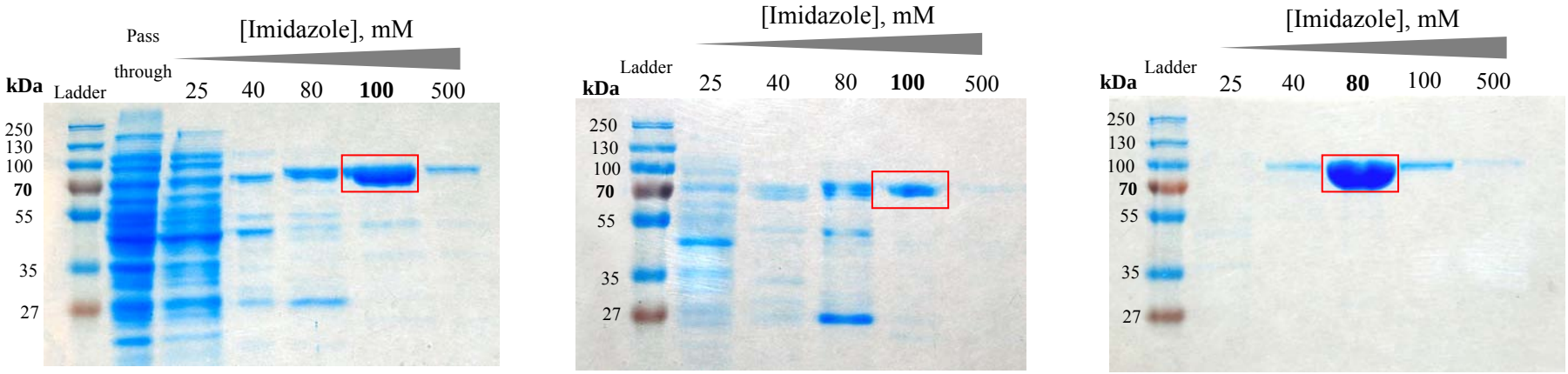

a. Tet(O)^{WT} **b. Tet(O)^{D131N}** **c. EF-G**

Figure 3.1 10% SDS-PAGE of purified Tet(O)^{WT}, Tet(O)^{D131N}, and EF-G

a. Tet(O)^{WT} was eluted at 100 mM imidazole, MW 72.5 kDa.
b. Tet(O)^{D131N} was eluted at 100 mM imidazole, MW 72.5 kDa.
c. EF-G was eluted at 80 mM imidazole, MW 77.5 kDa.

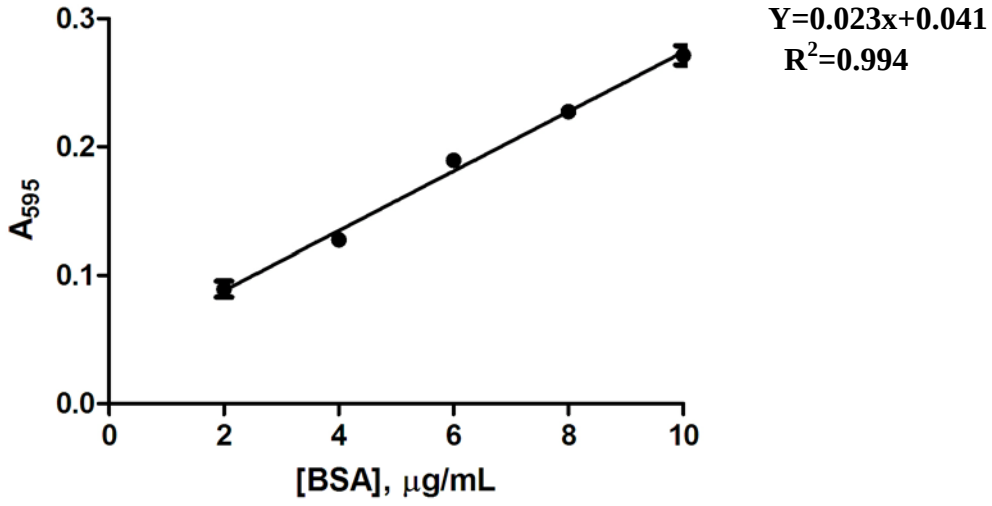

Figure 3.2 Standard curve of Bradford protein assay

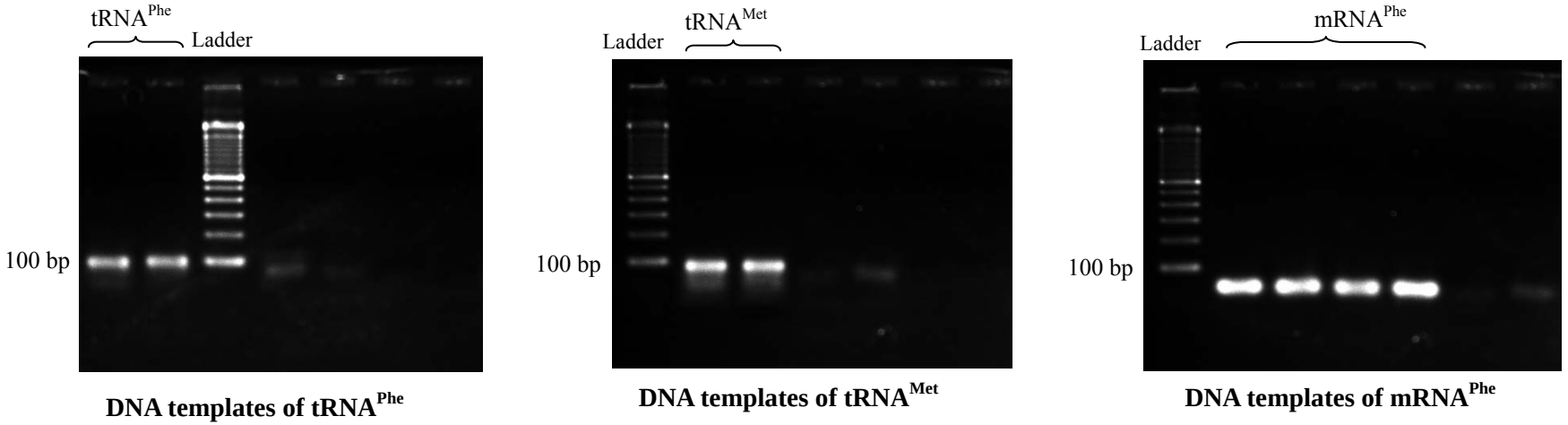

Figure 3.3 PCR products of DNA templates of $tRNA^{Phe}$, $tRNA^{Met}$ and $mRNA^{Phe}$ on 3% agarose gel

The gel was stained with ethidium bromide, and visualized under UV light.

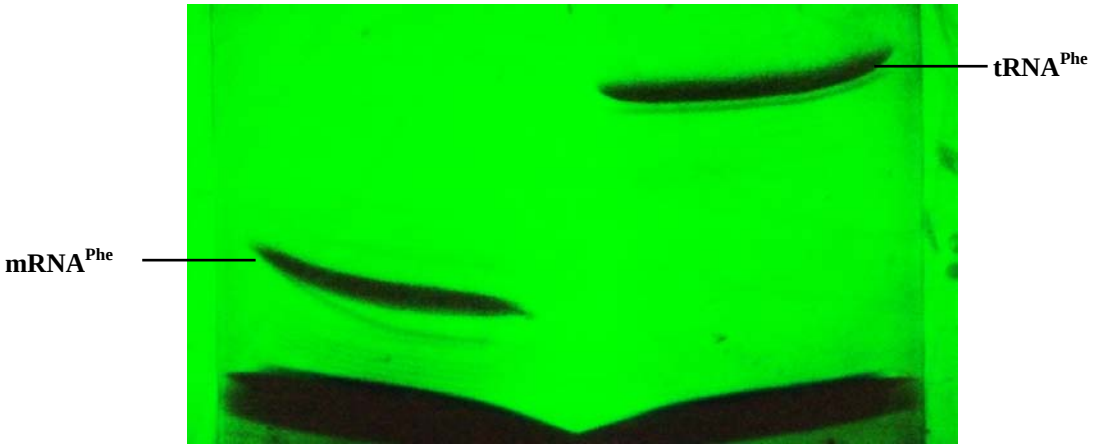

Figure 3.4 Transcribed mRNA^{Phe} and tRNA^{Phe} on 10% denaturing acrylamide gel visualized on a fluor-coated TLC plate by UV shadowing

The fluor-coated TLC plate appeared green; tRNA and mRNA were visualized as dark bands under the UV light.
The identical gel was obtained for tRNA^{Phe} and tRNA^{Met}.

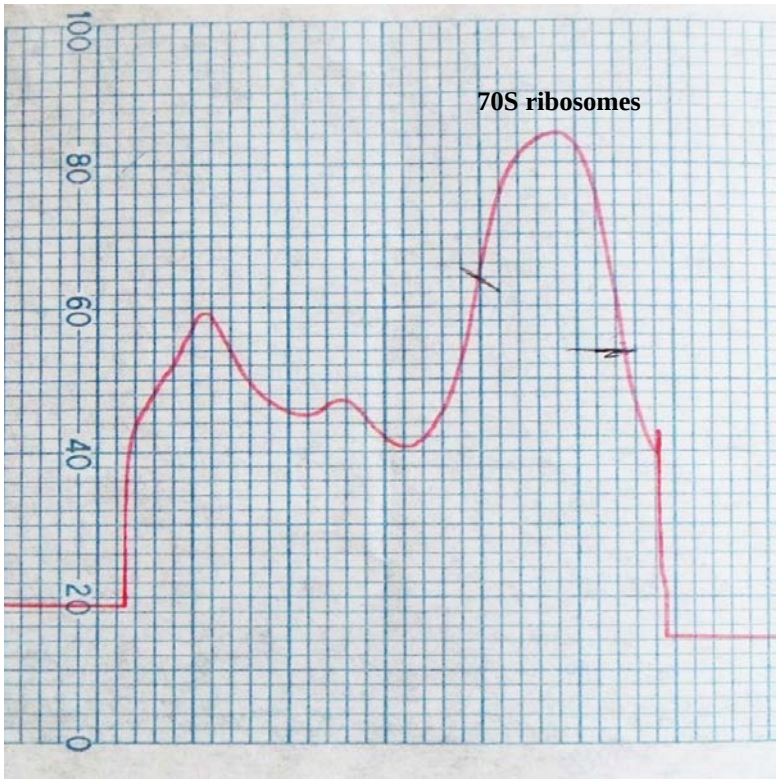

Figure 3.5 Tight-coupled 70S ribosomes in 10-40% sucrose gradient solution were identified and collected under a UV detector at 260 nm

a) Association of [3'-^{32}P]tRNA^{Met} to the ribosomal P-site

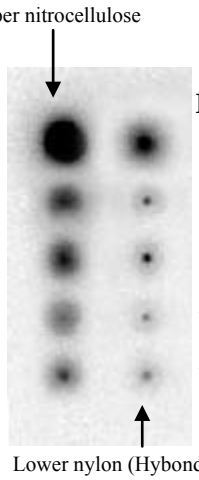

Dilution	Washed	% Bound
No	Yes	83.9
5 ×	No	84.7
5 ×	Yes	80.9
10 ×	No	85.1
10 ×	Yes	80.6

b) Association of [3'-^{32}P]tRNA^{Phe} to the ribosomal A-site

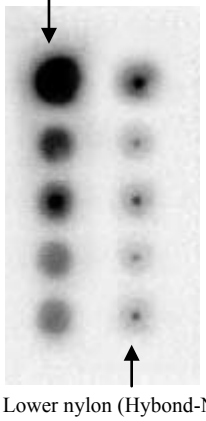

Dilution	Washed	% Bound
No	Yes	90.6
5 ×	No	87.8
5 ×	Yes	83.4
10 ×	No	83.6
10 ×	Yes	76.4

Figure 3.6 Association of [3'-^{32}P]tRNA^{Met} and [3'-^{32}P]tRNA^{Phe} to the P- and A-site of mRNA-programmed 70S ribosomes

Upper nitrocellulose membrane: traps tRNAs associated to the mRNA-programmed 70S ribosome
Lower nylon membrane: traps tRNAs dissociated from the mRNA-programmed 70S ribosome
Binding was assessed in original and diluted samples with and without washing the filter. Dilution was done to prevent filter saturation and induce dissociation of weakly bound tRNAs. Washing was done to remove loosely associated tRNAs from mRNA-programmed 70S ribosomes.

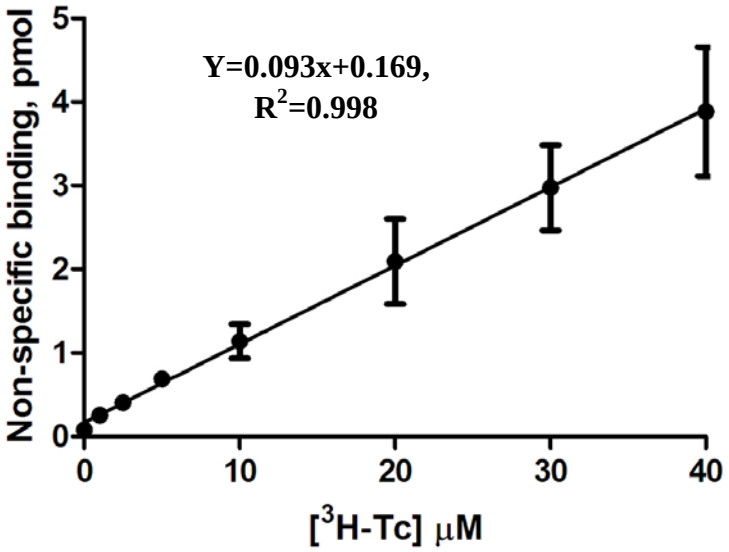

Figure 3.7 Non-specific binding of [^{3}H]-Tc (1-40 μM) to 0.45 μm nitrocellulose filters

n=4 experiments. Each experiment was done in triplicate. The values represent mean±SD.

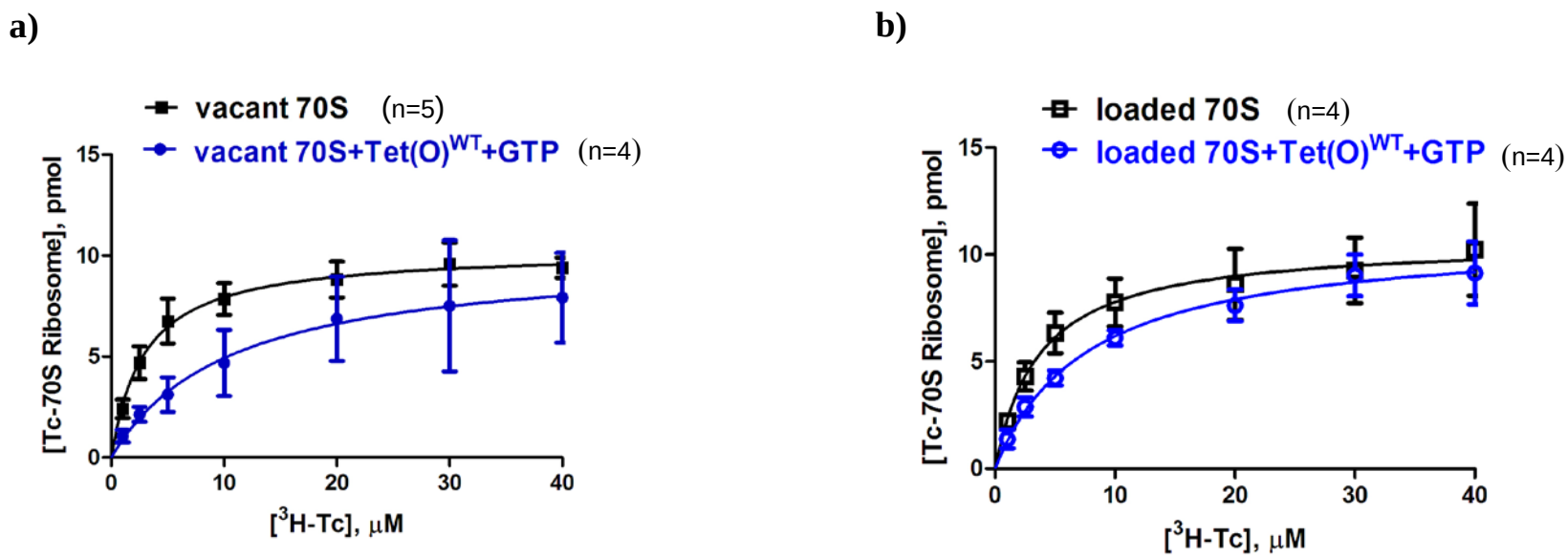

Figure 3.8 Binding of [^{3}H]-Tc to vacant and loaded 70S ribosomes in the absence and presence of Tet(O)^{WT}

The reactions were performed at increasing concentrations (1-40 μM) of [^{3}H]-Tc in the presence of: a) 0.5 μM vacant 70S ribosomes (■) , or 0.5 μM vacant 70S ribosomes + 2 μM Tet(O)^{WT} + 50 μM GTP (●); b) 0.5 μM loaded 70S ribosomes (□), or 0.5 μM loaded 70S ribosomes+ 2 μM Tet(O)^{WT} + 50 μM GTP (○).
Each experiment was done in triplicate. The values represent mean±SD.

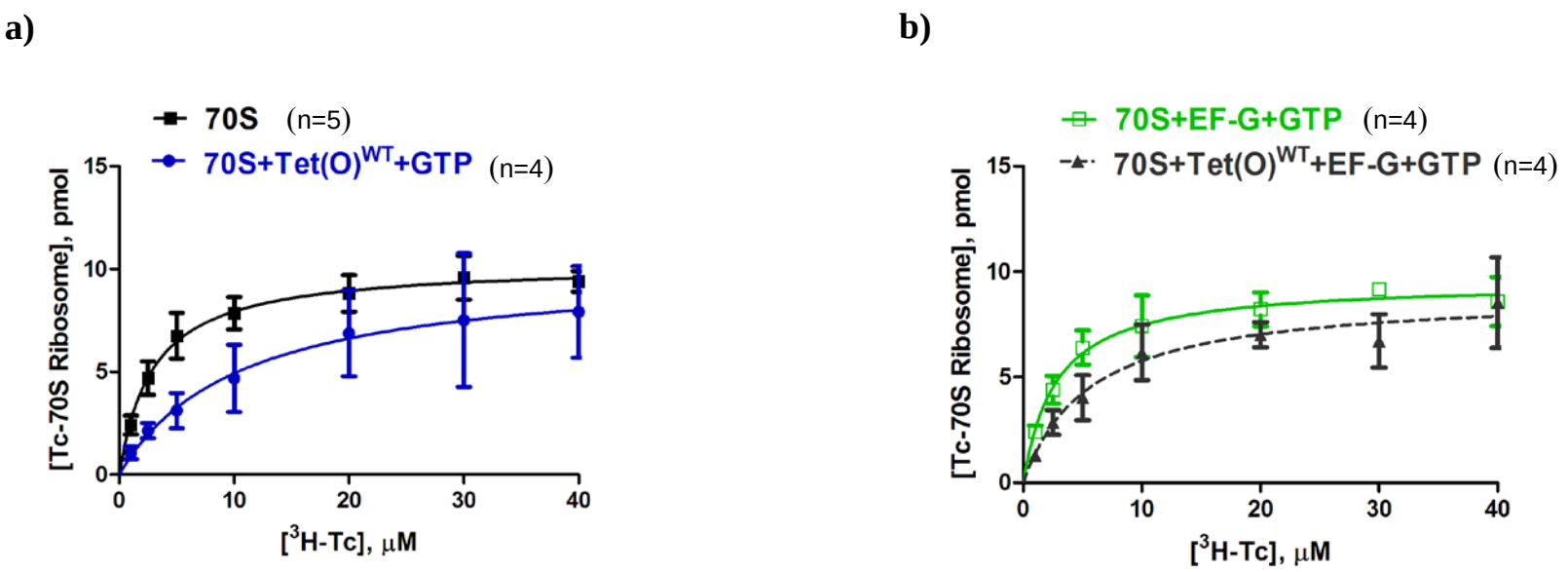

Figure 3.9 Binding of [^{3}H]-Tc to vacant 70S ribosomes in the absence and presence of Tet(O)^{WT} and/or EF-G

The reactions were performed at increasing concentrations (1-40 μM) of [^{3}H]-Tc with 0.5 μM vacant 70S ribosomes: a) in the absence of Tet(O)^{WT} or EF-G (■), or in the presence of 2 μM Tet(O)^{WT} + 50 μM GTP (●); b) in the presence of 2 μM EF-G + 50 μM GTP (□), or 2 μM Tet(O)^{WT}+ 2 μM EF-G + 50 μM GTP (▲).
Each experiment was done in triplicate. The values represent mean±SD.

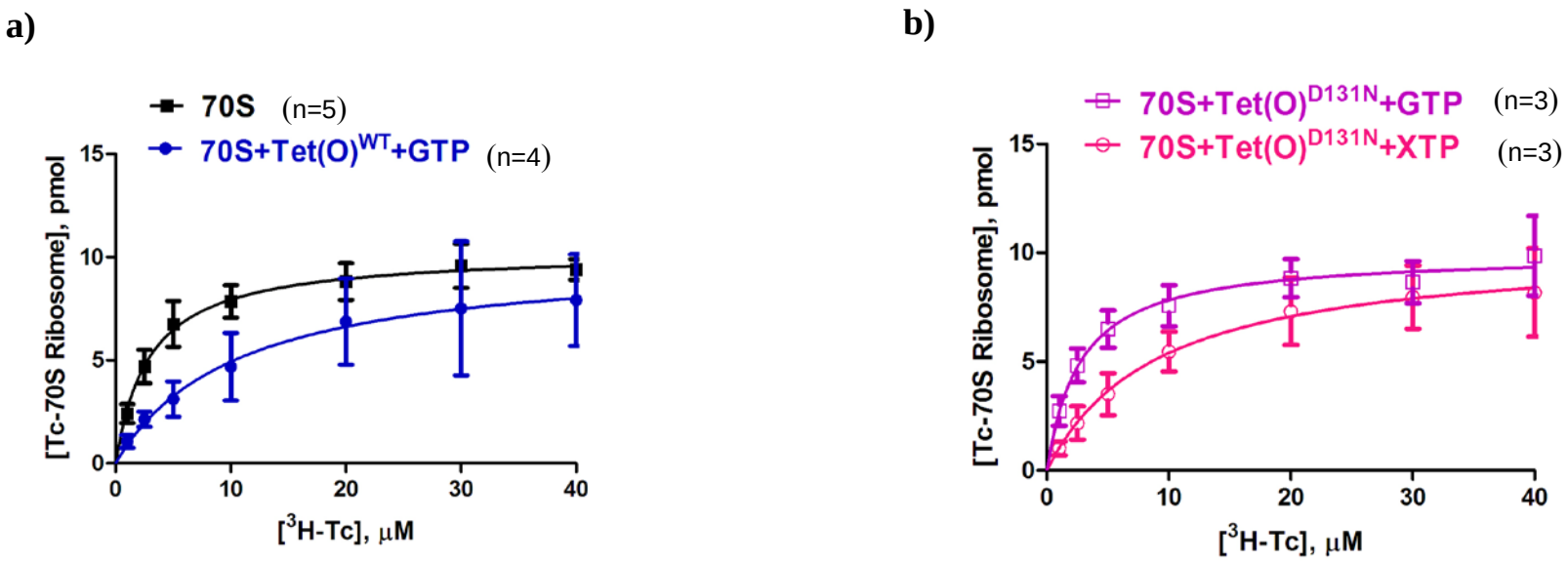

Figure 3.10 Binding of [^{3}H]-Tc to vacant 70S ribosomes in the presence of Tet(O)^{D131N} and GTP/XTP

The reactions were performed at increasing concentrations (1-40 μM) of [^{3}H]-Tc with 0.5 μM vacant 70S ribosomes: a) in the absence of Tet(O)^{WT} or Tet(O)^{D131N} (■), or in the presence of 2 μM Tet(O)^{WT} + 50 μM GTP (●); b) in the presence of 2 μM Tet(O)^{D131N} + 50 μM GTP (□), or 2 μM Tet(O)^{D131N} + 50 μM XTP (○).

Each experiment was done in triplicate. The values represent mean±SD.

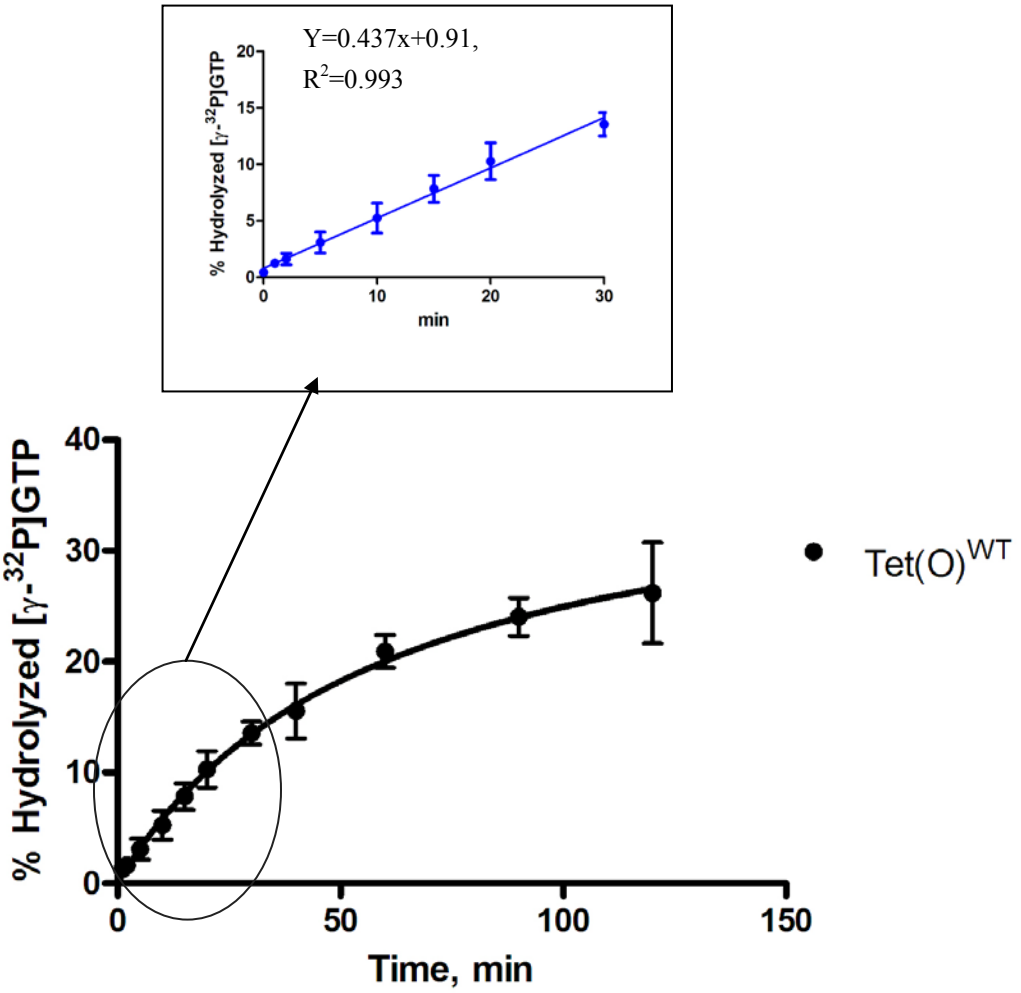

Figure 3.11 Time course of GTP hydrolysis of Tet(O)^{WT}

n=4, values represent mean±SD
The reactions containing 0.2 μM 70S ribosomes, 0.05 μM Tet(O)^{WT}, and 200 μM [γ-^{32}P]GTP were incubated at 37°C for 1, 2, 5, 10, 15, 20, 30, 40, 60, 90, 120 min.

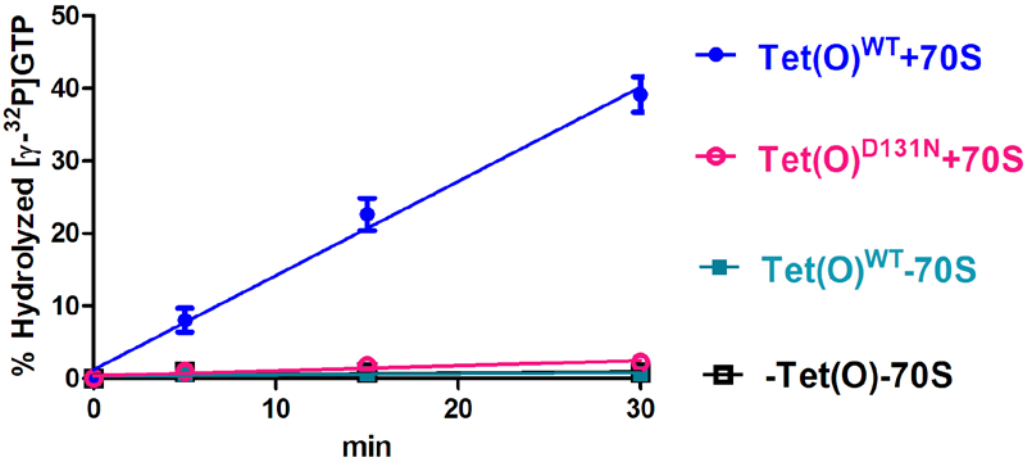

Figure 3.12 GTP hydrolysis of Tet(O)^{D131N}

n=4, values represented mean ± SD

The reactions were performed at 37°C for 5 min, 15min, 30 min at concentrations of 200 μM [γ-^{32}P]GTP in the presence of 0.05 μM Tet(O)^{WT} and 0.2 μM 70S ribosomes (●), or 0.05 μM Tet(O)^{D131N} and 0.2 μM 70S ribosomes (○), or 0.05 μM Tet(O)^{WT} alone (■), or in the absence of Tet(O) and 70S ribosome (□).

a)

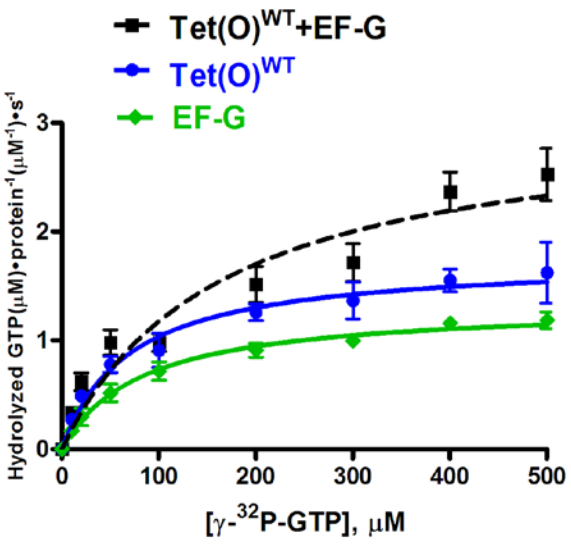

b)

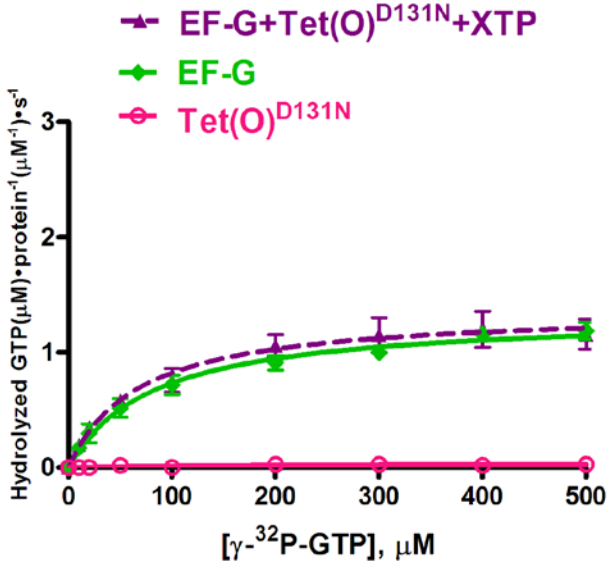

Figure 3.13 GTP hydrolysis of Tet(O)^{WT} and/or EF-G in the absence or presence of Tet(O)^{D131N}

The reactions were performed at concentrations of 10-500 μM of [γ-^{32}P]GTP and 0.2 μM vacant 70S ribosomes in the presence of : a) 0.05 μM EF-G (◆), or 0.05 μM Tet(O)^{WT} (●), or 0.05 μM Tet(O)^{WT}+0.05 μM EF-G (■); b) 0.05 μM Tet(O)^{D131N} (○), or 0.05 μM EF-G (◆), or 0.05 μM Tet(O)^{D131N}+0.05 μM EF-G+10-500 μM XTP (▲)

n=4, values represented mean±SD

Chapter 4 Discussion

4.1 *C. jejuni tet(O)^{WT}* gene conferred Tc^R to Tc^S *E. coli*

As expected, transformation with the *fusA* gene maintained Tc susceptible phenotype, which demonstrated that transformation of *E. coli* BL21(DE3) with the vector containing the gene encoding EF-G could not confer resistance to Tc.

Transformation with *C. jejuni tet(O)^{WT}* gene conferred Tc^R to Tc^S *E. coli* BL21(DE3) and *E. coli* TOP10, but IPTG-mediated overexpression of Tet(O) in *E. coli* BL21(DE3) was required to further increase the MIC to the same level (64 μg/mL) as reported previously for Tet(O)-mediated Tc^R in *C. jejuni* [67]. However, *E. coli* TOP10 could not overexpress Tet(O) in the presence of IPTG because it lacks T7 RNA polymerase [103], and therefore the Tc MIC is the same as observed in the absence of IPTG. These results suggest that the basal expression of *tet(O)^{WT}* is sufficient to cause resistance to Tc.

E. coli BL21(DE3) transformed with *tet(O)^{D131N}* gene remained Tc^S because GTP present in *E. coli* cannot be used as a substrate by Tet(O)^{D131N} XTPase, regardless of whether *tet(O)^{D131N}* gene is overexpressed in the presence of IPTG. XTP is the substrate required for Tet(O)^{D131N} XTPase activity, but *E. coli* cannot produce internal XTP [57, 81]. The addition of external XTP to the medium did not result in a Tc^R phenotype because the XTP was unaccessable to the Tet(O)^{D131N} XTPase. *E. coli* has the poor ability to transport guanosine across the

cytoplasmic membrane [141], which may account for the poor ability to transport xanthosine as well due to the similar structure of guanine and xanthine base (see Figure 1.7).

4.2 pET200 vector with T7*lac* promoter resulted in high-level expression

A major bottleneck for the investigation of the mechanism of Tet(O)-mediated Tc^R is the ability to obtain large amounts of purified biologically functional Tet(O) protein. Attempts to overexpress the $Tet(O)^{WT}$ protein were unsuccessful until an improved procedure was developed by Thakor *et al.* [72]. The improved method was able to achieve a high level of purity with good yield of $Tet(O)^{WT}$. Early attempts to overexpress and purify Tet(O) were unsuccessful [59, 62]. Even attempts to overexpress and purify Tet(M) protein resulted in poor yields with approximately only 0.023 mg/g wet cell weight [111].

In the previous studies, $Tet(O)^{WT}$ was expressed in *E. coli* by prokaryotic expression vectors (e.g. pMS119EH) with *tac*, λP_L or T7 promoters, but failed to yield sufficient amounts for detection by SDS-PAGE despite the presence of the Tc^R phenotype [59, 62]. The expression of $Tet(O)^{WT}$ was largely improved by using the pET200 vector with T7*lac* promoter as described by Thakor *et al.* [72]. This improved method resulted in yields of 0.33-0.44 mg/g wet cell weight with greater than 90% protein purity.

The pET vectors are a powerful expression system and widely used for the

cloning and expression of recombinant proteins in *E. coli* [112]. In the pET200 vector, expression of the heterologous gene is controlled by a strong bacteriophage T7 promoter that has been modified to contain a *lac* operator sequence [103]. The T7 promoter drives high-level, IPTG-inducible expression of the interested gene in *E. coli* BL21 (DE3). The *lac* operator serves as a binding site for the *lac* repressor (encoded by the *lac*I gene) and functions to further repress T7 RNA polymerase-induced basal transcription of the gene of interest in *E. coli* BL21 (DE3) for cases in which the expressed gene is toxic or detrimental to the growth of the host cell [113, 114]. *E.coli* BL21 (DE3) contains the λDE3 lysogen which carries the T7 RNA polymerase gene under the control of the lacUV5 promoter and the *lac*I gene encoding the *lac* repressor [113]. The strain is compatible with the T7 *lac*O promoter system and has the advantage of being deficient in both *lon* and *ompT* proteases [113, 115]. The lack of these two proteases reduces degradation of heterologous proteins expressed in the strain [113].

Besides harboring a kanamycin resistance gene for selection in *E. coli*, the pET200 vector also has a N-terminal affinity tag composed of six consecutive histidine residues (His_6-tag) that strengthen expression of recombinant protein and facilitate one-step purification of the recombinant protein on IMAC [115] with purity ≥ 90%.

4.3 Yields of Tet(O)^{WT}, Tet(O)^{D131N} and EF-G are dependent upon protein solubility

The recombinant protein yield depends on the solubility of a protein [115, 116]. In the present study, the recombinant Tet(O)^{WT}, Tet(O)^{D131N} and EF-G were overexpressed and purified similarly, but yielded different amounts of protein. EF-G had the highest mg protein per g wet cell mass yield (8-9 mg/g), followed by Tet(O)^{WT} (0.5-0.6 mg/g), and Tet(O)^{D131N} (0.2-0.3 mg/g). As compared with the yield for EF-G, a much lower average yield was obtained for Tet(O)^{WT} and Tet(O)^{D131N} (~15-fold and ~34-fold respectively). This lower yield may be explained by the toxic effects of Tet(O) protein overexpression on the bacterial cells and differences in protein solubility as outlined in the following sections.

4.3.1 High levels of Tet(O) inhibits protein synthesis

Even in the absence of Tc, high amounts of Tet(O) inhibit protein synthesis. When the concentration of Tet(O) exceeds the concentration of 70S ribosomes by 1.5-fold, protein synthesis is inhibited by up to 20% [62]. This suggests that overexpression of Tet(O) is toxic to bacterial cells and contributes to the lower yield compared with overexpression of EF-G.

4.3.2 Protein solubility determines yield

Wilkinson and Harrison (1991) developed a model to predict the solubility of

a protein and the probability of inclusion body formation on the basis of the amino acid composition of a protein [117]. A statistical analysis of the composition of 81 proteins that do and do not form inclusion bodies in *E. coli* concluded that six parameters are correlated with inclusion body formation: charge average, turn-forming residue fraction, cysteine fraction, proline fraction, hydrophilicity, and total number of residues [117]. The first two parameters are strongly correlated with inclusion body formation, while the last four parameters show a weak correlation. According to the first two main parameters (charge average and turn-forming residue fraction), the canonical variable CV-CV' was produced to predict the protein solubility according to the following equation [118].

$$CV=\lambda_1\left(\frac{N+G+P+S}{n}\right)+\lambda_2\left|\left(\frac{(R+K)-(D+E)}{n}-0.03\right)\right|$$

Where: n = number of amino acids in protein

N,G,P,S = number of Asn, Gly, Pro, or Ser residues, respectively.

R,K,D,E = number of Arg, Lys, Asp, or Glu residues, respectively.

λ_1, λ_2 = coefficients (15.43 and -29.56, respectively)

CV' is the discriminant equal to 1.71. If CV-CV' is positive, the protein is predicted to be insoluble, while if CV-CV' is negative, the protein is predicted to be soluble [118]. The CV-CV' values of -0.4, 0.0 and 1.1 represent probabilities of solubility of 60%, 50% and 25%, respectively [119].

Based on this model, the protein solubility of $Tet(O)^{WT}$, $Tet(O)^{D131N}$ and

EF-G was predicted with the aid of a protein solubility prediction website (Recombinant Protein Solubility Prediction, School of Chemical Engineering and Materials Science, University of Oklahoma, http://biotech.ou.edu/). Both $Tet(O)^{WT}$ and $Tet(O)^{D131N}$ are composed of 639 amino acids, but the one amino acid difference causes a difference in CV-CV' values where: $Tet(O)^{WT}$ is -0.22, and $Tet(O)^{D131N}$ is -0.15. In contrast, EF-G consists of 704 amino acids and has a CV-CV' value of -0.36. Thus the chance of soluble protein overexpression in *E. coli* is greatest for EF-G (58.8%), followed by $Tet(O)^{WT}$ (55.2%), and $Tet(O)^{D131N}$ (53.4%). The differences of solubility of the three proteins overexpressed in *E. coli* may partly explain the different protein yields.

4.3.3 Substitution of D to N decreases Tet(O) solubility

It has been shown that single amino acid residues can have a major impact on protein solubility and minimize the formation of inclusion bodies [120, 121]. The solubility of the trimethoprim-resistant type S1 dihydrofolate reductase was increased by changing the 130 position amino acid from uncharged asparagine (N) to negatively charged aspartate (D) [120]. It is therefore not unexpected that changing the 131 position amino acid of $Tet(O)^{WT}$ from D to N decreased the solubility of $Tet(O)^{D131N}$. The lower solubility of $Tet(O)^{D131N}$ resulted in the requirement of a lower induction temperature for overexpression and consequently a lower yield than obtained for $Tet(O)^{WT}$.

4.3.4 Induction at low growth temperature increases protein solubility

High-level expression of recombinant proteins in *E. coli in vivo* often results in their accumulation in insoluble aggregates as inclusion bodies. The inclusion body proteins are, in general, misfolded and thus biologically inactive. They need elaborate solubilization, refolding and purification procedures in order to recover their functional bioactivity [122, 123]. The overall yield of bioactive protein from inclusion bodies is only around 15-25% of the total protein and accounts for the major cost in the production of recombinant proteins from *E. coli* [124]. Consequently, soluble expression of functional proteins in *E. coli* is in high demand.

A simple and effective strategy to improve the solubility of overexpressed recombinant proteins and to minimize inclusion body formation, is the use of low induction temperature (15-30°C) [115, 117, 125-127]. Induction of recombinant green fluorescent protein (GFP) in *E. coli* BL21(DE3) with vector pET21-b at 37°C resulted in 58.8% of the recombinant protein present in the insoluble cell fraction [125]. However, at 30°C and 16°C, 54.4% and 16.9%, respectively, of the GFP produced was found in the insoluble cell fraction, indicating that low induction temperature positively influences GFP solubility [125]. This strategy has also improved the solubility of a number of difficult proteins including human interferon-2, subtilisin E, ricin A chain, bacterial luciferase, Fab fragments,

β-lactamase, rice lipoxygenase L-2, soybean lypoxygenase L-1, kanamycin nuclotidyltransferase and rabbit muscle glycogen phosphorylase etc. [125, 126, 128].

In the present study the recombinant Tet(O) and EF-G were induced at sub-optimal growth temperature ($Tet(O)^{WT}$ and EF-G at 30°C, $Tet(O)^{D131N}$ at 18°C). The low induction temperature contributed to the improved solubility of overexpressed recombinant Tet(O) and resulted in a higher protein yield than reported previously [59, 62].

At the optimum temperature (37°C) for its growth, *E. coli* tends to accumulate heterologous proteins in insoluble forms [129], especially in a T7 RNA polymerase-based expression system [115]. At the sub-optimum temperature (15-30°C), the low temperature decreases the protein production rates and thus allows newly transcribed recombinant protein enough time to fold properly [115, 125]. A direct consequence of temperature reduction is the partial elimination of heat shock proteases that are induced under overexpression conditions [130]. Furthermore, the activity and expression of a number of *E. coli* chaperones are increased at temperatures around 30°C [126]. The aggregation reaction is in general favored at higher temperatures due to the strong temperature dependence of hydrophobic interactions that determine the aggregation reaction [131]. Thus, lower temperature during induction should be used as the default induction temperature [115].

4.4 tRNA binding to the P- and A-site of mRNA-programmed 70S ribosomes does not affect Tet(O)-mediated Tc release

In this study, for the first time, a quantitative comparison of the binding affinity of [^{3}H]-Tc to vacant and loaded 70S ribosomes in the absence and presence of Tet(O)^{WT} was performed by the nitrocellulose filter binding assay. The results revealed that there were no significant differences between the affinity of Tc for vacant or loaded 70S ribosomes in the absence or presence of Tet(O)^{WT} (see section 3.4.1). Tc has been reported to specifically inhibit the accommodation of tRNA to ribosomal A-site, and also conditionally inhibit the accommodation of tRNA to ribosomal P-site when the ratio of tRNA to 70S ribosome is over 0.7 [132]. In the present study, excess tRNA (tRNA:70S =1.5) was added in the absence of Tc to ensure the binding of tRNA to the ribosomal P- and A- site. In the model proposed by Connell *et al*., Tc prefers to bind the POST state ribosome which has an empty A-site like the vacant 70S ribosome used in this experiment [57]. It is unclear whether Tc can bind to the ribosomal A-site in the presence of aa-tRNA or whether aa-tRNA in the A-site of the loaded ribosomes is ejected upon Tc binding.

Within bacteria, aa-tRNA is delivered by the EF-Tu ternary complex to the empty ribosomal A-site [23, 88]. Structural studies demonstrated when Tc is present, it binds close to the empty ribosomal A-site and causes a conformational change which makes it impossible for EF-Tu to deliver aa-tRNA to the A-site [30,

31]. These studies do not examine the structure of occupied A-site ribosomes when Tc is present, so it is not known whether Tc binds to the occupied A-site ribosome, or what effect it may have on ribosome structure. In the present study, the A-site has been loaded with aa-tRNA without the help of EF-Tu in the absence of Tc *in vitro*. When Tc was added, it was still able to bind to the A-site occupied ribosome. However, it is unknown whether Tc binding caused a conformational change that would result in the release of the bound A-site tRNA, and possibly the bound P-site tRNA as well. If true, this would support the observed similarities in K_d of Tc binding to vacant or loaded 70S ribosomes in the absence or presence of $Tet(O)^{WT}$ (see Figure 3.8, Table 3.2). The tRNAs rapidly associate to mRNA-programmed ribosomes but dissociate much more slowly [107]. It is unknown whether Tc affects tRNA dissociation. Alternatively, if the tRNAs remain bound to the ribosomal A- and P-sites after Tc binding, the similarities of Tc K_d in vacant or loaded 70S ribosomes suggest that the Tc ribosomal binding site is unaffected by ribosomal A- and P-site occupation.

The similar affinity of Tc binding to vacant or loaded 70S ribosomes indicated that the occupancy of ribosomal P- and A-sites did not affect Tet(O)-mediated Tc release, therefore vacant 70S ribosomes were used as the default 70S ribosome state for studies of ribosome-bound Tc release.

4.5 Challenges in the determination of Tet(O)-mediated Tc release

When Tet(O)^{WT} was absent, the high binding affinity of Tc for 70S ribosomes was demonstrated by a low K_d (2.9±0.7 μM), which was in good agreement with the previously reported value (K_d=2-20 μM) [62, 72, 133]. Although earlier studies reported a 6-fold reduction in binding affinity of Tc for 70S ribosomes in the presence of Tet(O)^{WT} (K_d=30 μM [62], 20.4 μM [72]), only a 3.6-fold reduction (K_d=10.6±4.1 μM) was observed in the present study. The following points may explain this difference:

First, different preparations of Tet(O) may have inconsistent functional activities arising from variations in overexpression and purification procedures. Different plasmids and expression hosts resulted in varying success in attempts to obtain the purified functional Tet(O) protein. Trieber *et al.* used plasmid pMS119EH and *E. coli* MRE600/pTetOH to express Tet(O), and reported a high K_d for Tc binding to the ribosomes in the presence (30 μM) of Tet(O) [62]. In contrast, Thakor *et al.* used plasmid pET200 and *E. coli* BL21(DE3) to express Tet(O), and reported a lower K_d for Tc binding to the ribosomes in the presence (20.4 μM) of Tet(O) [72]. In the present study, the same plasmid and expression host were used to express Tet(O) as described by Thakor *et al.*, but K_d was even lower (10.6±4.1 μM).

The discrepancy between the values obtained in the present study compared with Thakor *et al.* who used the same protocol, likely arise from several reasons.

The present study performed multiple replicate experiments to establish a mean value whereas previous studies only reported a single experimental value. No SD error was reported for values of K_d. This suggested the experiment was not done more than once. In this present study, each value of K_d represents the average of at least three experiments where each experiment was done in triplicate. Accordingly, the mean K_d values reported in this study include SD as a measure of their precision.

Earlier studies also did not subtract background counts of [^{3}H]-Tc associated with the nitrocellulose filter (non-specific filter binding) from the counts for the specific binding of [^{3}H]-Tc-70S ribosome trapped on the filter. The background binding of [^{3}H]-Tc to the filter increased linearly with increasing concentrations of [^{3}H]-Tc (see Figure 3.7). The non-specific [^{3}H]-Tc binding represented about 10% of counts at low Tc concentrations (1-10 μM), and up to 30% of counts at high Tc concentrations (20-40 μM). Overestimation of the K_d for Tc-70S ribosome binding will occur if there is no correction for non-specific [^{3}H]-Tc binding. This is likely a contributing factor for the higher K_d reported previously [62, 72].

In addition, different preparations of 70S ribosomes may have dissimilar activities. The activity of typical ribosome preparations vary from 55% to 85% because these preparations include different ribosome states [100, 101, 107]. Active 70S ribosomes are capable of association with mRNA and tRNA to participate in protein synthesis. Batch to batch variation in 70S ribosome

preparations may contribute to variability in the assessment of Tc K_d for Tc-70S ribosome binding. More than one batch of 70S ribosomes was required to complete the experiments. However, values for Tc binding to different preparations of 70S ribosomes provided remarkably reproducible values in the present study (2.9±0.7 μM) which agree with previously reported values of 3.4 μM [72] and 5 μM [62]. The wider range of K_d (2-20 μM) reported in earlier papers (before 1990) may be due to the use of different methods [62, 133, 134].

4.6 EF-G interferes with Tet(O)-mediated Tc release

The present study was the first report to compare the binding affinities of Tc to 70S ribosomes in the absence or presence of EF-G and/or Tet(O). As expected, EF-G did not alter the binding affinity of Tc for 70S ribosomes and could not release bound Tc (see Figure 3.9b; Table 3.3). In contrast, $Tet(O)^{WT}$ decreased the binding affinity of Tc for 70S ribosomes ~3.8-fold (see Figure 3.9a; Table 3.3) as compared with EF-G, which is consistent with the release of Tc from the ribosome.

$Tet(O)^{WT}$ is an EF-G like GTPase, and binds to the site on the ribosome which overlaps the binding site for EF-G [56, 76]. When both EF-G and $Tet(O)^{WT}$ were present, the binding affinity of Tc for 70S ribosomes was reduced by half the value observed when only $Tet(O)^{WT}$ was present (See Figure 3.9; Table 3.3). In other words, the ability of Tet(O) to release Tc from the 70S ribosomes in the

presence of EF-G was reduced by 50% as compared to when only Tet(O)^{WT} was present. This suggests that EF-G may compete with Tet(O)^{WT} for binding to the ribosome, and thereby impair Tet(O)-mediated Tc release. There are no other reports in the literature that have examined the effect of EF-G on RPP-mediated Tc release in the investigation of the mechanism of Tc^{R}.

4.7 Tet(O)^{D13N}•XTP and Tet(O)^{WT}•GTP are equally able to release ribosome-bound Tc

All RPP-mediated Tc^{R} was thought to occur by the same mechanism [16, 54]. Previous studies proposed that binding of the Tet(O)^{WT}•GTP complex to the 70S ribosomes is required for the release of Tc from 70S ribosomes. GTP hydrolysis was demonstrated to be necessary for both the release of bound Tc and Tet(M) from the 70S ribosomes [63, 64]. However, it was proposed that GTP hydrolysis is not necessary for Tet(O)^{WT}-mediated Tc release from 70S ribosomes, but is required to release bound Tet(O)^{WT} [58, 62]. In the presence of non-hydrolyzable GTP analog (GMPPNP), Tet(O)^{WT} was able to release ribosome-bound Tc, suggesting that GTP hydrolysis was not necessary for Tc release. However, when GMPPNP was present, Tc release depended upon a high concentration of Tet(O)^{WT}, which inhibited protein synthesis, even when Tc was absent [58, 62]. This inhibitory effect on protein synthesis was also reported for high concentrations of Tet(M) [63]. Since only low levels of Tet(O)^{WT} are likely to

exist *in vivo* [62, 72], GTP hydrolysis would be necessary for Tet(O) to continuously recycle to release ribosome-bound Tc and restore protein synthesis.

The present study is the first report of Tc release from 70S ribosomes by $Tet(O)^{D131N}$•XTP. $Tet(O)^{D131N}$ could not release Tc from 70S ribosomes in the presence of GTP (see Figure 3.10b; Table 3.4) because it was unable to utilize GTP as a substrate (see Figure 3.12). Without the correct substrate, $Tet(O)^{D131N}$ may not bind to the 70S ribosomes because it cannot form a complex with GTP (see section 1.5.5, figure 1.7). In contrast, $Tet(O)^{D131N}$ was able to release Tc from 70S ribosomes in the presence of XTP to a similar level as observed in the presence of $Tet(O)^{WT}$ and GTP (see Figure 3.10a; Table 3.4). This indicated $Tet(O)^{D131N}$ and $Tet(O)^{WT}$ were equally able to promote the release of Tc from the ribosome when their individual specific enzyme substrates were available for hydrolysis. The present study confirmed the previous report that the presence of correct substrate is necessary for Tet(O) to release ribosome-bound Tc [62]. This supports the requirement of the binding of $Tet(O)^{WT}$•GTP complex or $Tet(O)^{D131N}$ •XTP complex to the 70S ribosome for Tc release. The binding of $Tet(O)^{WT}$•GTP complex to the 70S ribosome also triggers GTP hydrolysis of $Tet(O)^{WT}$. GTP hydrolysis is necessary for Tet(O) release from 70S ribosomes, which allows Tet(O) to repeatedly cycle to release ribosome-bound Tc and restore protein elongation.

The present study also confirmed the previous report that ~50% of

ribosome-bound Tc was released by Tet(O) when the concentration of Tc was 5 μM [62]. However, at high concentrations of Tc (20 μM), all of the Tc binding sites become occupied on the 70S ribosomes. Thereby when Tet(O) is present, it can only release ~30% of ribosome-bound Tc (Figure 4.1) because Tet(O) can only release bound Tc from the primary binding site [58]. The exponential 2 phase decay equation accurately differentiates the rapid Tc release from the primary Tc binding site mediated by Tet(O) versus the slower Tc release from the secondary Tc binding sites.

4.8 Proposed changes in 70S ribosome conformation induced by Tc-binding is not required for Tet(O)^{WT} binding

Both Tet(O) and EF-G are ribosome-dependent GTPases. GTP hydrolysis is essential for Tet(O) and EF-G to dissociate from the 70S ribosomes to allow protein synthesis continue [23, 62, 76, 88]. Thakor *et al.* was the first to report the values of the affinity constant (apparent K_m) and the rate constant (k_{cat}/K_m) of Tet(O)^{WT} for GTP, and compared these with the values for EF-G [72]. In the present study, the apparent K_m values for Tet(O)^{WT} (69.0±19.8 μM) and EF-G (81.5±16.0 μM) for GTP agreed with previously reported results (84±5 μM and 80±5 μM, respectively), which demonstrate that both GTPases have a similar affinity for GTP [72]. The apparent K_m of EF-G was also in agreement with an earlier reported value for EF-G (K_m=30-100 μM) [135].

The GTPase catalytic efficiency (k_{cat}/K_m) of Tet(O)^{WT} was reported to be ~2.5-fold lower than for EF-G [72]. However, there was an error in the reporting of k_{cat} in this paper, which renders any further consideration of the k_{cat}/K_m data invalid. The present study revealed the catalytic efficiency (k_{cat}/K_m) of Tet(O)^{WT} was ~1.5-fold higher than for EF-G (see Figure 3.13, Table 3.5). This change was a numerical significant difference ($p<0.05$), but perhaps not a biologically significant one. If the biological activity of Tet(O)^{WT} was significantly higher than EF-G, Tet(O)^{WT} would hydrolyze GTP more quickly than EF-G, which would imply that Tet(O)^{WT} recycles on and off the ribosome more rapidly than EF-G. However, since this difference in GTPase activity was less than 2-fold, it is more likely that the GTPase activities of Tet(O)^{WT} and EF-G are similar to each other. This is supported by their nearly identical G-domain structure (see Figure 1.5).

Connell *et al.* established that Tet(O) prefers to bind to POST state ribosomes which has an empty A-site [57], while EF-G prefers to bind to PRE state ribosomes which has an occupied A-site [136]. In the present study, GTPase activity of Tet(O) and EF-G was investigated with empty A-site (vacant) ribosomes. The higher k_{cat}/K_m of Tet(O) as compared with EF-G was consistent with the preferential binding of Tet(O) to POST state 70S ribosomes.

4.9 The presence of Tet(O)^{D131N} does not interfere with GTP hydrolysis of EF-G

The binding of Tet(O)^{WT} or EF-G to the 70S ribosomes is critical for stimulation of their individual GTPase activity. Therefore, GTP hydrolysis may be used to indirectly assess the binding of either Tet(O)^{WT} or EF-G to the ribosome. The GTPase activity of EF-G was differentiated from the combined GTPase activities of Tet(O)^{WT} and EF-G when Tet(O)^{D131N} was incubated with EF-G because Tet(O)^{D131N} XTPase could not hydrolyze GTP. This was the first report that permitted the differentiation of the binding of Tet(O) to the ribosome from EF-G by the indirect measurement of GTPase activity. The results (see section 3.5.4) revealed that the presence of Tet(O)^{D131N} did not affect the kinetics of GTP hydrolysis of EF-G, which implies that Tet(O) does not appear to compete directly with EF-G for binding to the 70S ribosome. In contrast, Tet(M) has been observed to compete with EF-G for binding to the ribosome, and has stronger ability to bind the ribosome than EF-G [64]. The different results for Tet(O) and Tet(M) may be due to the different experimental methods. In this study, GTP hydrolysis assay was used to indirectly determine the binding of Tet(O) and EF-G to the 70S ribosome (see section 2.10.3). In contrast, gel filtration assay was used to demonstrate the competitive binding of Tet(M) and EF-G to the 70S ribosome [64]. [^{3}H]-Tet(M) and unlabelled EF-G, or [^{3}H]-EF-G and unlabelled Tet(M) were incubated with 70S ribosomes in the presence of GTP and fusidic acid. The extent

of radio-labelled protein binding to the ribosome was monitored by gel filtration chromatography. Fusidic acid is an antibiotic which disrupts protein synthesis by stabilizing EF-G binding to the ribosome following GTP hydrolysis, thereby preventing the dissociation of EF-G from the ribosome [137, 138]. Consequently, only Tet(M) can repeatedly cycle on and off the ribosome following GTP hydrolysis. In contrast, in this study both Tet(O)^{D131N} and EF-G were allowed to cycle repeatedly on and off the ribosome following XTP and GTP hydrolysis, respectively. This dynamic on-off binding of Tet(O)^{D131N} and EF-G to the ribosome more closely resembles the *in vivo* conditions.

In vivo, Tet(O) is proposed to be present in concentrations less than or equal to that of EF-G [59, 62]. Therefore in the present study, equal amounts of Tet(O)^{D131N} and EF-G were used to mimic maximal *in vivo* conditions, which may reflect the physiological binding conditions. However, competitive binding between Tet(M) and EF-G was observed by incubating 3- and 10-fold higher concentrations of unlabelled competitor (Tet(M) or EF-G) with radio-labelled proteins ([^{3}H]-EF-G or [^{3}H]-Tet(M)). Therefore, studies of Tet(O) in the presence of excess EF-G (competitor) may provide further insight into whether Tet(O) competes with EF-G for binding to the 70S ribosome.

4.10 Summary

Investigation of the mechanism of Tet(O)-mediated Tc^R may provide new

strategies for the development of novel antibiotics to circumvent RPP-mediated Tc^R and the treatment of serious campylobacterioses and other infections. This thesis reports a series of novel findings regarding the kinetic interactions of Tc, Tet(O) and EF-G with 70S ribosomes, which help to characterize the mechanism of Tet(O)-mediated Tc^R.

1) The proposed model (see Figure 1.8) suggests Tc prefers to bind the POST-state ribosomes, which is supported by other reports of Tc binding to empty A-site riboosmes; however Tc binding was not assessed for occupied A-site ribosomes [62, 72]. In this thesis, Tc was observed to bind equally well to empty or occupied A-site ribosomes.
2) $Tet(O)^{D131N}$ was functionally identical to $Tet(O)^{WT}$. Both proteins were able to release similar amounts of ribosome-bound Tc, even though their enzyme specificity was different. The kinetic studies performed with $Tet(O)^{D131N}$ provided evidences to demonstrate that $Tet(O)^{WT}$, like Tet(M), requires binding to the 70S ribosome as a $Tet(O)^{WT}$•GTP complex to release ribosome-bound Tc. This supports the need for GTP hydrolysis for Tet(O) to repeatedly recycle on and off 70S ribosomes to release Tc.
3) The higher catalytic efficiency of Tet(O) GTPase as compared with EF-G GTPase suggests more rapid cycling of Tet(O) on and off empty A-site ribosomes. This provides additional evidence that compared with EF-G, Tet(O) preferentially binds to POST state ribosomes which have empty

A-sites [57]. However the increased catalytic efficiency of Tet(O) may not be biologically significant; rather it may be similar to EF-G.

4) The reduction of Tet(O)-mediated Tc release by EF-G suggests equal concentrations of Tet(O) and EF-G compete for binding to empty A-site ribosomes. However, this competitive binding could not be demonstrated in the presence of equal concentrations of Tet(O) and EF-G when their binding was indirectly measured by GTP hydrolysis. This was likely because the concentration of 70S ribosomes was not less than the concentrations of Tet(O) and EF-G.

Although these findings contribute to the knowledge of the kinetics of Tc release by Tet(O), further investigation is required in order to clarify whether Tet(O) directly competes with EF-G for binding to the 70S ribosomes. This will help to understand the mechanism of Tet(O)-mediated Tc^R and develop strategies to overcome Tc^R infections, such as Tc^R *Campylobacter* infections.

Food animals, particularly poultry and beef cattle, act as sources and reservoirs of human *Campylobacter* infections. Reduction or elimination of *C. jejuni* in food animals is an essential measure to improve the food safety and minimize the public health problem. The increasing rates of resistance to the current drug of choice (erythromycin) used in the treatment of *Campylobacter* infections may increase the demand for alternative antimicrobial agents.

Beyond developing novel antibiotics, the more important strategies for the

prevention of the spread of antibiotic resistant *C. jejuni* from animals to humans, is to regulate the use of antibiotics for the treatment of infections, withdraw antibiotic use in animals for growth promotion, and advocate the proper handling of animals, as well as the food derived from animals. However, Tc^R is ubiquitous in the environment as it is present in the bacteria of marine life, wild birds and animals, as well as domestic and food animals [16]. As a consequence, it is inevitable that Tc^R bacteria will appear in human infections. Strategies to overcome Tc^R would provide much needed alternatives for the treatment of Tc^R infections.

4.11 Concluding Remarks

The thesis has provided a further understanding of the kinetic mechanism of Tet(O)-mediated Tc^R. In this thesis, EF-G appeared to compete with Tet(O), and thereby impair Tet(O)-mediated Tc release. GTP hydrolysis was essential for Tet(O) to dissociate from the ribosome so that it could repeatedly recycle to release Tc from the ribosome. In this way, GTP hydrolysis was an indirect measure of the cycle of Tet(O) binding and release from the ribosome. These findings have the potential to guide a new strategy to overcome Tet(O)-mediated Tc^R by interrupting GTP hydrolysis of Tet(O) through inhibition of its association or dissociation from the 70S ribosomes without affecting other GTPase proteins in bacteria. This strategy is similar to the inhibition of EF-G GTPase activity by

fusidic acid, which prevents the dissociation of EF-G from the ribosome and inhibits protein synthesis. A similar analog could be developed to inhibit Tet(O) GTPase activity to prevent the dissociation of Tet(O) from the ribosome, and thereby inhibit protein synthesis. This novel analog would then be effective for the treatment of infections caused by bacteria with the *tet(O)* gene. If this new therapeutic agent was reserved as a last resort for the treatment of severe human infections with bacteria carrying the *tet(O)* gene (e.g. only hospitalized patients), and was not used in agriculture, the development of resistance to this agent would be slow.

4.12 Future Directions:

4.12.1 To investigate competitive binding of Tet(O) and EF-G to 70S ribosomes

4.12.1.1 Effect of increasing concentrations of competitor protein

Investigation of the binding of Tet(O) and EF-G to the 70S ribosomes in the presence of increasing concentrations of competitor (EF-G or Tet(O) respectively) will further clarify whether Tet(O) and EF-G compete with each other to bind to the 70S ribosomes in the absence or presence of Tc.

a) GTP hydrolysis as an indirect measurement of Tet(O) and EF-G binding

In the absence of Tc, if the binding is competitive, the GTPase activity of

EF-G or Tet(O) should decrease with increasing concentrations of competitor (Tet(O) or EF-G, respectively). If the binding is not competitive, the GTPase activity of EF-G or Tet(O) should not change with increasing concentrations of competitor (Tet(O) or EF-G, respectively). $Tet(O)^{D131N}$ will permit assessment of EF-G GTPase activity when EF-G is present with $Tet(O)^{WT}$. Fusidic acid will permit assessment of $Tet(O)^{WT}$ GTPase activity when $Tet(O)^{WT}$ is present with EF-G.

In Tc^{R} bacterial cells, EF-G cannot bind to the empty ribosomal A-site and therefore cannot activate its GTPase activity when Tc is present [76, 136]. In the present study, EF-G bound to the empty A-site ribosomes and hydrolyzed GTP in the absence of Tc, but the GTP hydrolysis was not measured in the presence of Tc. Earlier studies suggest that EF-G cannot hydrolyze GTP in the presence of Tc because it cannot recognize the ribosome conformational change caused by Tc [76]. If increasing concentrations of $Tet(O)^{D131N}$ is present with excess XTP, ribosome-bound Tc will be released by $Tet(O)^{D131N}$ and XTP hydrolysis will cause release of $Tet(O)^{D131N}$ from the ribosome. The A-site will then be available for EF-G to bind to the ribosome which can be detected by GTP hydrolysis.

In contrast, GTPase activity of Tet(O) is not affected by the presence of Tc because Tet(O) can recognize the ribosome conformational change caused by Tc and release the bound Tc from the 70S ribosomes. In the presence of fusidic acid, EF-G can bind to the ribosome, but cannot hydrolyze GTP and therefore cannot

dissociate from the ribosome. When $Tet(O)^{WT}$ is present with increasing concentrations of EF-G in the presence of Tc and fusidic acid, only Tet(O) would be able to hydrolyze GTP. If EF-G competes with Tet(O) for ribosome binding, Tet(O) will release bound Tc to allow EF-G to bind, but EF-G will become locked on the ribosome by fusidic acid. The EF-G-blocked sites will prevent further binding of Tc and Tet(O). Accordingly, if EF-G and Tet(O) compete for binding to the same ribosomal site, the GTPase activity of Tet(O) should decrease with the increasing concentrations of EF-G to reflect the decreasing number of binding sites available.

The GTP hydrolysis assay is a feasible, economical method for the indirect measurement of Tet(O) and EF-G binding to 70S ribosomes. This method measures the GTP hydrolysis stimulated upon protein binding to the ribosome, but does not directly measure binding. The limitation of this method is that it cannot detect the binding of Tet(O) and EF-G to 70S ribosomes if GTP hydrolysis does not occur (e.g. when the protein release from the ribosome is blocked).

b) Fluorescent-labelled Tet(O) or EF-G for the direct measurement of their binding to ribosomes

It is known that the His-tag, an oligohistidine sequence ($(His)_n$, $n \geq 6$), tightly interacts with transition-metal complexes (e.g. nitrilotriacetic acid (NTA) complex of Ni^{2+}), thereby the His-tag is widely used for purification of recombinant

proteins by IMAC [139]. The selective interaction between the His_6-tag and the metal complexes is also applicable for site-specific fluorescent labeling of proteins [140]. The derivatives of cyanine fluorochromes Cy3 and Cy5 with one or two pendant NTA-Ni^{2+} can be used for specific labeling of His_6-tagged proteins (Figure 4.2) [140]. In the present study, recombinant Tet(O) and EF-G carry a His_6-tag for one-step purification by IMAC, thereby they could be individually fluorescent-labelled by utilizing NTA- Ni^{2+}-chromophores for binding studies. The protein-bound ribosome complexes and the free protein would be separated using a filter (100 kDa). The large fluorescent-labelled protein-bound ribosome complexes (EF-G*-70S or Tet(O)*-70S) will be trapped on the filter, while the free or unbound Tet(O) or EF-G will be washed through the filter. If the binding is competitive, the fluorescent signal of the protein-bound ribosome complexes will be reduced with the increasing concentration of competitor (Tet(O) or EF-G respectively). If the binding is not competitive, the fluorescent signal of the protein-bound ribosome complexes will not change with increasing concentrations of competitor.

The use of fluorescent-labelled Tet(O) or EF-G is a safe, easy, and direct method to assess their binding to the ribosome as compared with the indirect assessment by [γ-^{32}P]GTP hydrolysis or the direct assessment by [^{3}H] labeled Tet(M) or EF-G used previously [64].

4.12.2 To determine the effect of Tc on ribosome-bound tRNAs

In order to clarify whether Tc binding causes the release of bound ribosomal A-site tRNA *in vitro*, (and perhaps P-site tRNA) as discussed in section 4.4, the dissociation rate of [3'-^{32}P]tRNAs from 70S ribosomes could be determined with the double-filter binding assay as described in section 2.8 with some modications. If Tc binding causes the release of 70S ribosome-bound tRNAs, the percent dissociated [3'-^{32}P]tRNAs on the lower nylon membrane will increase as compared with the absence of Tc. If Tc binding does not release bound tRNAs, the percent associated [3'-^{32}P]tRNAs on the upper nitrocellulose membrane will be the same as compared with the absence of Tc.

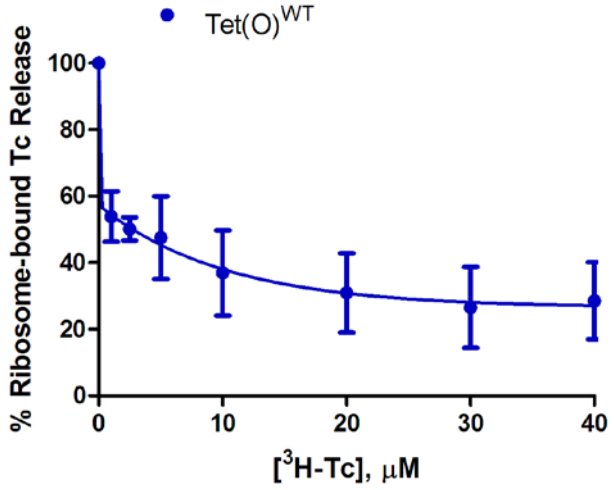

Figure 4.1 Percent of ribosome-bound Tc released by Tet(O)^{WT}

The percent of ribosome-bound Tc released by Tet(O) was obtained by subtracting the amount of ribosome-bound [^{3}H]-Tc with increasing concentrations of Tc in the presence of Tet(O) from the maximum [^{3}H]-Tc bound to 70S ribosome in the absence of Tet(O) (Figure 3.8a). The exponential 2 phase decay equation accurately fits the relationship between Tc release and increasing Tc concentration.

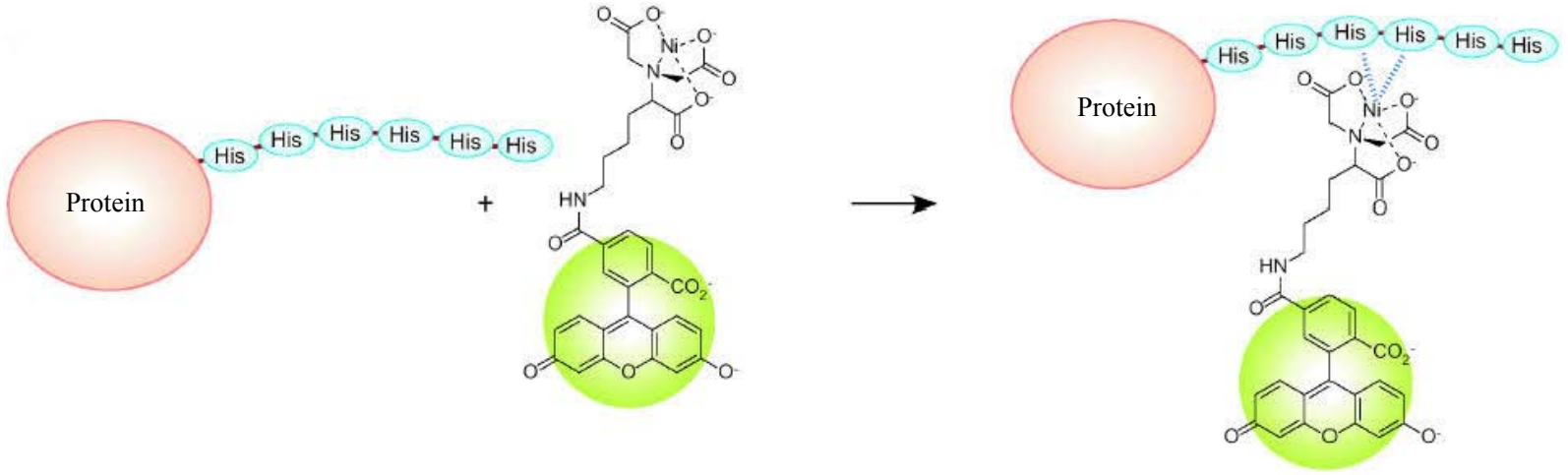

Figure 4.2 A His_6-tag protein is fluorescent-labelled by nitrilotriacetic acid (NTA) complex of Ni^{2+} with fluorochromes

References:

[1] Moore JE, Corcoran D, Dooley JS, Fanning S, Lucey B, Matsuda M, et al. *Campylobacter*. Vet.Res. 2005 May-Jun;36(3):351-382.

[2] Rao MR, Naficy AB, Savarino SJ, Abu-Elyazeed R, Wierzba TF, Peruski LF, Abdel-Messih I, Frenck R, Clemens JD. Pathogenicity and convalescent excretion of *Campylobacter* in rural Egyptian children. Am J Epidemiol. 2001 Jul; 154(2):166-173

[3] Gibreel A, Taylor DE. Macrolide resistance in *Campylobacter jejuni* and *Campylobacter coli*. J.Antimicrob.Chemother. 2006 Aug;58(2):243-255.

[4] Allos BM, Blaser MJ. *Campylobacter jejuni* and the expanding spectrum of related infections Clin Infect Dis. 1995 May;20(5):1092-1099; quiz 1100-1.

[5] Blaser MJ. Epidemiologic and clinical features of *Campylobacter jejuni* infections. J. Infect Dis. 1997 Dec;176 (Suppl 2):S103-S105.

[6] Coker AO, Isokpehi RD, Thomas BN, Amisu KO, Obi CL. Human campylobacteriosis in developing countries. Emerg Infect Dis. 2002 Mar; 8(3):237-244.

[7] Senok AC, Botta GA. *Campylobacter* enteritis in the Arabian Gulf. J. Infect Dev Ctries. 2009 Mar;3(2):74-82

[8] Mead PS, Slutsker L, Dietz V, McCaig LF, Bresee JS, Shapiro C, Griffin PM, Tauxe RV. Food-related illness and death in the United States. Emerg Infect Dis. 1999 Sep-Oct; 5(5):607-625

[9] Ciampa N, Finley R, Fleury MD, Flint J, Nesbitt A, Murray R, et al. Canadian Integrated Surveillance Report: *Salmonella*, *Campylobacter*, verotoxigenic *E. coli* and *Shigella*, from 2000-2004. Canada Communicable Disease Report 2009 Dec; 35S2: 1-50. Available from: URL: http://www.phac-aspc.gc.ca/publicat/ccdr-rmtc/09vol35/35s3/index-eng.php#toc

[10] Galanis E. *Campylobacter* and bacterial gastroenteritis. CMAJ 2007 Sep 11;177(6):570-571.

[11] Godschalk PC, Heikema AP, Gilbert M, Komagamine T, Ang CW, Glerum J, et al. The crucial role of *Campylobacter jejuni* genes in anti-ganglioside antibody induction in Guillain-Barre syndrome. J.Clin.Invest. 2004 Dec;114(11):1659-1665.

[12] Allos BM. *Campylobacter jejuni* Infections: update on emerging issues and trends. Clin.Infect.Dis. 2001 Apr 15;32(8):1201-1206.

[13] Engberg J, Aarestrup FM, Taylor DE, Gerner-Smidt P, Nachamkin I. Quinolone and macrolide resistance in *Campylobacter jejuni* and *C. coli*: resistance mechanisms and trends in human isolates. Emerg.Infect.Dis. 2001 Jan-Feb;7(1):24-34.

[14] Aarestrup FM, Engberg J. Antimicrobial resistance of thermophilic *Campylobacter*. Vet.Res. 2001 May-Aug;32(3-4):311-321.

[15] Alfredson DA, Korolik V. Antibiotic resistance and resistance mechanisms in *Campylobacter jejuni* and *Campylobacter coli*. FEMS Microbiol.Lett. 2007 Dec;277(2):123-132.

[16] Chopra I, Roberts M. Tetracycline antibiotics: mode of action, applications, molecular biology, and epidemiology of bacterial resistance. Microbiol.Mol.Biol.Rev. 2001 Jun;65(2):232-260.

[17] Chopra I, Hawkey PM, Hinton M. Tetracyclines, molecular and clinical aspects. J.Antimicrob.Chemother. 1992 Mar;29(3):245-277.

[18] Chopra I. Tetracycline analogs whose primary target is not the bacterial ribosome. Antimicrob.Agents Chemother. 1994 Apr;38(4):637-640.

[19] Levy SB. Chapter 2 The disease and the cure: the microscopic world of bacterial and antibiotics. In: The antibiotic paradox: how the misuse of antibiotics destroys their curative powers. 2nd ed. Cambridge, MA: Perseus Pub.; 2002: 15-56.

[20] Roberts MC. Tetracycline therapy: update. Clin.Infect.Dis., 2003 Feb; 36(4): 462-467.

[21] Cate JH, Yusupov MM, Yusupova GZ, Earnest TN, Noller HF. X-ray crystal structures of 70S ribosome functional complexes. Science 1999 Sep 24;285(5436):2095-2104.

[22] Yusupov MM, Yusupova GZ, Baucom A, Lieberman K, Earnest TN, Cate JH, et al. Crystal structure of the ribosome at 5.5 A resolution. Science 2001 May 4;292(5518):883-896.

[23] Spahn CM, Nierhaus KH. Models of the elongation cycle: an evaluation. Biol.Chem. 1998 Jul;379(7):753-772.

[24] Wilson DN, Nierhaus KH. The ribosome through the looking glass. Angew.Chem.Int.Ed Engl. 2003 Aug 4;42(30):3464-3486.

[25] Nilsson J, Nissen P. Elongation factors on the ribosome. Curr Opin Struct Biol. 2005 Jun;15(3):349-354

[26] Wimberly BT, Brodersen DE, Clemons WM,Jr, Morgan-Warren RJ, Carter AP, Vonrhein C, et al. Structure of the 30S ribosomal subunit. Nature 2000 Sep; 407(6802):327-339.

[27] Ban N, Nissen P, Hansen J, Moore PB, Steitz TA. The complete atomic structure of the large ribosomal subunit at 2.4 A resolution. Science 2000 Aug; 289(5481):905-920.

[28] Schluenzen F, Tocilj A, Zarivach R, Harms J, Gluehmann M, Janell D, et al. Structure of functionally activated small ribosomal subunit at 3.3 angstroms resolution. Cell 2000 Sep;102(5):615-623.

[29] Schuwirth BS, Borovinskaya MA, Hau CW, Zhang W, Vila-Sanjurjo A, Holton JM, et al. Structures of the bacterial ribosome at 3.5 A resolution. Science 2005 Nov;310(5749):827-834.

[30] Brodersen DE, Clemons WM,Jr, Carter AP, Morgan-Warren RJ, Wimberly BT, Ramakrishnan V. The structural basis for the action of the antibiotics tetracycline, pactamycin, and hygromycin B on the 30S ribosomal subunit. Cell 2000 Dec;103(7):1143-1154.

[31] Pioletti M, Schlunzen F, Harms J, Zarivach R, Gluhmann M, Avila H, et al. Crystal structures of complexes of the small ribosomal subunit with tetracycline, edeine and IF3. EMBO J. 2001 Apr;20(8):1829-1839.

[32] Schnappinger D, Hillen W. Tetracyclines: antibiotic action, uptake, and resistance mechanisms. Arch.Microbiol. 1996 Jun;165(6):359-369.

[33] Lima AA, Lima NL, Pinho MC, Barros Junior EA, Teixeira MJ, Martins MC, et al. High frequency of strains multiply resistant to ampicillin, trimethoprim-sulfamethoxazole, streptomycin, chloramphenicol, and tetracycline isolated from patients with shigellosis in northeastern Brazil during the period 1988 to 1993. Antimicrob.Agents Chemother. 1995 Jan;39(1):256-259.

[34] Goldstein FW, Kitzis MD, Acar JF. N,N-dimethylglycyl-amido derivative of minocycline and 6-demethyl-6-desoxytetracycline, two new glycylcyclines highly effective against tetracycline-resistant gram-positive cocci. Antimicrob.Agents Chemother. 1994 Sep;38(9):2218-2220.

[35] Padungton P, Kaneene JB. *Campylobacter* spp. in human, chickens, pigs and their antimicrobial resistance. J.Vet.Med.Sci. 2003 Feb;65(2):161-170.

[36] Moore JE, Barton MD, Blair IS, Corcoran D, Dooley JS, Fanning S, et al. The epidemiology of antibiotic resistance in *Campylobacter*. Microbes Infect. 2006 Jun;8(7):1955-1966.

[37] Gaudreau C, Gilbert H. Antimicrobial resistance of *Campylobacter jejuni* subsp. jejuni strains isolated from humans in 1998 to 2001 in Montreal, Canada. Antimicrob.Agents Chemother. 2003 Jun;47(6):2027-2029.

[38] Gibreel A, Tracz DM, Nonaka L, Ngo TM, Connell SR, Taylor DE. Incidence of antibiotic resistance in *Campylobacter jejuni* isolated in Alberta, Canada, from 1999 to 2002, with special reference to tet(O)-mediated tetracycline resistance. Antimicrob.Agents Chemother. 2004 Sep;48(9):3442-3450.

[39] Taylor DE, Chang N, Garner RS, Sherburne R, Mueller L. Incidence of antibiotic resistance and characterization of plasmids in *Campylobacter jejuni* strains isolated from clinical sources in Alberta, Canada Can.J.Microbiol. 1986

Jan; 32 (1): 28-32.

[40] Kos VN, Keelan M, Taylor DE. Antimicrobial susceptibilities of *Campylobacter jejuni* isolates from poultry from Alberta, Canada. Antimicrob.Agents Chemother. 2006 Feb;50(2):778-780.

[41] Inglis GD, Morck DW, McAllister TA, Entz T, Olson ME, Yanke LJ, et al. Temporal prevalence of antimicrobial resistance in *Campylobacter* spp. from beef cattle in Alberta feedlots. Appl.Environ.Microbiol. 2006 Jun;72(6):4088-4095.

[42] Rosengren,L.B.; Waldner,C.L.; Reid-Smith,R.J.; Valdivieso-Garcia,A. Associations between antimicrobial exposure and resistance in fecal *Campylobacter* spp. from grow-finish pigs on-farm in Alberta and Saskatchewan, Canada J.Food Prot., 2009 Mar; 72(3): 482-489.

[43] Cook A, Reid-Smith R, Irwin R, McEwen SA, Valdivieso-Garcia A, Ribble C. Antimicrobial resistance in *Campylobacter*, *Salmonella*, and *Escherichia coli* isolated from retail turkey meat from southern Ontario, Canada. J.Food Prot. 2009 Mar;72(3):473-481.

[44] Larkin C, Van Donkersgoed C, Mahdi A, Johnson P, McNab B, Odumeru J. Antibiotic resistance of *Campylobacter jejuni* and *Campylobacter coli* isolated from hog, beef, and chicken carcass samples from provincially inspected abattoirs in Ontario. J.Food Prot. 2006 Jan;69(1):22-26.

[45] Roberts MC. Epidemiology of tetracycline-resistance determinants. Trends Microbiol. 1994 Oct;2(10):353-357.

[46] Taubes G. The bacteria fight back. Science 2008 Jul;321(5887):356-361.

[47] Poole K. Mechanisms of bacterial biocide and antibiotic resistance. J.Appl.Microbiol. 2002;92 Suppl:55S-64S.

[48] Sefton AM. Mechanisms of antimicrobial resistance: their clinical relevance in the new millennium. Drugs 2002;62(4):557-566.

[49] Roberts MC. Update on acquired tetracycline resistance genes. FEMS Microbiol.Lett. 2005 Apr 15;245(2):195-203.

[50] Levy SB. Chapter 4 Antibiotic Resistance: Microbial Adaptation and Evolution. In: The antibiotic paradox: how the misuse of antibiotics destroys their curative powers. 2nd ed. Cambridge, MA: Perseus Pub.; 2002: 71-114.

[51] Roberts MC. Tet mechanisms of resistance. Distribution of *tet* resistance genes among gram-negative bacteria. Distribution of tetracycline resistance genes among gram-positive bacteria, *Mycobacterium*, *Mycoplasma*, *Nocardia*, *Streptomyces* and *Ureaplasma*. Available from: URL: http://faculty.washington.edu/marilynr/

[52] Speer BS, Bedzyk L, Salyers AA. Evidence that a novel tetracycline resistance gene found on two Bacteroides transposons encodes an NADP-requiring oxidoreductase. J.Bacteriol. 1991 Jan;173(1):176-183.

[53] Burdett V. Streptococcal tetracycline resistance mediated at the level of protein synthesis. J.Bacteriol. 1986 Feb;165(2):564-569.

[54] Roberts MC. Chapter 2: Tetracycline resistance due to ribosomal protection proteins. In: White DG, Alekshun MN, McDermott PF., editors. Frontiers in antimicrobial resistance: attribute to Stuart B. Levy. ASM Press, Washington DC. 2005: 19-28.

[55] Leipe DD, Wolf YI, Koonin EV, Aravind L. Classification and evolution of P-loop GTPases and related ATPases. J.Mol.Biol. 2002 Mar;317(1):41-72.

[56] Connell SR, Tracz DM, Nierhaus KH, Taylor DE. Ribosomal protection proteins and their mechanism of tetracycline resistance. Antimicrob.Agents Chemother. 2003 Dec;47(12):3675-3681.

[57] Connell SR, Trieber CA, Dinos GP, Einfeldt E, Taylor DE, Nierhaus KH. Mechanism of Tet(O)-mediated tetracycline resistance. EMBO J. 2003 Feb; 22(4):945-953.

[58] Connell SR, Trieber CA, Stelzl U, Einfeldt E, Taylor DE, Nierhaus KH. The tetracycline resistance protein Tet(O) perturbs the conformation of the ribosomal decoding centre. Mol.Microbiol. 2002 Sep;45(6):1463-1472.

[59] Manavathu EK, Fernandez CL, Cooperman BS, Taylor DE. Molecular studies on the mechanism of tetracycline resistance mediated by Tet(O). Antimicrob.Agents Chemother. 1990 Jan;34(1):71-77.

[60] Sanchez-Pescador R, Brown JT, Roberts M, Urdea MS. Homology of the TetM with translational elongation factors: implications for potential modes of tetM-conferred tetracycline resistance. Nucleic Acids Res. 1988 Feb;16(3):1218.

[61] Parmeggiani A, Swart GW, Mortensen KK, Jensen M, Clark BF, Dente L, et al. Properties of a genetically engineered G domain of elongation factor Tu. Proc.Natl.Acad.Sci.U.S.A. 1987 May;84(10):3141-3145.

[62] Trieber CA, Burkhardt N, Nierhaus KH, Taylor DE. Ribosomal protection from tetracycline mediated by Tet(O): Tet(O) interaction with ribosomes is GTP-dependent. Biol.Chem. 1998 Jul;379(7):847-855.

[63] Burdett V. Tet(M)-promoted release of tetracycline from ribosomes is GTP dependent. J.Bacteriol. 1996 Jun;178(11):3246-3251.

[64] Dantley KA, Dannelly HK, Burdett V. Binding interaction between Tet(M) and the ribosome: requirements for binding. J.Bacteriol. 1998 Aug;180(16):4089-4092.

[65] Taylor DE, DeGrandis SA, Karmali MA, Fleming PC. Transmissible tetracycline resistance in *Campylobacter jejuni*. Lancet 1980 Oct;2(8198):797.

[66] Taylor DE, Garner RS, Allan BJ. Characterization of tetracycline resistance plasmids from *Campylobacter jejuni* and *Campylobacter coli*. Antimicrob.Agents Chemother. 1983 Dec;24(6):930-935.

[67] Taylor DE. Plasmid-mediated tetracycline resistance in *Campylobacter jejuni*: expression in *Escherichia coli* and identification of homology with streptococcal class M determinant. J.Bacteriol. 1986 Mar;165(3):1037-1039.

[68] Manavathu EK, Hiratsuka K, Taylor DE. Nucleotide sequence analysis and expression of a tetracycline-resistance gene from *Campylobacter jejuni*. Gene 1988;62(1):17-26.

[69] Nirdnoy W, Mason CJ, Guerry P. Mosaic structure of a multiple-drug-resistant, conjugative plasmid from *Campylobacter jejuni*. Antimicrob.Agents Chemother. 2005 Jun;49(6):2454-2459.

[70] Sougakoff W., Papadopoulou B., Nordmann P., Courvalin P. Nucleotide sequence and distribution of gene *tetO* encoding tetracycline resistance in *Campylobacter coli*. 1987;44(1):153-159.

[71] Avrain L, Vernozy-Rozand C, Kempf I. Evidence for natural horizontal transfer of tetO gene between *Campylobacter jejuni* strains in chickens. J.Appl.Microbiol. 2004;97(1):134-140.

[72] Thakor NS, Wilson KS, Scott PG, Taylor DE. An improved procedure for expression and purification of ribosomal protection protein Tet(O) for high-resolution structural studies. Protein Expr.Purif. 2007 Oct;55(2):388-394.

[73] Nissen P. & Nyborg J. EF-G and EF-Tu Structures and Translation Elongation in Bacteria. 2004;2:1-5.

[74] Krab IM, Parmeggiani A. EF-Tu, a GTPase odyssey. Biochim.Biophys.Acta 1998 Nov;1443(1-2):1-22.

[75] Thakor NS, Nechifor R, Scott PG, Keelan M, Taylor DE, Wilson KS. Chimeras of bacterial translation factors Tet(O) and EF-G. FEBS Lett. 2008 Apr 16;582(9):1386-1390.

[76] Spahn CM, Blaha G, Agrawal RK, Penczek P, Grassucci RA, Trieber CA, et al. Localization of the ribosomal protection protein Tet(O) on the ribosome and the mechanism of tetracycline resistance. Mol.Cell 2001 May;7(5):1037-1045.

[77] Jacquet E, Parmeggiani A. Structure-function relationships in the GTP binding domain of EF-Tu: mutation of Val20, the residue homologous to position 12 in p21. EMBO J. 1988 Sep;7(9):2861-2867.

[78] Zavialov AV, Hauryliuk VV, Ehrenberg M. Guanine-nucleotide exchange on ribosome-bound elongation factor G initiates the translocation of tRNAs. J. Biol. 2005 Jun;4(2):9.

[79] Taylor DE, Jerome LJ, Grewal J, Chang N. Tet(O), a protein that mediates ribosomal protection to tetracycline, binds and hydrolyses GTP. Can. J. Microbiol. 1995, 41: 965-970.

[80] Kobayashi T, Nonaka L, Maruyama F, Suzuki S. Molecular evidence for the ancient origin of the ribosomal protection protein that mediates tetracycline resistance in bacteria. J.Mol.Evol. 2007 Sep;65(3):228-235.

[81] Hwang YW, Miller DL. A mutation that alters the nucleotide specificity of elongation factor Tu, a GTP regulatory protein. J.Biol.Chem. 1987 Sep 25;262(27):13081-13085.

[82] Schmidt G, Lenzen C, Simon I, Deuter R, Cool RH, Goody RS, Wittinghofer A. Biochemical and biological consequences of changing the specificity of p21ras from guanosine to xanthosine nucleotides. Oncogene. 1996 Jan;12(1):87-96.

[83] Yu B, Slepak VZ, Simon MI. Characterization of a Goalpha mutant that binds xanthine nucleotides. J. Biol Chem. 1997 Jul; 272(29):18015-18019.

[84] Barbieri MA, Hoffenberg S, Roberts R, Mukhopadhyay A, Pomrehn A, Dickey BF, Stahl PD. Evidence for a symmetrical requirement for Rab5-GTP in in vitro endosome-endosome fusion. J. Biol Chem. 1998 Oct; 273(40): 25850-25855.

[85] Martemyanov KA, Gudkov AT. Domain IV of elongation factor G from *Thermus thermophilus* is strictly required for translocation. FEBS Lett. 1999 Jun 11;452(3):155-159.

[86] Martemyanov KA, Yarunin AS, Liljas A, Gudkov AT. An intact conformation at the tip of elongation factor G domain IV is functionally important. FEBS Lett. 1998 Aug 28;434(1-2):205-208.

[87] Savelsbergh A, Matassova NB, Rodnina MV, Wintermeyer W. Role of domains 4 and 5 in elongation factor G functions on the ribosome. J.Mol.Biol. 2000 Jul;300(4):951-961.

[88] Connell SR, Takemoto C, Wilson DN, Wang H, Murayama K, Terada T, et al. Structural basis for interaction of the ribosome with the switch regions of GTP-bound elongation factors. Mol.Cell 2007 Mar;25(5):751-764.

[89] Tijerina P, Mohr S, Russell R. DMS footprinting of structured RNAs and RNA-protein complexes. Nat.Protoc. 2007;2(10):2608-2623.

[90] Moazed D, Noller HF. Interaction of antibiotics with functional sites in 16S ribosomal RNA. Nature 1987 Jun;327(6121):389-394.

[91] Chopra I. Glycylcyclines: third-generation tetracycline antibiotics. Curr.Opin.Pharmacol. 2001 Oct;1(5):464-469.

[92] Mullangi PK, Pankey GA. Tigecycline in critical care. Crit.Care Clin. 2008 Apr;24(2):365-375.

[93] Bergeron J, Ammirati M, Danley D, James L, Norcia M, Retsema J, et al. Glycylcyclines bind to the high-affinity tetracycline ribosomal binding site and evade Tet(M)- and Tet(O)-mediated ribosomal protection. Antimicrob.Agents Chemother. 1996 Sep;40(9):2226-2228.

[94] Iredell J, Thomas L, Power D, Mendes E. Tigecycline resistance in Australian antibiotic-resistant Gram-negative bacteria. J.Antimicrob.Chemother. 2007 Apr;59(4):816-818.

[95] Navon-Venezia S, Leavitt A, Carmeli Y. High tigecycline resistance in multidrug-resistant *Acinetobacter baumannii*. J.Antimicrob.Chemother. 2007 Apr;59(4):772-774.

[96] Reid GE, Grim SA, Aldeza CA, Janda WM, Clark NM. Rapid development of *Acinetobacter baumannii* resistance to tigecycline. Pharmacotherapy 2007 Aug;27(8):1198-1201.

[97] Werner G, Gfrorer S, Fleige C, Witte W, Klare I. Tigecycline-resistant *Enterococcus faecalis* strain isolated from a German intensive care unit patient. J.Antimicrob.Chemother. 2008 May;61(5):1182-1183.

[98] Kohler RE, Ron EZ, Davis BD. Significance of the free 70 s ribosomes in *Escherichia coli* extracts. J.Mol.Biol. 1968 Aug;36(1):71-82.

[99] van Diggelen OP, Bosch L. The association of ribosomal subunits of *Escherichia coli*. 1. Two types of association products differing in their apparent sedimentation coefficient. Eur.J.Biochem. 1973 Nov;39(2):499-510.

[100] Blaha G, Stelzl U, Spahn CM, Agrawal RK, Frank J, Nierhaus KH. Preparation of functional ribosomal complexes and effect of buffer conditions on tRNA positions observed by cryoelectron microscopy. Methods Enzymol. 2000;317:292-309.

[101] Phillips LA, Franklin RM. The in vivo distribution of bacterial polysomes, ribosomes, and ribosomal subunits. Cold Spring Harb.Symp.Quant.Biol. 1969;34:243-253.

[102] Spedding G. Isolation and analysis of ribosomes from prokaryotes, eukaryotes and organelles. In: Spedding G. Ribosomes and Protein Synthesis: A Practical Approach. Oxford University Press, Oxford, UK, 1990:1–27.

[103] Invitrogen Corporation. Champion™ pET Directional TOPO Expression Kits: Five-minute, directional TOPO Cloning of blunt-end PCR products into vectors for high-level, inducible expression in *E. coli*. User manual, Version H, 2006 Oct:1-43

[104] Cammack KA, Wade HE. The sedimentation behaviour of ribonuclease-active and -inactive ribosomes from bacteria. Biochem.J. 1965 Sep;96(3):671-680.

[105] Salaj-Smic E. Colicinogeny of Escherichia coli MRE 600. Antimicrob.Agents Chemother. 1978 Nov;14(5):797-799.

[106] Bradford MM. A rapid and sensitive method for the quantitation of microgram quantities of protein utilizing the principle of protein-dye binding. Anal.Biochem. 1976 May 7;72:248-254.

[107] Fahlman RP, Uhlenbeck OC. Contribution of the esterified amino acid to the binding of aminoacylated tRNAs to the ribosomal P- and A-sites. Biochemistry 2004 Jun 15;43(23):7575-7583.

[108] Hassur SM, Whitlock HW,Jr. UV shadowing--a new and convenient method for the location of ultraviolet-absorbing species in polyacrylamide gels. Anal.Biochem. 1974 May;59(1):162-164.

[109] Ledoux S, Uhlenbeck OC. [3'-^{32}P]-labeling tRNA with nucleotidyltransferase for assaying aminoacylation and peptide bond formation. Methods 2008 Feb;44(2):74-80.

[110] Wong I, Lohman TM. A double-filter method for nitrocellulose-filter binding: application to protein-nucleic acid interactions. Proc.Natl.Acad.Sci.U.S.A. 1993 Jun;90(12):5428-5432.

[111] Burdett V. Purification and characterization of Tet(M), a protein that renders ribosomes resistant to tetracycline. J.Biol.Chem. 1991 Feb 15;266(5):2872-2877.

[112] Pan SH, Malcolm BA. Reduced background expression and improved plasmid stability with pET vectors in BL21 (DE3). BioTechniques 2000 Dec;29(6):1234-1238.

[113] Studier FW, Rosenberg AH, Dunn JJ, Dubendorff JW. Use of T7 RNA polymerase to direct expression of cloned genes. Methods Enzymol. 1990;185:60-89.

[114] Dubendorff JW, Studier FW. Controlling basal expression in an inducible T7 expression system by blocking the target T7 promoter with lac repressor. J.Mol.Biol. 1991 May;219(1):45-59.

[115] Structural Genomics Consortium, China Structural Genomics Consortium, Northeast Structural Genomics Consortium, Graslund S, Nordlund P, Weigelt J, et al. Protein production and purification. Nat.Methods 2008 Feb;5(2):135-146.

[116] Hannig G, Makrides SC. Strategies for optimizing heterologous protein expression in Escherichia coli. Trends Biotechnol. 1998 Feb;16(2):54-60.

[117] Wilkinson DL, Harrison RG. Predicting the solubility of recombinant proteins in Escherichia coli. Biotechnology (N.Y) 1991 May;9(5):443-448.

[118] Davis GD, Elisee C, Newham DM, Harrison RG. New fusion protein systems designed to give soluble expression in Escherichia coli. Biotechnol.Bioeng., 1999 Nov; 65(4): 382-388.

[119] Koschorreck M, Fischer M, Barth S, Pleiss J. How to find soluble proteins: a comprehensive analysis of alpha/beta hydrolases for recombinant expression in E. coli. BMC Genomics 2005 Apr;6(1):49.

[120] Dale GE, Broger C, Langen H, D'Arcy A, Stuber D. Improving protein solubility through rationally designed amino acid replacements: solubilization of the trimethoprim-resistant type S1 dihydrofolate reductase. Protein Eng. 1994 Jul;7(7):933-939.

[121] Izard J, Parker MW, Chartier M, Duche D, Baty D. A single amino acid substitution can restore the solubility of aggregated colicin A mutants in Escherichia coli. Protein Eng. 1994 Dec;7(12):1495-1500.

[122] Villaverde A, Carrio MM. Protein aggregation in recombinant bacteria: biological role of inclusion bodies. Biotechnol.Lett. 2003 Sep;25(17):1385-1395.

[123] Vallejo LF, Rinas U. Strategies for the recovery of active proteins through refolding of bacterial inclusion body proteins. Microb.Cell.Fact. 2004 Sep; 3(1):11.

[124] Singh SM, Panda AK. Solubilization and refolding of bacterial inclusion body proteins. J.Biosci.Bioeng. 2005 Apr;99(4):303-310.

[125] Vera A, Gonzalez-Montalban N, Aris A, Villaverde A. The conformational quality of insoluble recombinant proteins is enhanced at low growth temperatures. Biotechnol.Bioeng. 2007 Apr;96(6):1101-1106.

[126] Sorensen HP, Mortensen KK. Soluble expression of recombinant proteins in the cytoplasm of Escherichia coli. Microb.Cell.Fact. 2005 Jan;4(1):1.

[127] Makrides SC. Strategies for achieving high-level expression of genes in Escherichia coli. Microbiol.Rev. 1996 Sep;60(3):512-538.

[128] Vasina JA, Baneyx F. Expression of aggregation-prone recombinant proteins at low temperatures: a comparative study of the Escherichia coli cspA and tac promoter systems. Protein Expr.Purif. 1997 Mar;9(2):211-218.

[129] Zhang Y, Olsen DR, Nguyen KB, Olson PS, Rhodes ET, Mascarenhas D. Expression of eukaryotic proteins in soluble form in Escherichia coli. Protein Expr.Purif. 1998 Mar;12(2):159-165.

[130] Chesshyre JA HA. Low tempteratures stabilize interferon a-2 against proteolysis in Methylophilus methylotrophus and Escherichia coli. 1989(31):158-162.

[131] Kiefhaber T, Rudolph R, Kohler HH, Buchner J. Protein aggregation in vitro and in vivo: a quantitative model of the kinetic competition between folding and aggregation. Biotechnology (N.Y) 1991 Sep;9(9):825-829.

[132] Geigenmuller U, Nierhaus KH. Tetracycline can inhibit tRNA binding to the ribosomal P site as well as to the A site. Eur.J.Biochem. 1986 Dec 15;161(3):723-726.

[133] Tritton TR. Ribosome-tetracycline interactions. Biochemistry 1977 Sep 6;16(18):4133-4138.

[134] Goldman RA, Cooperman BS, Strycharz WA, Williams BA, Tritton TR. Photoincorporation of tetracycline into Escherichia coli ribosomes. FEBS Lett. 1980 Aug;118(1):113-118.

[135] Parmeggiani A, Sander G. Properties and regulation of the GTPase activities of elongation factors Tu and G, and of initiation factor 2. Mol.Cell.Biochem. 1981 Mar;35(3):129-158.

[136] Valle M, Zavialov A, Sengupta J, Rawat U, Ehrenberg M, Frank J. Locking and unlocking of ribosomal motions. Cell 2003 Jul 11;114(1):123-134.

[137] Tanaka N, Kinoshita T, Masukawa H. Mechanism of protein synthesis inhibition by fusidic acid and related antibiotics. Biochem Biophys Res Commun. 1968 Feb;30(3):278-283.

[138] Falck E, Hautala JT, Karttunen M, Kinnunen PK, Patra M, Saaren-Seppala H, et al. Interaction of fusidic acid with lipid membranes: Implications to the mechanism of antibiotic activity. Biophys.J. 2006 Sep;91(5):1787-1799.

[139] Crowe J, Dobeli H, Gentz R, Hochuli E, Stuber D, Henco K. 6xHis-Ni-NTA chromatography as a superior technique in recombinant protein expression/purification. Methods Mol.Biol. 1994;31:371-387.

[140] Kapanidis AN, Ebright YW, Ebright RH. Site-specific incorporation of fluorescent probes into protein: hexahistidine-tag-mediated fluorescent labeling with (Ni^{2+}:nitrilotriacetic Acid (n)-fluorochrome conjugates. J.Am.Chem.Soc. 2001 Dec;123(48):12123-12125.

[141] Craig JE, Zhang Y, Gallagher MP. Cloning of the nupC gene of Escherichia coli encoding a nucleoside transport system, and identification of an adjacent insertion element, IS 186. Mol Microbiol. 1994 Mar;11(6):1159-1168.